



UNIVERSITÀ DEGLI STUDI DI SALERNO



UNIVERSITÀ DEGLI STUDI DI SALERNO  
Dipartimento di Farmacia

Dottorato di Ricerca  
in **Scienze del Farmaco**  
Ciclo XXIX — Anno accademico 2016/2017

### ***Tesi di Dottorato in***

***Design, synthesis and biological studies of new  
mitochondrial modulators improving  
neurological deficits in experimental models of  
Huntington's disease.***

Dottorando

Dott. *Francesca Di Cristo*

Tutore

Chiar.mo Prof. *Carmela Saturnino*

Co-tutore

Chiar.mo Prof. *Gianfranco Peluso*

Coordinatore: Chiar.mo Prof. *Gianluca Sbardella*



# Index

## Abstract

## Introduction

<b>1. Huntington's chorea</b> .....	11
1.1 Genetics of Huntington's disease .....	12
1.2 Huntingtin protein .....	14
1.2.1 Physiological role of huntingtin protein.....	15
1.2.2 Mutant huntingtin: loss and gain of function .....	16
<b>2. Mitochondrial matters in Huntington's disease</b> .....	19
2.1 Mitochondrial dysfunctions .....	19
2.2 Abnormal mitochondrial biogenesis .....	21
2.3 Abnormal mitochondrial dynamics .....	23
2.4 PGC-1 $\alpha$ , mitochondrial dysfunction and Huntington's disease.....	26
<b>3. Current therapeutic approaches for Huntington's disease</b> .....	29
3.1 Gene and protein therapy .....	29
3.2 Therapies specifically acting on protein aggregate .....	31
3.3 Mitochondria targeted therapeutic approaches .....	32
3.3.1 Regulators of mitochondrial dynamics .....	33
3.3.2 PGC-1 $\alpha$ as a therapeutic target in HD.....	34
<b>4. Mildronate: a possible candidate for HD treatment</b> .....	37
4.1 Mildronate: a mitochondrial modulator .....	37
4.2 Mildronate as neuroprotective drug .....	39
<b>5. Aim</b> .....	43

<b>6. Materials and methods</b> .....	47
6.1 Design and synthesis of mildronate structurally related compounds...	47
6.1.1 General procedure for the synthesis of amides 3a-v .....	48
6.1.2 General procedure for the synthesis of ammonium salts 4a-v ...	55
6.2 Biological <i>in vitro</i> assay.....	61
6.2.1 Cell culture and treatments.....	61
6.2.2 Cell proliferation assay .....	61
6.2.3 Western blotting .....	62
6.2.4 RNA isolation and quantitative Real-time PCR.....	62
6.2.5 Statistical Analyses .....	63
6.3 Mitotracker fluorescence assay .....	63
6.4 Biological assay in <i>Drosophila melanogaster</i> .....	63
6.4.1 <i>Drosophila melanogaster</i> stocks and crosses .....	63
6.4.2 Climbing behavioral assay .....	64
6.4.3 Data Interpretation and Statistical Analysis .....	66
6.5 Biological assay in <i>Caenorhabditis elegans</i> .....	67
6.5.1 <i>Caenorhabditis elegans</i> strain.....	67
6.5.2 Mechanosensory behavioral assay .....	67
6.5.3 Data Interpretation and Statistical Analysis.....	68
<b>7. Results</b> .....	71
7.1 Mildronate biological activity in <i>in vitro</i> HD model .....	71
7.1.1 Mildronate and mHtt aggregation .....	73
7.2 Synthesis of mildronate structurally related compounds: 4a-v .....	75
7.3 Evaluation of mildronate structurally related compounds in <i>in vitro</i> HD models .....	83
7.3.1 Mildronate structurally related compounds and mHtt aggregation .....	86

7.4	Modulation of <i>Pgc-1α</i> mRNA expression by mildronate and its structurally related analogues.....	89
7.5	Regulation of mitochondrial dynamics by mildronate and its structurally related compounds .....	92
7.6	Rescue of neurological deficits in HD animal model by mildronate and its structurally related compounds .....	96
7.6.1	<i>Drosophila melanogaster</i> HD stock.....	96
7.6.2	Mildronate and its structurally related compounds on neuronal deficits in the HD <i>Drosophila</i> model.....	97
7.7	<i>Caenorhabditis elegans</i> HD strain .....	103
7.7.1	Mildronate and its structurally related compounds on neuronal deficits in the HD <i>C.elegans</i> model .....	105
<b>8.</b>	<b>Discussion</b> .....	<b>111</b>
<b>9.</b>	<b>References</b> .....	<b>117</b>



# **Abstract**



Huntington's disease (HD) is an adult-onset, neurodegenerative disorder. It is a genetic dominantly inherited disease caused by a polyglutamine (polyQ) expansion mutation in the huntingtin protein (Htt). Because of its lack of valid treatment, development of more effective therapeutics for HD is urgently required. Recently, pharmacological strategies that modulate mitochondrial dynamics have shown promising results in several HD models. Mildronate, [3-(2,2,2-trimethylhydrazinium) propionate; THP; MET-88], a compound able to improve mitochondrial dysfunction, has demonstrated protective effects on a wide range of neuropathological events, as in case of Parkinson's and Alzheimer's disease. Interestingly, in the current study we found that mildronate can effectively improve motor function in the *Drosophila melanogaster* stock *elav-HTT.128Q.FL* and in *Pmec-3htt57Q128::GFP Caenorhabditis elegans* strain, both animal models overexpressing human mutant Htt. This improvement is evident by the significant increase in performance on the behavioral assays after mildronate treatment. In an effort to increase the activity of mildronate, we have designed, synthesized, and characterized 22 compounds, among which 4 display superior ability to reduce pathological biomarkers of HD as well as ameliorate mitochondrial dynamics in *in vitro* and *in vivo* assays in comparison to mildronate. In particular, the selected compounds decrease the level of HD aggregates in *STHdh<sup>Q109/109</sup>* transfected cells more significantly than mildronate, without affecting the level of transfected normal or mutant Htt. Finally, all the compounds have shown the ability to decrease significantly the mitochondrial fragmentation in *STHdh<sup>Q109/109</sup>* and to reduce motor deficits in the animal models. This result confirms that perturbation in mitochondrial dynamics may contribute to the onset and progression of neurodegenerative disorders and that correcting mitochondrial fragmentation, reduces motor deficits in HD animals.



# Introduction



## 1. Huntington's chorea

Huntington's disease (HD) is an adult-onset, neurodegenerative and genetic disorder. It is an orphan disease affecting fewer than 10 people per 100,000 in the Caucasian population [1].

HD is clinically characterized by a combination of motor, affective and cognitive deficits which result in a slow progressive neuronal degeneration in selected brain areas, including the caudate and putamen of the striatum, cerebral cortex, hippocampus, hypothalamus and sub-thalamus [2].

The main clinical features are motor disturbances (chorea, dystonia, bradykinesia, rigidity), behavioral and psychiatric impairment (irritability, impulsivity, depression, apathy, anxiety) and cognitive decline (executive dysfunction, inattention, dementia) along with sleep disturbances and weight loss [3] [4] .

Most clinical features of Huntington's disease can be attributed to central nervous system (CNS) degeneration, but there are other aspects mediated outside the CNS, including weight loss, metabolic dysfunction and endocrine disturbances. [5]. Within the brain, there is massive striatal neuronal cell death, with up to 95% loss of GABAergic medium spiny projection neurons.

Furthermore, there is atrophy in cerebral cortex, subcortical white matter, thalamus, specific hypothalamic nuclei and other brain areas [6].

HD symptoms typically manifest between the ages of 35 and 45 years, then progress slowly approximately 15 to 20 years until death.

## 1.1 Genetics of Huntington's disease

HD is a genetic disease with an autosomal dominant inheritance.

The disease-causing gene mutation consists of an expanded polyglutamine repeats (CAG repeats) in the coding region of exon 1 in IT-15 gene. The gene is located on chromosome 4p16.3 and it codes for a 347 kilo-Daltons ubiquitrary protein named huntingtin (Htt).

The length of the (CAG) $n$  domain in IT-15 gene is genetically unstable and susceptible to expansion. In its wild-type form, it contains 8-26 glutamine residues. Intermediate numbers of repeats, between 27 and 35, are not associated with disease expression but they can be meiotically unstable in paternal transmission: the CAG length may expand in paternal transmission, resulting in the disease in descendents. Repeats of 36–39 are associated with reduced penetrance , whereas repeats of 40 or larger are associated with disease expression (fig.1) [7] .

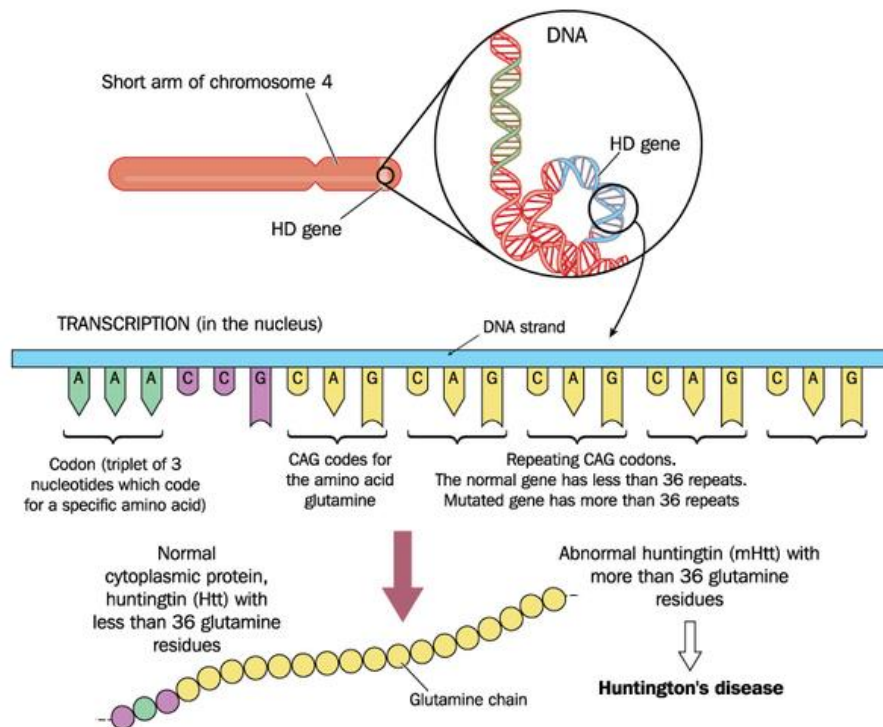


**Figure 1.** Huntington mutated gene. The length of the (CAG) $n$  domain in wild-type form is 8-26 glutamine residues. Intermediate numbers of repeats, between 27 and 35, are not associated with disease expression but they can be meiotically unstable; repeats of 36 or larger are associated with disease expression.  
Source: <https://ghr.nlm.nih.gov/condition/huntington-disease>.

The disease is inherited with age-dependent penetrance: there is a strong inverse relationship between age at onset and number of CAG repeats.

Classic adult onset between the ages of 35 and 45 is associated with repeat lengths between 40 and 49. CAG lengths greater than 50 are typically associated with onset between 20 and 30 years of age. Longer CAG repeats predict juvenile HD (JHD), which constitutes about 5% of all HD case and occurs prior to the age of 21. Within JHD, repeat lengths longer than 60 are associated with age of onset between 10 and 20, and more than 80 can manifest in childhood onset, where the diagnosis is prior the age of 10 (fig.2) [8].

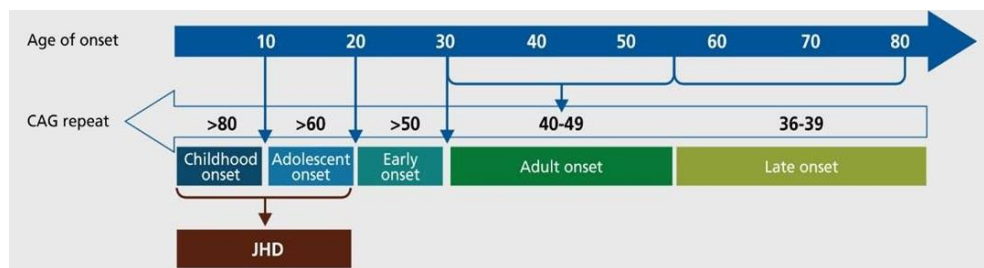


**Figure 2.** In HD the length of CAG repeat is inversely related to age of onset. This relationship is reported with approximations of age of onset based on repeat length. JHD, juvenile Huntington disease.

Source: P.C. Nopoulos, Dialogues in Clinical Neuroscience, 2016.

## 1.2 Huntingtin protein

Huntingtin (Htt) is a large protein of 3,144 amino acids, ubiquitously expressed with the highest levels in CNS neurons and in the testes.

Htt has been found in different cellular locations, where it may act as a scaffold protein for the activation and correct assembly, in time and space, of specific molecular partners and pathways.

Intracellularly, Htt is associated with various organelles, including the nucleus, endoplasmic reticulum and Golgi complex and it is also found in neurites and at synapses, where it associates with vesicular structures [9].

It has many potential domains, but their activities are not fully understood.

The polyglutamine region is an important portion of the mammalian protein: its physiological function is to regulate interaction among wild-type huntingtin and several partners.

Huntingtin also contains the so-called HEAT (Huntingtin, Elongator factor3, PR65/A regulatory subunit of PP2A, and Tor1) repeats, ~40-amino-acid-long sequences involved in protein-protein interactions [10].

Their distribution within the Htt protein might confer a scaffolding role for protein complex formation. The HEAT repeats are very similar in terms of number, sequence and distribution along the length of the protein [11].

Downstream of these regions are three caspase and calpain cleavage sites typically conserved in vertebrate [12]. Cleaved fragments of Htt are observed in the nucleus, but their activity is yet unclear. Maybe cellular status might affect proteolysis process, as shown in different studies that reported increased proteolysis in diseased brain [13].

### **1.2.1 Physiological role of huntingtin protein**

Wild-type huntingtin (wtHtt) is involved in several important cell activities. With its large number of protein-protein interaction domains, has been found to interact with more than 200 other proteins [14].

A large number of Htt protein interactors are involved in microtubule-based axon trafficking. Huntingtin-associated protein 1 (HAP1) mediates the interaction between Htt, microtubule motor proteins and their co-factors, including kinesin, dynactin, and dynein [15].

Wild Htt plays a crucial function in embryonic development: its complete inactivation in huntingtin-knockout mice leads to embryonic lethality. Other study has shown that greatly reduced Htt levels are insufficient to support normal mouse development [16].

After gastrulation, huntingtin becomes important for neurogenesis: a lower dose of wHtt leads to defects in the epiblast with consequent neurogenesis reduction and serious malformations of the cortex and striatum [17].

Wild Htt is also crucial for establishing and maintaining neuronal identity, especially in the cortex and striatum region. Furthermore, it is important for

the survival of mammalian neurons, in which it regulates many cell functions, such as neuronal gene transcription, and axonal and vesicular transport [12].

Additionally, wHtt has an antiapoptotic role. Several studies established that wHtt is neuroprotective in brain cells exposed to apoptotic stimuli, such as serum deprivation, mitochondrial toxins or the transfection of death genes [18]. The neuronal inactivation of huntingtin led to apoptotic cells in the hippocampus, cortex and striatum [19].

Wild-type protein level increase improves neuroprotection: it suggests a gene-dosage effect [20].

Investigations highlighted molecular mechanisms of Htt antiapoptotic role: it prevents cell death by inhibiting both the processing of pro-caspase 9 and the formation of the pro-apoptotic protein interactor of huntingtin-interacting protein 1 [21].

Wild Htt has also been associated to brain-derived neurotrophic factor (BDNF), an important trophic factor in HD.

Loss or reduction in wild-type huntingtin activity might decrease BDNF support to striatal neurons and disturb their transport along the cortico-striatal afferents [22].

Finally wHtt interacts with a lot of cytoskeletal and synaptic vesicle proteins essential for exo- and endocytosis at synaptic terminals [23].

### **1.2.2 Mutant huntingtin: loss and gain of function**

Numerous studies postulate that neurodegeneration results from a toxic “gain and/or loss of function” of mutant Htt (mHtt) including enhanced protease activity, protein misfolding, disruption of axonal transport, changes in electrophysiological properties or induction of apoptotic mechanisms. However, most of these hypotheses do not explain the selective loss of GABAergic medium spiny neurons in HD.

Mutation of CAG length in huntingtin leads to protein misfolding, promoting an abnormal and toxic aggregation process, which triggers the formation of intracellular insoluble aggregates, called inclusion bodies [24].

The rate of aggregation is proportional to the length of polyQ expansion [25]. Indeed, the presence of an expanded polyglutamine tract in the mutant protein induces a conformational change which is believed to trigger a pathogenic cascade. The toxic structure includes a compact anti-parallel  $\beta$ -sheets conformation, in which the strands are held together by intra- and intermolecular hydrogen bonds. The abnormal folded protein can aggregate and form fibrillar structures, likewise in other neurodegenerative diseases such as Alzheimer's disease, Parkinson's disease and prion disorders [26].

Extensive research using cell cultures, animal models and postmortem brains from HD patients suggests that, following the aggregation process, multiple cellular changes can induce neuronal damage, such as transcriptional deregulation, altered calcium homeostasis, aberrant protein-protein interaction, abnormal mitochondrial dynamics and impaired axonal transport (fig.3) [27].

Among these, abnormal mitochondrial dynamics seems to be strongly associated with HD pathogenesis and progression.

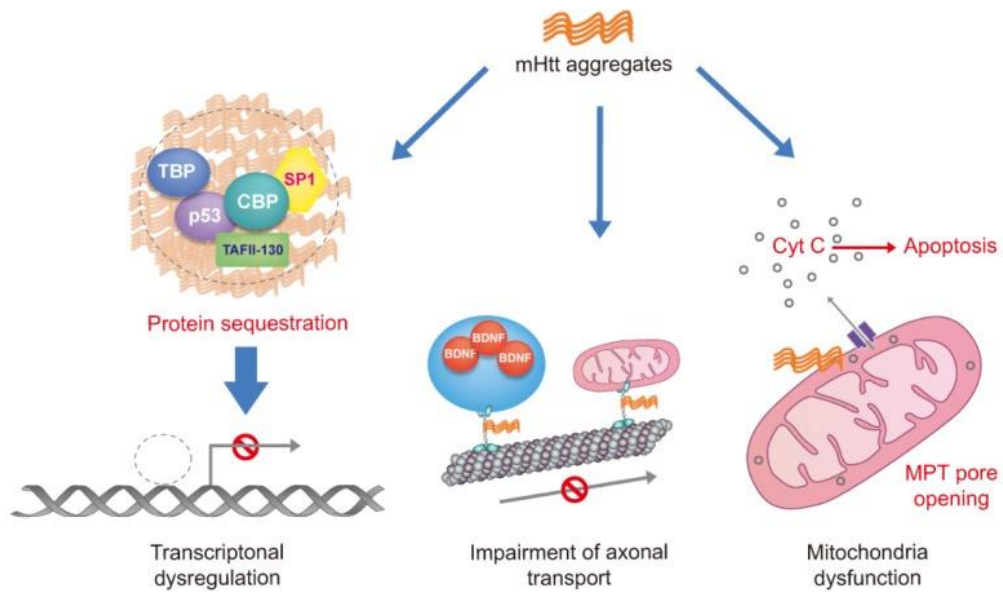


**Figure 3.** Potential molecular pathogenesis of toxicity of mHtt aggregates. Mutant huntingtin may sequester transcription factors leading to transcriptional dysregulation of many genes. Moreover, mHtt causes defects in trafficking of vesicle and cellular organelle such as mitochondria. Finally, mHtt directly influence to decrease the  $\text{Ca}^{2+}$  threshold for mitochondrial permeability transition (MPT) pore opening, leading to Cyt c release and apoptosis.

Source: Kim S., Experimental Neurology, 2014.

## **2. Mitochondrial matters in Huntington's disease**

It is a well-known fact that mitochondrial oxidative phosphorylation provides the major source of ATP in neurons. From the classical viewpoint, adequate levels of ATP are essential to maintain the neuronal plasma membrane potential via the sodium–potassium ATPase, which consumes about 40% of the energy. In addition, mitochondria are an important intracellular  $\text{Ca}^{2+}$  sequestration system, and especially synaptic mitochondria are indispensable for neurotransmitter reserve pool mobilization in the presynaptic compartment. Due to these important features, mitochondria can modulate neuronal excitability and synaptic transmission. In addition, more recent evidence shows that mitochondria in neurons are highly dynamic organelles undergoing extensive fusion, fission, and have sophisticated mechanisms for quality control, which is extremely relevant for a dependable long-lasting function of these post-mitotic cells, working in highly specialized networks and being not subject to further selection mechanisms.

### **2.1 Mitochondrial dysfunctions**

Recent research has revealed multiple alterations in mitochondria, in HD progression and pathogenesis, including: (i) reduced enzymatic activity in several components of oxidative phosphorylation, including complexes II, III and IV of the electron transport chain, in HD postmortem brains and HD mouse models, suggesting that mitochondria are involved in HD pathogenesis; (ii) low mitochondrial ATP and decreased mitochondrial ADP uptake in HD knock-in striatal cells and lymphoblasts from patients with HD, revealing expanded polyglutamine repeats; (iii) defective calcium-induced

mitochondrial permeability in HD cell lines and HD mice; (iv) mHtt-induced defective mitochondrial trafficking in HD primary neurons; (v) age-dependent mitochondrial (mt)DNA damage and mtDNA deletions in HD-affected neurons; and (vi) biochemical, confocal and electron microscopy studies revealed structurally damaged mitochondria with broken cristae and small and round mitochondria in HD-affected neurons [28].

Current evidence suggests that mHtt might directly or indirectly impair mitochondria function [29].

Direct mechanisms are supported by evidence that mHtt associates with brain mitochondria, and that acute exposure of mitochondria isolated from rat brain to pathological-length polyQ constructs perturbs mitochondria functionality, resulting in an increase of reactive oxygen species (ROS) production [30] [31]. However, the precise mechanisms through polyQ constructs increase ROS formation and if these apply to mHtt full-length or fragments remain uncertain [29].

Evidence showing enhanced oxidative stress in HD brains includes an increase in accumulation of lipofuscin, a product of unsaturated fatty acid peroxidation, strand breaks in DNA and the accumulation of oxidative DNA damage products 8-hydroxy-2'-deoxyguanosine in HD brain and blood [32]. A further relevant indicator of increased oxidative stress is the induction of oxidative defense mechanisms including mitochondrial and cytoplasmic superoxide dismutase in HD brains of humans and transgenic animals [33].

Abnormalities in some of the key mitochondrial enzymes involved in glucose metabolism, including the pyruvate dehydrogenase complex (PDHC) and the tricarboxylic acid (TCA) cycle, may contribute to mitochondrial dysfunction [34]. Follow-up studies performed upon HD patient material documented significant reductions in the enzymatic activities of complexes II, III, and IV of the mitochondrial oxidative phosphorylation pathway in caudate and putamen, [35], [36], [37]. This deficiency of respiratory chain complex has

been found in postmortem studies of symptomatic HD patients but not in presymptomatic patients, suggesting that respiratory chain defects are a secondary phenomenon in the pathogenesis of HD [35], [38].

Alternatively, it was proposed an indirect mechanisms of action for mHtt. Mutant Htt induces transcriptional deregulation by interfering with transcription factors, cluttering gene promoters and even through direct DNA binding [39]. An example of an indirect mechanism underlying HD mitochondrial dysfunction is the mHtt-p53 interaction. Mutant protein binds p53 and up-regulates its nuclear levels and transcriptional activity, thus inducing expression of mitochondria associated proteins and up-regulation of ROS levels [40].

A recent paper indicates a shift toward a larger free/bound NADH ratio (shift toward anaerobic glycolysis) in the cytosolic region in the presence of mHtt. This might indicate depletion of ATP production and an increase in oxidative stress that can eventually lead to cell death [41]. Moreover it has been shown that NADH interaction with regulatory proteins such as C-terminal-binding protein (CtBP) and sirtuins influences their transcriptional activity: thus result lead to the hypothesis that an increase in nuclear NADH leads to transcriptional dysregulation [42].

## **2.2 Abnormal mitochondrial biogenesis**

Mitochondrial biogenesis requires a tight coordination between the nuclear, cytosolic and mitochondrial compartments, since only a minority (13 proteins) of the full mammalian mitochondrial proteome (about 1100 to 1500 proteins) is locally encoded in the mtDNA [43], [44]. The transcriptional co-activator PGC-1 $\alpha$  is considered the master regulator of the mitochondrial biogenesis

program, acting in concert with nuclear respiratory factors NRF1 and NRF2 [45].

Proteins translated in the cytosol may be targeted to mitochondria via positively charged N-terminal presequences recognized by the translocase of the outer membrane (TOM), and then transferred to the translocase of the inner membrane (TIM23) in a membrane potential-dependent manner [46]. Proteins within the TIM23 complex may fully translocate to the mitochondrial matrix or insert into the inner membrane, where some will integrate into respiratory complexes [47] [48].

Impaired PGC-1 $\alpha$  signaling and defective mitochondrial biogenesis were implicated in the mechanisms of striatal vulnerability in HD following data from PGC-1 $\alpha$  knockout mice. These PGC-1 $\alpha$ <sup>-/-</sup> mice exhibited behavioral changes consistent with neurodegeneration, presenting spongiform lesions primarily in the striatum and, less prominently, in the motor cortex and hippocampus [49]. More recently, PGC-1 $\alpha$  suppression in cultured neurons was found to contribute to mHtt-induced increases in extrasynaptic NMDAR activity and vulnerability to excitotoxic insults [50]. In wild-type mice, PGC-1 $\alpha$  mRNA levels were identical in striatum and cortex, but mitochondrial/nuclear DNA ratios (mtDNA/nDNA) and citrate synthase activity were higher in the striatum [51] [52]. Interestingly, in R6/2 HD mice, PGC-1 $\alpha$  mRNA levels were similarly decreased in the striatum and cortex; however, only the striatum presented decreased mtDNA/nDNA, suggesting that the striatum may be particularly susceptible to reduced PGC-1 $\alpha$  expression [51].

In early-stage HD patients, PGC-1 $\alpha$  mRNA levels were decreased in the striatum (caudate nucleus), but not in the hippocampus or cerebellum [53], [54]. Within the striatum, data from CAG140 knock-in mice showed that PGC-1 $\alpha$  mRNA levels were decreased in MSNs and increased in cholinergic interneurons, which are mostly spared in HD [53]. The mechanism by which

striatal PGC-1 $\alpha$  transcription is differently affected in MSNs and interneurons is unknown. Nevertheless, mHtt is thought to repress PGC-1 $\alpha$  transcription by associating with the promoter region and interfering with the activation functions of the transcription factors CREB and TAF4 [53].

### **2.3 Abnormal mitochondrial dynamics**

Mitochondrial dynamics are crucial events that determine mitochondrial morphology and size as well as mitochondrial distribution and function. This morphological plasticity of mitochondria results from the equilibrium between fusion and fission processes. Fused mitochondrial networks are important for energy dissipation to distant areas of the neuron and complementation of mitochondrial DNA gene products. Because mitochondria have double membranes, mitochondrial fusion is necessarily a well-coordinated and multistep process, where the outer and inner mitochondrial membranes fuse by independent events. These fusion processes involve specific and distinct sets of proteins that show distinct mitochondrial sublocalization. The mitofusins Mfn1 and Mfn2 are transmembrane proteins embedded in the mitochondrial outer membrane which function depends on GTPase activity whereas Opa1 is localized in the mitochondrial intermembrane space as soluble forms or tightly attached to the inner mitochondrial membrane being responsible for the inner membrane fusion.

Instead, fission is required for inheritance and partitioning of organelles during cell division, for the release of pro-apoptotic factors from the mitochondrial intermembrane space and for the turnover of damaged organelles by mitophagy. The central protein player appears to be Drp1, an evolutionarily conserved dynamin-related protein, member of the dynamin family of

GTPases. Since Drp1 is mainly cytosolic, receptor-like molecules on the mitochondrial membrane are necessary to efficiently recruit Drp1 for fission. Different outer-membrane proteins have been proposed as Drp1-receptors, including Fis1, Mff and the two homologous proteins Mid49 and Mid51.

Thus, any perturbation in mitochondrial dynamics particularly those affecting the proteins that control the complementary processes of fission and fusion may increase neuronal susceptibility to brain injuries and contribute to the onset and progression of distinct neurodegenerative disorders.

In neurons that express mHtt, an imbalance between fission and fusion was found to lead to abnormalities in mitochondrial structure and function, and to damaged neurons. Several studies have reported such abnormal mitochondrial dynamics in patients with HD, HD mouse models, damaged HD lymphoblasts, HD cell lines and primary neurons that express mHtt [55].

### **2.3.1 Aberrant mitochondrial fission in HD**

Mitochondria alterations in HD were first reported over four decades ago in ultrastructural studies on HD brain biopsies showing aberrant dense mitochondria with sparse cristae [56]. Consistent with these findings, recent studies have demonstrated that mitochondrial dynamics in HD are unbalanced towards fission. Thus, mitochondria from human HD lymphoblasts or from murine HD primary striatal cultures were found greatly fragmented with higher susceptibility to apoptotic stimuli [57].

This aberrant mitochondrial fragmentation was correlated with increased levels of Drp1 and Fis1 and decreased expression of Mitofusins and Opa1 [58]. Though the underlying mechanisms are not yet completely understood, the expression of mHtt has emerged as the key casual factor. mHtt can

enhance mitochondrial fission by direct association with the mitochondrial surface and with the fission protein Drp1 promoting its GTPase activity [31] [59]. This interaction could facilitate abnormal assembly of Drp1 oligomers on the surface of mitochondria, thereby activating fission. Indeed, mHtt-induced mitochondrial fragmentation and cell death can be rescued by a dominant negative form of Drp1, supporting the idea that Drp1 activation is a major target of mHtt-induced toxicity.

Nevertheless, the bases of the increased sensitivity of mitochondria to fragmentation in HD striatum have not been elucidated. Interestingly, mitochondria from the striatum express higher levels of Drp1-receptor Fis1 and are more inherently shifted towards fission than mitochondria in cortical brain areas [60]. Therefore, it has been hypothesized that this increase in striatal Fis1 levels may contribute to enhance the susceptibility of striatal neurons to mHtt-induced up-regulation of Drp1 activity leading to neuronal cell death.

mHtt-mediated mitochondrial fragmentation may also contribute to defects in mitochondrial transport. Neurons expressing exon-1 Htt with 46 polyQ show excessive mitochondrial fragmentation together with a decrease in both anterograde and retrograde mitochondrial transport and velocity that was even more pronounced in neurons expressing exon-1 Htt with 97 polyQ [59]. Moreover, in neurons from BACHD mice excessively fragmented mitochondria have altered mitochondrial biogenesis, remain in the soma and cannot be transported to neuronal processes, ultimately leading to synaptic deficiencies [61] [62].

Interestingly, emerging evidence indicates a role for the transcriptional coactivator PGC-1 $\alpha$ , as key upstream regulator of the mitochondrial dynamics machinery. The results obtained by a study on postnatal growth of the heart support the following conclusions: 1) PGC-1 $\alpha$  coactivator is necessary for normal mitochondrial maturation, and dynamics, during postnatal

development; 2) PGC-1 $\alpha$  coactivator regulates expression of a subset of genes involved in mitochondrial fusion and fission; 3) PGC-1 $\alpha$  directly stimulates transcription of the Mfn1 gene by coactivating the orphan nuclear receptor ERR $\alpha$ ; and 4) PGC-1 $\alpha$  coactivator is required for high level expression of nuclear- and mitochondrial-encoded genes involved in mitochondrial energy transduction and OXPHOS pathways, and for full respiratory capacity [63].

## **2.4 PGC-1 $\alpha$ , mitochondrial dysfunction and Huntington's disease**

Peroxisome proliferator-activated receptor (PPAR)- $\gamma$  coactivator-1 (PGC-1) family of coactivators plays a crucial role in integrating signaling pathways, tailoring them to best suit the changing cellular and systemic milieu. The first and perhaps the best studied member of the PGC-1 family of coactivators is PGC-1 $\alpha$ , which interacts with a broad range of transcription factors, including nuclear respiratory factors, NRF-1 and NRF-2, and the nuclear receptors, PPAR $\alpha$ , PPAR $\delta$ , PPAR $\gamma$ , estrogen related receptor  $\alpha$  (ERR $\alpha$ ) [64]. These transcription factors, in turn, regulate the expression of many nuclear-encoded mitochondrial genes, such as Cyt c, complexes I–V and the mitochondrial transcription factor A (Tfam) [65]. Activation of the mitochondrial genes leads to increased enzymatic capacity for fatty-acid  $\beta$ -oxidation, Krebs cycle, and OXPHOS. Importantly, PGC-1 $\alpha$  also induces the expression of genes involved in heme biosynthesis, ion transport, mitochondrial protein translation and protein import and stimulates respiratory function. In light of the above, PGC-1 $\alpha$  is aptly termed a master co-regulator of mitochondrial function.

In recent years, impaired PGC-1 $\alpha$  expression and/or function has emerged as a common underlying cause of mitochondrial dysfunction in HD. There is substantial evidence for impairment of PGC-1 $\alpha$  levels and activity in HD [53] [54]. Involvement of PGC-1 $\alpha$  in HD was first suggested by the findings that PGC-1 $\alpha$  knockout mice exhibit mitochondrial dysfunction, defective bioenergetics, a hyperkinetic movement disorder and striatal degeneration, which are features also observed in HD [49].

Impaired PGC-1 $\alpha$  function and levels occur in striatal cell lines, transgenic mouse models of HD and in postmortem brain tissue from HD patients, and interference of mutant huntingtin with the CREB/TAF4 complex was shown to be instrumental in this impairment [53].

Mutant Htt also increases transglutaminase (Tgase) activity, which impairs transcription of PGC-1 $\alpha$ , whereas Tgase inhibitors reverse this impairment both *in vitro* as well as in *Drosophila* [66]. Microarray expression data from the caudate nucleus of HD patient postmortem brain tissue showed that there was reduced expression of 24 out of 26 PGC-1 $\alpha$  target genes [54]. It is also showed that the pathologic grade-dependent significant reduction in numbers of mitochondria in striatal spiny neurons correlated with reductions in PGC-1 $\alpha$  and Tfam [58]. PGC-1 $\alpha$  also plays a role in the suppression of oxidative stress, and it induces mitochondrial uncoupling proteins and antioxidant enzymes, including copper/zinc superoxide dismutase (SOD1), manganese SOD (SOD2), and glutathione peroxidase (Gpx-1) [67]. Indeed, spongiform degeneration of striatum is a well-known feature of HD and similar lesions occur in SOD2 null mice [68]. In concert with the reduced PGC-1 $\alpha$  expression in the brains of R6/2 transgenic mice, it has been demonstrated that the oxidative stress response genes such as hemeoxygenase-1 (HO-1), Nrf-2 and Gpx1 are also reduced, resulting in increased oxidative stress as shown by an increase in oxidative damage markers such as MDA and 8-OHdG [69].



### **3. Current therapeutic approaches for Huntington's disease**

Although many advances have been made in the clinical, genetic and neuropathological knowledge after the discovery of the HD genetic cause, at the time there are no effective therapies available to stop or prevent the progression of Huntington's disease.

Several pharmacological approaches are currently undergoing studies in preclinical models and in clinical trials. Many drugs have been evaluated for their ability to reduce choreatic movements, such as neuroleptics, benzodiazepines, antiepileptics, acetylcholinesterase inhibitors and glutamate antagonists. Recently, the monoamine depletor tetrabenazine (TBZ) has shown to be effective in reducing chorea in HD (tab.1 ) [70].

Recent data propose the use of stem cell therapy, to replace the lost striatal neurons.

In conclusion, there is no effective therapy for HD yet, hence urging the need to develop novel therapeutic strategies.

#### **3.1 Gene and protein therapy**

HD, a single-gene disorder, can be a good candidate for gene therapy. Reducing mutant Htt expression may offer a treatment for HD. RNA interference (RNAi) that blocks production of the dysfunctional Htt protein has emerged as a potential therapeutic strategy for HD. Short RNAs including short interfering RNA (siRNA), short hairpin RNA (shRNA), and microRNA (miRNA) molecules can bind to the Htt mRNA and trigger a cascade of events that results in the degradation of the mRNA. In a HD transgenic R6/2 mouse model, siRNAs against the *Htt* gene inhibited expression of transgenic mHtt

and reduced brain atrophy and neural inclusion accompanied with a rescue of motor deficits and an increase in survival [71].

A study using Adenovirus-mediated delivery of shRNA for transgenic HD N171-82Q mouse model showed results as a decrease of mHtt mRNA expression and a complete elimination of mutant HTT-positive inclusions with improved behavioral deficits [72].

Overall, these results suggest that a reduction of mHtt expression can improve the HD phenotype in mice. Non allele-specific Htt silencing approach would save the cost of developing individual therapy for HD patients, but the ideal gene therapy approach is to target specifically the mHtt as it represents the safest strategy.

Antisense oligonucleotides (ASOs), the short synthetic single stranded oligonucleotides that are complementary to a chosen sequence, can be used to suppress mHtt specifically. ASO infusion study showed sustained improvement of HD symptoms was achieved following a transient reduction of Htt in HD mouse model [73].

Another upstream therapeutic approach targeting mHtt is to clear misfolded proteins by increasing its degradation through therapeutic upregulation of the ubiquitin-proteasome pathway [74].

Mutant Htt might also be cleared through enhancement of chaperones molecular activity, which can promote refolding of misfolded proteins. Recent data suggest that overexpression of one or both of the chaperones HSP104 and HSP27 can suppress mHtt-mediated neurotoxicity in HD [75].

Despite the best efforts of researchers around the world, gene and/or protein therapy as an alternative to existing pharmacological treatments for HD still poses one of the greatest technical challenges in modern medicine due to the problems with toxicity, immune activation and tumorigenic response.

### 3.2 Therapies specifically acting on protein aggregate

Several studies are aimed to search anti-aggregation molecules able to inhibit oligomerization of  $\beta$ -sheet containing peptide [76].

Azo-dye congo-red intraperitoneally injected to R6/2 HD transgenic mice after onset of symptoms leads to the clearance of mHtt aggregates *in vivo* and shows protective effects on survival, motor dysfunction and weight loss [77].

Likewise to Azo-dye congo-red, the disaccharide trehalose also prevents the polyQ aggregation in R6/2 transgenic mouse model and it also improves survival, striatal atrophy, weight loss and motor impairments [78].

On the other side both congo-red and trehalose cannot cross blood-brain barrier [79]. In addition to these small molecules, polyglutamine binding peptide 1 (QBP1) also significantly has shown to suppresses polyQ aggregation in fly HD model [80].

Other approaches support the utilization of RNA aptamers, short RNA oligonucleotides, which bind their target molecules with high affinity.

In a recent study they were selected which bound specifically to the mHtt N-terminal fragment and they showed ability in inhibiting its aggregation *in vitro* model of HD. Aptamers were able to solubilize mHtt fragment and inhibit sequestration of essential cellular proteins [81].

Karpuj and colleagues suggest that inhibition of transglutaminase (TGase) could be considered a new therapeutical approach to HD [82].

TGase seems to be significant to the HD pathogenesis, promoting the formation of the protein aggregates via cross-linking huntingtin.

The inhibition of TGase activity through competitive inhibitor cystamine in transgenic mice expressing exon-1 of mutant huntingtin interferes with the course of their HD-like disease.

Data show that cystamine prolong survival, decreases tremor and irregular movements and improves weight loss [83] [82].

### **3.3 Mitochondria targeted therapeutic approaches**

Increasing evidence shows the significant involvement of mitochondrial dysfunction in the pathogenesis of HD. Therefore several therapeutic strategies are aimed to surmount such mitochondrial impairments [84].

Bioenergetics agents able to enhance normal mitochondrial function and improve mitochondrial bioenergetic defects have been evaluated. Among them, Creatine has been demonstrated to be beneficial and to exert neuroprotective effects in transgenic HD mouse. It is a naturally occurring guanidine compound involved in buffering energy within the cell [85]. Similarly, Coenzyme Q (CoQ) is a component of the electron transport chain as well as a crucial antioxidant in mitochondrial and lipid membranes. CoQ10 administration has been shown to be beneficial in transgenic mouse models of HD [84].

An interesting agent for therapeutic intervention in HD patients suffering from diabetes is exendin-4 (Ex-4), a FDA-approved antidiabetic glucagon-like peptide 1 receptor agonist [86].

It acts by targeting both peripheral and neuronal deficits: Ex-4 treatment ameliorated abnormalities in peripheral glucose regulation and suppressed cellular pathology in brain of HD mouse model. The treatment also improved motor function and extended their survival time. These clinical improvements were correlated with reduced accumulation of mHtt protein aggregates in brain cells [87].

Reduced expression of antioxidant enzymes and increased oxidative damage occur in both HD transgenic mice and in postmortem brain tissue and body fluids of HD patients. A particularly interesting approach to correct this pathological condition is using the antioxidant TEMPOL linked to gramicidin (XJB-5-131), which localizes it to the inner mitochondrial membrane.

Administration of XJB-5-131 to a transgenic mouse model of HD resulted in improvement in mitochondrial function, reduced generation of ROS, reduced loss of striatal neurons, and amelioration of behavioral deficits [88].

Another approach to ameliorating oxidative damage is to activate the Nrf2/ARE transcriptional pathway, which leads to increased expression of hemoxygenase 1, NADPH-oxidoreductase, antioxidant enzymes, heat shock proteins, and enzymes which synthesize glutathione. It has been showed that administration of the triterpenoids CDDO-ethylamide and CDDO-trifluoroethylamide reduced oxidative stress, improved motor impairment, reduced striatal atrophy and increased survival in a transgenic mouse model [60].

### **3.3.1 Regulators of mitochondrial dynamics**

The imbalance between mitochondrial fusion/fission events plays a critical role in the pathogenesis of HD. Indeed, excessive fission in HD is a critical player in the striatal vulnerability that characterizes this disease. This phenomenon originates and is enhanced in the striatum due to mHtt expression but also to the intrinsic susceptibility of striatal mitochondria to neuronal insults. Pharmacological approaches that modulate mitochondrial fragmentation in order to prevent striatal degeneration have shown promising results in several HD models. For instance, treatments with the selective inhibitor of Drp1, P110, corrected defects in mitochondrial function and reduced cell death in multiple HD cell models derived from either mice or patients, including patient GABAergic striatal neurons differentiated from patient-induced pluripotent stem cells [89]. Moreover, in HD transgenic mice, P110 corrected mitochondrial fragmentation, cristae disruption and respiratory inactivity that were associated with reduced motor deficits, neuropathology,

and mortality. Another study reported the beneficial effects of Mdivi1, a cell-permeable selective mitochondrial fission inhibitor that arrests GTPase Drp1 activity by blocking the self-assembly of Drp1, resulting in a reversible formation of elongated and tubular mitochondria. Mdivi1-treated HD striatal cells showed restored mitochondrial dynamics and function through down-regulation of fission genes and increased expression of fusion and synaptic genes [90]. Other pharmacological strategies addressed to prevent mitochondrial dysfunction, such as mitochondrial calcium mishandling and defective motility, have shown neuroprotective effects [91] [60].

In sum, all these studies suggest that retrieval of mitochondrial integrity is a critical step in reducing the vulnerability of striatal MSNs in HD.

### **3.3.2 PGC-1 $\alpha$ as a therapeutic target in HD**

PGC-1 $\alpha$  is now increasingly being recognized as an important therapeutic target for HD. As discussed above, there is plethora of evidence for impaired PGC-1 $\alpha$  expression and/or function in HD, therefore pharmacologic/transcriptional activation of PGC-1 $\alpha$  pathway is expected to have neuroprotective effects. Indeed, overexpression of PGC-1 $\alpha$  was shown to enhance the mitochondrial membrane potential and to reduce mitochondrial toxicity in *in vitro* models of HD [54]. Lentiviral delivery of PGC-1 $\alpha$  to the striatum of R6/2 HD mice completely prevented striatal atrophy at the site of PGC-1 $\alpha$  injection [53]. Another potential approach to activate the PGC-1 $\alpha$  pathway, and thereby improve mitochondrial function, is via activation of peroxisome proliferator-activated receptors (PPARs). The PPARs are a subfamily of nuclear receptors, which are ligand-modulated transcription factors that regulate gene-expression programs of metabolic pathways. PPAR agonists increase oxidative phosphorylation capacity in mouse and human cells, and enhance mitochondrial biogenesis. Administration of a PPAR $\gamma$

agonist, thiazolidinedione, was shown to produce beneficial effects on weight loss, mutant huntingtin aggregates and global ubiquitination profiles in R6/2 mice [92]. Earlier, it was shown in STHdh<sup>Q111</sup> cells, that PPAR $\gamma$  activation by rosiglitazone prevents the mitochondrial dysfunction and oxidative stress that occurs when mutant striatal cells are challenged with pathological increases in calcium [93]. Recently, it was shown that bezafibrate, which is a pan-PPAR agonist, improved expression of PGC-1 $\alpha$  and downstream target genes, improved behavioral deficits, survival, and striatal atrophy and reduced oxidative damage, in the R6/2 transgenic mouse model of HD [69].

Another potential mechanism by which PGC-1 $\alpha$  confers neuroprotection is by its antioxidant activity. It is well known that PGC-1 $\alpha$  plays an important role in the suppression of oxidative stress, and it induces mitochondrial uncoupling proteins and antioxidant enzymes, including SOD1, SOD2 (MnSOD), and Gpx-1 [67]. The mitochondrial antioxidant enzymes form the first line of defense against mitochondrial ROS, including SOD2, the enzyme that scavenges superoxide anion to produce H<sub>2</sub>O<sub>2</sub>, and peroxiredoxin III (Prx3), V (Prx5), mitochondrial thioredoxin (Trx2), and mitochondrial thioredoxin reductase (TrxR2). PGC-1 $\alpha$  was found to be directly associated with the regulatory promoter sequences of SOD2, UCP-2 and Prx5. Importantly, UCP-2 has already been proposed to be a direct target of PGC-1 $\alpha$  transcriptional regulation [94]. GC-1 $\alpha$  controls expression of SIRT3 in mitochondria, which in turn activates SOD2 by deacetylating it and reduces ROS [95].

Therefore, therapeutic approaches targeting PGC-1 $\alpha$  may be beneficial both in improving mitochondrial function and biogenesis as well as in restoring the expression of antioxidant enzymes and ameliorating oxidative damage in HD.

Recently Tsunemi et al. showed that increased PGC-1 $\alpha$  function could ameliorate neuronal loss and some of the neurological symptoms of HD, by crossing mice inducibly overexpressing PGC-1 $\alpha$  with a transgenic mouse model of HD. The authors found that PGC-1 $\alpha$  overexpression virtually

eradicates aggregates of mutant huntingtin protein in the brains of the HD mice [96]. They further showed that PGC-1 $\alpha$ 's ability to induce clearance of mutant huntingtin protein aggregates stems from its capacity to switch on the expression of TFEB, a master regulatory transcription factor that activates genes in the autophagy-lysosome pathway of protein turnover [97]. These findings highlight the important role of PGC-1 $\alpha$  in maintaining mitochondrial quality control, in accelerating mitochondrial biogenesis and increasing ATP generation.

A number of other approaches to modulating PGC-1 $\alpha$  and ameliorating mitochondrial dysfunction also have great promise. Activation of SIRT1 results in deacetylation of PGC-1 $\alpha$  which increases its activity. Increased SIRT1 is neuroprotective in transgenic mouse models of HD, while a deficiency exacerbates the phenotype and reduces survival of HD transgenic mice [98] [99].

Another approach to activating sirtuins is to increase NAD<sup>+</sup> levels which can be achieved with administration of nicotinamide precursors, such as nicotinamide riboside [100]. This has the advantage of activating both SIRT1 and SIRT3, leading to increased PGC-1 $\alpha$ , as well as induction of antioxidant enzymes, and SIRT3 mediated increases in SOD2 and mitochondrial reduced glutathione.

## 4. Mildronate: a possible candidate for HD treatment

Assuming that mitochondrial dysfunctions, including a wide range of additional metabolic abnormalities, have a leading role in the HD pathogenesis, a drug able to correct such mitochondrial abnormalities may be taken into account.

### 4.1 Mildronate: a mitochondrial modulator

Mildronate (meldonium; 3-(2,2,2-trimethylhydrazinium) propionate; THP; MET-88) is an antiischemic drug developed at the Latvian Institute of Organic Synthesis (OSI) and clinically used in several countries [101]. It is a small molecule with positively charged nitrogen and negatively charged oxygen, capable to interact and form a cyclic conformation (figure 4).

It belongs to the aza-butyrobetaine class of compounds.

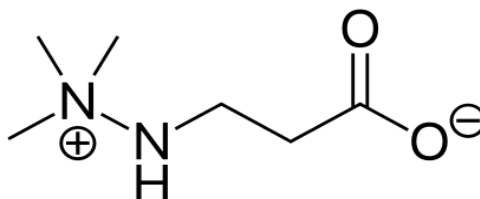


**Figure 4.** Chemical structure of mildronate.

Its mechanism of action includes lowering of l-carnitine availability in body tissues. L-carnitine is needful for the carnitine palmitoyltransferase-1 (CPT1)-dependent transport of long-chain fatty acids (FA) to the mitochondria for  $\beta$ -oxidation. Therefore, mildronate-induced decreased l-carnitine availability lead to a reduction of the of long-chain FA translocation into mitochondria,

resulting in decreased fatty acid  $\beta$ -oxidation. This involves a lesser accumulation of cytotoxic intermediate and decreased free radicals production, both correlated to FA  $\beta$ -oxidation [102].

Additionally mildronate treatment induces a PPAR- $\alpha$ /PGC1- $\alpha$  signaling pathway activation [103]. The enhancement in the nuclear content of PPAR- $\alpha$ /PGC1- $\alpha$  lead to an increased activation of the peroxisomes proliferation and the subsequent stimulation of peroxisomal FA oxidation [104].

Then the mildronate-induced decrease in l-carnitine availability protects mitochondria against an FA metabolite overload by reducing translocation of long-chain fatty acids (FA) to the mitochondria and redirecting FA metabolism from mitochondria to peroxisomes.

The decreased l-carnitine content resulting from mildronate treatment also affects glucose metabolism regulation, inducing increases in gene and protein expression related to glucose metabolism [105] [106]. Several studies suggest that the availability of acylcarnitines determines the interplay between FA and glucose metabolism.

The way through which hypothetically mildronate induces changes in glucose metabolism is by acting in the Randle cycle, as a compensatory mechanism of decreased CPT1-dependent FA oxidation in mitochondria [107].

Moreover the upregulation of pyruvate decarboxylase (PDC) genes expression found in mildronate-treated animal hearts, together with the lowering in lactate concentrations in ischemic hearts, indicate that mildronate treatment might also stimulate aerobic oxidation of glucose [108].

Thus, a lowering in l-carnitine availability induced by mildronate involves not only FA metabolism modulation but also glucose utilization stimulation, resulting in an optimised balance between glucose and FA oxidation.

## **4.2 Mildronate as neuroprotective drug**

In addition to the cardioprotective field, ongoing studies suggest mildronate also acts as a neuroprotective agent, providing evidences for its delivery into the brain.

It is already used in neurological clinics for the treatment of brain circulation disorders and recent data also show its protective action against azidothymidine-induced degenerative and inflammatory changes in mouse brain tissue [101] [109]. In addition, several evidences show that mildronate may stimulate learning and memory by acting on the expression of hippocampal proteins which are involved in synaptic plasticity. This mechanism probably involves also the ability of mildronate to regulate the expression of neuro-glial proteins attributed to neuroinflammation and apoptosis. All these evidences support that mildronate can deserve attention as neuroprotective drug [110].



**Aim**



## 5. Aim

Because of its devastating disease burden and lack of valid treatment, development of more effective therapeutics for Huntington's disease is urgently required. The most pressing unmet need in Huntington disease is for a therapeutic that shows evidence of disease modification — slowing, preventing or even reversing the disease in mutation carriers. Despite a multitude of therapeutic targets, few are well-validated and therapeutic successes of new treatments (i.e., gene therapy) in model systems have failed to translate to patients, partly because of the difficulty of applying these treatments in living humans. Indeed, delivery is a challenge: the most part of the agents proposed require direct administration to the central nervous system — intrathecally into the lumbar cerebrospinal fluid for antisense oligonucleotides and intraparenchymally or intraventricularly, encoded by a viral vector or infused under pressure, for RNA interference.

One mystery is the extent to which the treatment of the mitochondrial dysfunction characterizing Huntington disease, by agents acting directly or indirectly on mitochondrial dynamics and/or function, might be capable of modifying the course of the disease as some experimental studies have suggested. Here, we examined the effects of neo-synthesized derivatives of meldonium on mutant Htt accumulation and toxicity in cellular and animal models of HD.

Mildronate (meldonium; 3-(2,2,2-trimethylhydrazinium)propionate; THP; MET-88) is a neuro- and cardio-protective drug, which mechanism of action is based on the regulation of energy metabolism pathways through l-carnitine lowering effect.

Since l-carnitine is involved in the metabolism of fatty acids, the decline in its levels stimulates glucose metabolism and induces a compensatory activation of the PGC1- $\alpha$  signaling pathway.

We have designed, synthesized, and characterized 22 compounds; some of these display superior huntingtin aggregate inhibition relative to the commercially available mildronate. To identify the potential neuroprotective role of these molecules, the mildronate structurally related compounds were screened in a *Drosophila melanogaster* and *Caenorhabditis elegans* Huntington's disease model; all selected compounds showed a protective effect.

Taken together, our findings show that these new mildronate structurally related compounds are protective for HD transgenic animals and suggest that they could be novel drug candidates for treating Huntington's disease.

# **Materials and Methods**



## 6. Materials and methods

### 6.1 Design and synthesis of mildronate structurally related compounds

All reactions were performed using commercially available compounds without further purification. All used reagents were analytical grade and were purchased from Sigma-Aldrich (Milan-Italy). Column chromatographic purification of products was carried out using silica gel 60 (70–230 mesh, Merck). The NMR spectra were recorded on Bruker DRX 400, 300, 250 spectrometers (400 MHz, 300 MHz, 250 MHz,  $^1\text{H}$ ; 100 MHz, 75 MHz, 62.5 MHz  $^{13}\text{C}$ ). Spectra were referenced to residual  $\text{CHCl}_3$  (7.26 ppm,  $^1\text{H}$ , 77.23 ppm,  $^{13}\text{C}$ ). Coupling constants  $J$  are reported in Hz. Yields are given for isolated products showing one spot on a TLC plate and no impurities detectable in the NMR spectrum. Mass spectral analyses were carried out using an electrospray spectrometer Waters 4 micro quadrupole.

#### 4-(dimethylamino) butanoic acid hydrochloride **2**

A mixture of  $\gamma$ -amino butyric acid **1** (1g, 9.71 mmol), 1.94 mL of formaldehyde (59 mmol, 6 equivalent) and 2.52 mL of formic acid (67 mmol, 8.9 equivalents) was refluxed at 60°C for 16 hours. After cooling the solution, 1.2 mL of concentrated hydrochloric acid was added and the water removed under reduced pressure. Crystallization with acetonitrile gave a white solid. Yield: 71%. m.p. 97-98°C (acetonitrile). MS (ESI)  $m/z$ : 132.2 ( $\text{M}+\text{H}$ ) $^+$   $^1\text{H}$  NMR ( $\text{D}_2\text{O}$ , 300 MHz)  $\delta$ : 3.05-2.99 (m, 2H), 2.73 (s, 6H), 2.34 (t, 2H,  $J=7.2$ ), 1.90-1.79 (m, 2H).  $^{13}\text{C}$  NMR ( $\text{D}_2\text{O}$ , 75 MHz)  $\delta$ : 177.3, 58.5, 45.9, 33.8, 23.2.

### 6.1.1 General procedure for the synthesis of amides 3a-v

To a solution of **2** (50 mg, 0.31 mmol) in dichloromethane or tetrahydrofuran (1 mL) under magnetic stirring, dicyclohexylcarbodiimide (0.31 mmol), 1-hydroxybenzotriazole (0.31 mmol), triethylamine (0.45 mmol) and amine (0.25 mmol). The reaction was allowed to stir overnight at room temperature. The residue rinsed up with dichloromethane was extracted with 1N HCl: the acidic phase was basified with NaOH 1N, and extracted for three times with dichloromethane.

#### 4-(dimethylamino)-*N*-propylbutanamide **3a**

Waxy solid. Yield:75%. MS (ESI)  $m/z$ : 172.16(M+H)<sup>+</sup>. <sup>1</sup>H NMR (CDCl<sub>3</sub>, 400 MHz)  $\delta$ : 6.52 (bs, 1H), 3.17 (q, 2H,  $J$ = 6.6 Hz), 2.30-2.23 (m, 2H), 2.20 (m+s, 8H), 1.76 (t, 2H,  $J$ = 6.8 Hz), 1.49 (q, 2H,  $J$ = 7.2 Hz), 0.90 (t, 3H,  $J$ = 7.3 Hz). <sup>13</sup>C NMR(CDCl<sub>3</sub>, 100 MHz)  $\delta$ : 172.7, 58.1, 45.9, 42.6, 34.2, 24.1, 23.2, 11.2.

#### 4-(dimethylamino)-*N*-butylbutanamide **3b**

Waxy solid. Yield: 74%. MS (ESI)  $m/z$ : 186.17(M+H)<sup>+</sup>. <sup>1</sup>H NMR (CDCl<sub>3</sub>, 300 MHz)  $\delta$ : 6.50 (bs, 1H), 3.21 (q, 2H,  $J$ = 7.0 Hz), 2.47 (t, 2H,  $J$ = 6.8 Hz), 2.34 (s, 6H), 2.26 (t, 2H,  $J$ = 7.0 Hz), 1.86-1.81 (m, 2H), 1.48-1.43 (m, 4H), 0.90 (t, 3H,  $J$ = 7.2 Hz). <sup>13</sup>C NMR(CDCl<sub>3</sub>, 75 MHz)  $\delta$ : 172.7, 58.1, 45.9, 40.1, 34.2, 32.3, 24.1, 19.9, 13.8.

#### 4-(dimethylamino)-*N*-(prop-2-ynyl)butanamide **3c**

Waxy solid. Yield:72%. MS (ESI)  $m/z$ : 168.13(M+H)<sup>+</sup>. <sup>1</sup>H NMR (CDCl<sub>3</sub>, 300 MHz)  $\delta$ :7.67 (bs, 1H), 4.01-3.99 (m, 2H), 2.32 (q, 4H,  $J$ = 7.0 Hz), 2.21 (s, 6H+1H), 1.61 (q, 2H,  $J$ = 6.5 Hz). <sup>13</sup>C NMR(CDCl<sub>3</sub>, 75 MHz)  $\delta$ : 173.0, 78.1, 70.9, 58.1, 45.9, 33.3, 30.0, 24.1.

#### **4-(dimethylamino)-N-(3-methoxypropyl)butanamide 3d**

Waxy solid. Yield:74%. MS (ESI)  $m/z$ : 202.17(M+H)<sup>+</sup>. <sup>1</sup>H NMR (CDCl<sub>3</sub>, 400 MHz)  $\delta$ : 6.64 (bs, 1H), 3.42 (t, 2H,  $J$ = 5.4 Hz), 3.22 (s, 3H), 2.41 (t, 2H,  $J$ = 6.6 Hz), 2.18 (s, 10H), 1.78-1.73 (m, 4H). <sup>13</sup>C NMR (CDCl<sub>3</sub>, 100 MHz)  $\delta$ : 172.7, 71.7, 59.3, 58.1, 45.9, 36.7, 29.6, 24.1.

#### **4-(dimethylamino)-N-hexadecylbutanamide 3e**

Waxy solid. Yield:31%. MS (ESI)  $m/z$ : 354.5 (M+H)<sup>+</sup>. <sup>1</sup>H NMR (CDCl<sub>3</sub>, 400 MHz)  $\delta$ :6.44 (bs, 1H), 3.20 (t, 2H,  $J$ = 6.22 Hz), 2.29 (t, 2H,  $J$ =6.6 Hz), 2.23 (m+s, 8H), 1.77 (t, 2H,  $J$ = 6.8 Hz), 1.46 (s, 2H), 1.25 (s, 26H), 0.86 (d, 3H,  $J$ = 7.0 Hz). <sup>13</sup>C NMR (CDCl<sub>3</sub>, 100 MHz)  $\delta$ : 172.7, 58.1, 45.9, 40.4, 34.2, 31.9, 30.1, 29.7, 29.4, 26.8, 24.1, 22.8, 14.1.

#### **N-cyclohexyl-4-(dimethylamino)butanamide 3f**

Waxy solid. Yield:32%. MS (ESI)  $m/z$ : 212.3(M+H)<sup>+</sup>. <sup>1</sup>H NMR (CDCl<sub>3</sub>, 300 MHz)  $\delta$ :6.49 (bs, 1H), 3.72 (d, 1H,  $J$ = 4.0 Hz), 2.26 (d, 1H,  $J$ = 2.9 Hz), 2.25 (s, 6H), 1.89-1.58 (m, 8H), 1.54-1.06 (m, 7H). <sup>13</sup>C NMR (CDCl<sub>3</sub>, 75 MHz)  $\delta$ : 172.4, 58.1, 47.4, 45.9, 33.8, 34.5, 28.0, 24.1, 22.9.

#### **4-(dimethylamino)-1-(piperidin-1-yl)butan-1-one 3g**

Waxy solid. Yield: 81%. MS (ESI)  $m/z$ : 198.2 (M+H)<sup>+</sup>. <sup>1</sup>H NMR (CDCl<sub>3</sub>, 400 MHz)  $\delta$ : 3.68 (t, 2H,  $J$ = 5.4 Hz), 3.62 (t, 2H,  $J$ = 7.3 Hz), 2.43-2.36 (m, 4H), 2.19 (s, 6H), 1.78 (t, 2H,  $J$ = 7.6 Hz), 1.60 (d, 2H,  $J$ = 5.2 Hz), 1.53-1.50 (m, 4H). <sup>13</sup>C NMR (CDCl<sub>3</sub>, 100 MHz)  $\delta$ : 147.7, 58.1, 45.9, 44.8, 32.0, 25.6, 25.4, 24.4.

#### **4-(dimethylamino)-1-morpholinobutan-1-one 3h**

Waxy solid. Yield:76%. MS (ESI)  $m/z$ : 200.2(M+H)<sup>+</sup>. <sup>1</sup>H NMR (CDCl<sub>3</sub>, 300 MHz)  $\delta$ :3.62 (d, 6H,  $J$ =6.0 Hz), 3.46 (t, 2H,  $J$ =4.3 Hz), 2.36-2.26 (m, 4H),

2.18 (d, 6H,  $J=7.9$  Hz), 1.79 (t, 2H,  $J=7.3$  Hz).  $^{13}\text{C}$  NMR ( $\text{CDCl}_3$ , 75 MHz)  $\delta$ : 171.1, 66.3, 58.1, 45.9, 45.6, 32.0, 24.4.

#### **4-(dimethylamino)-1-(pyrrolidin-1-yl)butan-1-one 3i**

Waxy solid. Yield:95%. MS (ESI)  $m/z$ : 184.2(M+H) $^+$ .  $^1\text{H}$  NMR ( $\text{CDCl}_3$ , 300 MHz)  $\delta$ :3.51-3.37 (m, 4H), 2.34 (q, 4H,  $J=7.0$  Hz), 2.22 (s, 6H), 1.99-1.75 (m, 6H).  $^{13}\text{C}$  NMR ( $\text{CDCl}_3$ , 75 MHz)  $\delta$ : 174.7, 58.1, 48.8, 45.9, 32.0, 25.4, 24.4.

#### **4-(dimethylamino)-*N*-fenilbutanammide 3j**

Compound was purified by chromatography on silica gel in a gradient, using as eluent a mixture of  $\text{CHCl}_3/\text{CH}_3\text{OH}$  90:10 to elute the impurities and a mixture of  $\text{CH}_2\text{Cl}_2/\text{CH}_3\text{OH}/\text{Et}_3\text{N}$  90:10:0.2 to elute the compound as an oil .Yield: 35%. MS (ESI)  $m/z$ : 207.3 (M+H) $^+$ .  $^1\text{H}$  NMR ( $\text{CDCl}_3$ , 300 MHz)  $\delta$ : 9.77 (bs, 1H), 7.55 (d, 2H,  $J=7.7$  Hz), 7.31 (t, 2H,  $J=5.8$  Hz), 7.26 (bs, 1H), 2.55-2.53 (m, 4H), 2.37 (s, 6H), 1.93-1.89 (m, 2H).  $^{13}\text{C}$  NMR ( $\text{CDCl}_3$ , 75 MHz)  $\delta$ : 173.0, 138.5, 129.0, 124.4, 121.6, 58.1, 45.9, 33.8, 24.1.

#### **4-(dimethylamino)-*N*-(4-methoxyphenyl)butanamide 3k**

Compound was purified by chromatography on silica gel in a gradient, using as eluent a mixture of  $\text{CHCl}_3/\text{CH}_3\text{OH}$  90:10 to elute the impurities and a mixture of  $\text{CH}_2\text{Cl}_2/\text{CH}_3\text{OH}/\text{Et}_3\text{N}$  90:10:0.5 to elute the compound as an oil. Yield: 75%. MS (ESI)  $m/z$ : 236.3 (M+H) $^+$ .  $^1\text{H}$  NMR ( $\text{CDCl}_3$ , 300 MHz)  $\delta$ : 9.56 (bs, 1H), 7.45 (d, 2H,  $J=8.9$  Hz), 6.82 (d, 2H,  $J=8.9$  Hz), 3.75 (s, 3H), 2.57-2.49 (m, 4H), 2.38 (s, 6H), 1.92-1.87 (m, 2H).  $^{13}\text{C}$  NMR ( $\text{CDCl}_3$ , 75 MHz)  $\delta$ : 173.0, 156.3, 130.8, 122.6, 114.5, 58.1, 55.9, 45.9, 33.8, 24.1.

#### **4-(dimethylamino)-*N*-(3,4-dimethylphenyl)butanamide 3l**

Compound was purified by chromatography on silica gel in a gradient, using as eluent a mixture of CHCl<sub>3</sub>/CH<sub>3</sub>OH 90:10 to elute the impurities and a mixture of CH<sub>2</sub>Cl<sub>2</sub>/CH<sub>3</sub>OH/Et<sub>3</sub>N 90:10:0.5 to elute the compound. Oil. Yield: 67% MS (ESI) *m/z*: 235.3 (M+H)<sup>+</sup>. <sup>1</sup>H NMR (CDCl<sub>3</sub>, 300 MHz) δ: 9.41 (bs, 1H), 7.34 (s, 1H), 7.21 (d, 1H, *J*= 7.8 Hz), 7.03 (d, 1H, *J*= 7.8 Hz), 2.47-2.38 (m, 4H), 2.27 (s, 6H), 2.17 (s, 6H), 1.86-1.83 (m, 2H). <sup>13</sup>C NMR (CDCl<sub>3</sub>, 75 MHz) δ: 173.0, 137.1, 135.4, 132.5, 129.2, 118.5, 58.1, 45.9, 33.8, 24.1, 17.8.

#### **4-(dimethylamino)-N-(4-nitrophenyl)butanamide 3m**

To a solution of 4-nitroaniline (82.9 mg, 0.6 mmol, 2 eq) in pyridine (1 mL), phosphorous trichloride (26.2 μl, 0.3 mmol, 1 equivalent) at room temperature was added and stirring was kept for 1 hour. Then 50 mg of **5** (0.31 mmol) were put into the reaction mixture and temperature brought at 40°C for three hours. Pyridine was removed under vacuum and the residue rinsed with dichloromethane, was extracted with 1N HCl: the acidic phase was basified with NaOH 1N, and extracted for three times with dichloromethane. Product was obtained as an oil. Yield: 72%. MS (ESI)*m/z*: 252.3 (M+H)<sup>+</sup>. <sup>1</sup>H NMR (CDCl<sub>3</sub>, 400 MHz) δ: 8.16 (d, 2H, *J*= 9.0 Hz), 7.66 (d, 2H, *J*= 9.0 Hz), 2.56 (t, 2H, *J*= 6.2 Hz), 2.49 (t, 2H, *J*= 5.7 Hz), 2.34 (s, 6H), 1.86 (t, 2H, *J*= 5.9 Hz). <sup>13</sup>C NMR (CDCl<sub>3</sub>, 100 MHz) δ: 173.0, 144.6, 144.0, 122.5, 121.3, 58.1, 45.9, 33.8, 24.1.

#### **N-benzyl-4-(dimethylamino)butanamide 3n**

Compound was purified by chromatography on silica gel in a gradient, using as eluent a mixture of CHCl<sub>2</sub>/CH<sub>3</sub>OH 90:10 to elute the impurities and a mixture of CH<sub>2</sub>Cl<sub>2</sub>/CH<sub>3</sub>OH/Et<sub>3</sub>N 90:10:0.2 to elute the compound. Waxy solid. Yield: 87%. MS (ESI) *m/z*: 219.2 (M+H)<sup>+</sup>. <sup>1</sup>H NMR (CDCl<sub>3</sub>, 300 MHz) δ: 7.29 (q 5H, *J*= 6.4 Hz), 4.41 (d, 2H, *J*= 5.5 Hz), 2.34-2.17 (m, 4H), 2.08 (s, 6H), 1.18-1.75 (m, 2H). <sup>13</sup>C NMR (CDCl<sub>3</sub>, 75 MHz) δ: 173.0, 141.7, 128.6, 127.0, 126.8, 58.1, 45.9, 44.1, 34.2, 24.1.

***N*-(4-chlorobenzyl)-4-(dimethylamino)butanamide 3o**

Oil. Yield: 42%. MS (ESI)  $m/z$ : 255.8 (M+H)<sup>+</sup>. <sup>1</sup>H NMR (CDCl<sub>3</sub>, 300 MHz)  $\delta$ : 7.34-7.19 (m, 5H), 4.37 (d, 2H,  $J$ = 5.6 Hz), 2.34-2.26 (m, 4H), 2.11 (s, 6H), 1.80-1.76 (m, 2H). <sup>13</sup>C NMR (CDCl<sub>3</sub>, 75 MHz)  $\delta$ : 173.0, 139.8, 132.3, 128.7, 128.4, 58.1, 45.9, 34.2, 24.1.

**4-(dimethylamino)-*N*-(4-methoxybenzyl)butanamide 3p**

Oil. Yield: 49% MS (ESI)  $m/z$ : 251.3 (M+H)<sup>+</sup>. <sup>1</sup>H-NMR (CDCl<sub>3</sub>, 250 MHz)  $\delta$ : 7.19 (d, 2H,  $J$ = 8.6 Hz), 6.84 (d, 2H,  $J$ = 8.6 Hz), 4.32 (d, 2H,  $J$ = 5.4 Hz), 3.78 (s, 3H), 2.29-2.24 (m, 4H), 2.09 (s, 6H), 1.79-1.73 (m, 2H). <sup>13</sup>C NMR (CDCl<sub>3</sub>, 60 MHz)  $\delta$ : 173.0, 158.7, 134.0, 128.0, 114.1, 58.1, 55.9, 45.9, 44.1, 34.2, 24.1.

**4-(dimethylamino)-*N*-(4-nitrobenzyl)butanamide 3q**

Product was purified by chromatography on silica gel in a gradient, using as eluent a mixture of CHCl<sub>3</sub>/CH<sub>3</sub>OH 90:10 to elute the impurities and a mixture of CH<sub>2</sub>Cl<sub>2</sub>/CH<sub>3</sub>OH/Et<sub>3</sub>N 90:10:0.2 to elute the compound as an oil. Yield: 43%. MS (ESI)  $m/z$ : 266.1 (M+H)<sup>+</sup>. <sup>1</sup>H NMR (CDCl<sub>3</sub>, 300 MHz)  $\delta$ : 8.15 (d, 2H,  $J$ = 8.5 Hz), 7.77 (bs, 1H), 7.43 (d, 2H,  $J$ = 8.4 Hz), 4.49 (d, 2H,  $J$ = 5.8 Hz), 2.41-2.36 (m, 4H), 2.21 (s, 6H), 1.86-1.81 (m, 2H). <sup>13</sup>C NMR (CDCl<sub>3</sub>, 75 MHz)  $\delta$ : 173.0, 147.8, 146.4, 127.9, 120.9, 58.1, 45.9, 44.1, 34.2, 24.1.

**(*RS*)-4-(dimethylamino)-*N*-(1-phenylethyl)butanamide 3r**

Product was purified by chromatography on silica gel in a gradient, using as eluent a mixture of CHCl<sub>3</sub>/CH<sub>3</sub>OH 90:10 to elute the impurities and a mixture of CH<sub>2</sub>Cl<sub>2</sub>/CH<sub>3</sub>OH/Et<sub>3</sub>N 90:10:0.5 to elute the compound. Waxy solid. Yield: 30%. MS (ESI)  $m/z$ : 236.3 (M+H)<sup>+</sup>. <sup>1</sup>H NMR (CDCl<sub>3</sub>, 300 MHz)  $\delta$ : 7.43 (bs, 1H), 7.33-7.22 (m, 5H), 5.09-5.04 (m, 1H), 2.67 (t, 2H,  $J$ = 6.7 Hz), 2.49 (s,

6H), 2.37-2.34 (m, 2H), 1.95 (t, 2H,  $J = 6.8$  Hz), 1.47 (d, 3H,  $J = 6.5$  Hz).  $^{13}\text{C}$  NMR ( $\text{CDCl}_3$ , 75 MHz)  $\delta$ : 172.7, 143.5, 128.6, 127.0, 126.8, 58.1, 49.5, 45.9, 34.5, 24.1.

#### ***N*-(3,5-dimethoxybenzyl)-4-(dimethylamino)butanamide 3s**

Product was purified by chromatography on silica gel in a gradient, using as eluent a mixture of  $\text{CHCl}_3/\text{CH}_3\text{OH}$  90:10 to elute the impurities and a mixture of  $\text{CH}_2\text{Cl}_2/\text{CH}_3\text{OH}/\text{Et}_3\text{N}$  90:10:0.5 to elute the compound as an oil. Yield: 81%. MS (ESI)  $m/z$ : 281.2 ( $\text{M}+\text{H}$ ) $^+$ .  $^1\text{H}$  NMR ( $\text{CDCl}_3$ , 300 MHz)  $\delta$ : 7.21 (bs, 1H), 6.46 (s, 2H), 6.36 (s, 1H), 4.37 (d, 2H,  $J = 5.6$  Hz), 3.80 (s, 6H), 2.59 (t, 2H,  $J = 6.7$  Hz), 2.47-2.43 (m, 2H), 2.40 (s, 6H), 1.98-1.96 (m, 2H).  $^{13}\text{C}$  NMR ( $\text{CDCl}_3$ , 75 MHz)  $\delta$ : 173.0, 161.5, 143.7, 103.3, 98.4, 58.1, 55.9, 45.9, 44.7, 34.2, 24.1.

#### **4-(dimethylamino)-*N*-(4-methoxyphenylethyl)butanamide 3t**

Waxy solid. Yield: 92%. MS (ESI)  $m/z$ : 265.4 ( $\text{M}+\text{H}$ ) $^+$ .  $^1\text{H}$  NMR ( $\text{CDCl}_3$ , 250 MHz)  $\delta$ : 7.09 (d, 2H,  $J = 7.9$  Hz), 6.82 (d, 2H,  $J = 7.9$  Hz), 6.42 (bs, 1H), 3.77 (s, 3H), 3.48-3.43 (m, 2H), 2.73 (t, 2H,  $J = 7.0$  Hz), 2.23-2.17 (m, 4H), 2.13 (s, 6H), 1.75-1.69 (m, 2H).  $^{13}\text{C}$  NMR ( $\text{CDCl}_3$ , 60 MHz)  $\delta$ : 172.7, 157.9, 131.8, 128.8, 114.2, 58.1, 55.9, 45.9, 40.7, 35.7, 34.2, 24.1.

#### **4-(dimethylamino)-*N*-(4-nitrofenilet)butanamide 3u**

Product was purified by chromatography on silica gel in a gradient, using as eluent a mixture of  $\text{CHCl}_3/\text{CH}_3\text{OH}$  90:10 to elute the impurities and a mixture of  $\text{CH}_2\text{Cl}_2/\text{CH}_3\text{OH}/\text{Et}_3\text{N}$  90:10:0.2 to elute the compound as an oil. Yield: 46%. MS (ESI)  $m/z$ : 280.3 ( $\text{M}+\text{H}$ ) $^+$ .  $^1\text{H}$  NMR ( $\text{CDCl}_3$ , 300 MHz)  $\delta$ : 8.16 (d, 2H,  $J = 8.5$  Hz), 7.37 (d, 2H,  $J = 8.3$  Hz), 3.51 (t, 2H,  $J = 6.7$  Hz), 3.00-2.91 (m, 2H), 2.56 (t, 1H,  $J = 7.2$  Hz), 2.26-2.18 (m, 4H), 2.15 (s, 6H), 1.74 (t, 1H,  $J = 6.9$

Hz).  $^{13}\text{C}$  NMR ( $\text{CDCl}_3$ , 75 MHz)  $\delta$ : 172.7, 145.6, 128.7, 121.0, 58.1, 45.9, 40.7, 35.7, 34.2, 24.1.

**4-(dimethylamino)-*N*-(3-phenylpropyl)butanamide 3v**

Product was purified by chromatography on silica gel in a gradient, using as eluent a mixture of  $\text{CHCl}_3/\text{CH}_3\text{OH}$  90:10 to elute the impurities and a mixture of  $\text{CH}_2\text{Cl}_2/\text{CH}_3\text{OH}/\text{Et}_3\text{N}$  90:10:0.2 to elute the compound as an oil. Yield: 49%. MS (ESI) $m/z$ : 247.2 ( $\text{M}+\text{H}$ ) $^+$ .  $^1\text{H}$  NMR ( $\text{CDCl}_3$ , 300 MHz)  $\delta$ : 7.18 (q, 5H,  $J=6.4$  Hz), 6.95 (bs, 1H), 9.62 (t, 2H,  $J=5.9$  Hz), 2.60 (t, 2H,  $J=7.6$  Hz), 2.28 (t, 2H,  $J=6.8$  Hz), 2.17 (t, 8H,  $J=7.4$  Hz), 1.81-1.72 (m, 4H).  $^{13}\text{C}$  NMR ( $\text{CDCl}_3$ , 75 MHz)  $\delta$ : 172.7, 138.1, 128.9, 128.2, 126.1, 58.1, 45.9, 40.0, 34.2, 33.1, 29.1, 24.1.

### 6.1.2 General procedure for the synthesis of ammonium salts 4a-v

A solution of compounds **3a-z** (1 equiv.) in acetone (1 ml) was reacted with 2 equivalents of iodomethane and left overnight. Crystallization with diethyl ether afforded the desired products in good yields.

#### **4-(propylamino)-*N,N,N*-trimethyl-4-oxobutan-1-aminium iodide 4a**

White solid. Yield: 79%. m.p.:129-130 °C. MS (ESI)  $m/z$ : 187.2 (M+H)<sup>+</sup>. <sup>1</sup>H NMR (CDCl<sub>3</sub>, 300 MHz)  $\delta$ :6.61 (bs, 1H), 3.70-3.68 (m, 2H), 3.32 (s, 9H), 2.54 (t, 2H,  $J$ = 7.05 Hz), 2.22 (t, 2H,  $J$ = 7.2 Hz), 1.72 (s, 4H), 0.94 (t, 3H,  $J$ = 7.3 Hz). <sup>13</sup>C NMR (CDCl<sub>3</sub>, 75 MHz)  $\delta$ : 172.7, 66.0, 54.7, 42.6, 35.0, 23.2, 22.8, 11.2.

#### **4-(butylamino)-*N,N,N*-trimethyl-4-oxobutan-1-aminium iodide 4b**

Yellow powder. Yield:37%.m.p.:119-120°C. MS (ESI)  $m/z$ : 201.2 (M+H)<sup>+</sup>. <sup>1</sup>H NMR (CDCl<sub>3</sub>, 300 MHz)  $\delta$ :6.58 (bs, 1H), 3.33 (s, 9H), 3.20 (q, 2H,  $J$ = 6.9 Hz), 2.71 (s, 2H), 2.32 (t, 2H,  $J$ = 6.6 Hz), 1.77 (t, 2H,  $J$ = 6.8 Hz), 1.44 (t, 2H,  $J$ = 7.1 Hz), 1.33 (t, 2H,  $J$ = 7.6 Hz), 0.89 (t, 3H,  $J$ = 7.2 Hz). <sup>13</sup>C NMR (CDCl<sub>3</sub>, 75 MHz)  $\delta$ : 172.7, 66.0, 54.7, 40.1, 35.0, 32.3, 22.8, 19.9, 13.8.

#### **4-(prop-2-ynylamino)-*N,N,N*-trimethyl-4-oxobutan-1-aminium iodide 4c**

Pale yellow powder. Yield: 36%. m.p.:145°C (dec.). MS (ESI)  $m/z$ : 183.15 (M+H)<sup>+</sup>. <sup>1</sup>H NMR (CDCl<sub>3</sub>, 300 MHz)  $\delta$ :7.62 (bs, 1H), 4.01-3.98 (m, 2H), 3.31 (s, 9H), 2.32 (q, 4H,  $J$ = 7.0 Hz), 2.21 (m,1H), 1.61 (q, 2H,  $J$ = 6.5 Hz). <sup>13</sup>C NMR (CDCl<sub>3</sub>, 300 MHz)  $\delta$ : 173.0, 78.1, 70.9, 66.0, 54.7, 34.1, 30.0, 22.8.

#### **4-(methoxypropylamino)-*N,N,N*-trimethyl-4-oxobutan-1-aminium iodide 4d**

White powder. Yield: 78%. m.p.:137-138°C. MS (ESI)  $m/z$ : 217.3 (M+H)<sup>+</sup>. <sup>1</sup>H NMR (CDCl<sub>3</sub>, 300 MHz)  $\delta$ :6.69 (bs, 1H), 3.83-3.46 (m, 2H), 3.47 (t, 2H,  $J$ =

5.8 Hz), 3.33 (s, 3H), 3.38-3.35 (m+s, 11H), 2.44 (d, 2H,  $J=6.6$  Hz), 2.17-2.14 (m, 2H), 1.79 (t, 2H,  $J=6.1$  Hz)..  $^{13}\text{C}$  NMR ( $\text{CDCl}_3$ , 75 MHz)  $\delta$ : 172.7, 71.7, 66.0, 59.3, 54.7, 36.7, 35.0, 29.6, 22.8.

**4-(hexadecylamino)-*N,N,N*-trimethyl-4-oxobutan-1-aminium iodide 4e**

Tan powder. Yield: 71%. M.p. 139-140°C. MS (ESI)  $m/z$ : 369.4 (M+H)<sup>+</sup>.  $^1\text{H}$  NMR ( $\text{CDCl}_3$ , 300 MHz)  $\delta$ : 6.23 (bs, 1H), 3.65-3.63 (m, 2H), 3.27 (s, 9H), 2.53-2.52 (m, 2H), 2.22-2.20 (m, 2H), 1.51 (d, 10H,  $J=8.5$  Hz), 1.27 (d, 20H,  $J=7.5$  Hz), 0.92 (t, 3H,  $J=9.4$  Hz).  $^{13}\text{C}$  NMR ( $\text{CDCl}_3$ , 75 MHz)  $\delta$ : 172.7, 66.0, 54.7, 40.4, 35.0, 31.9, 30.1, 29.7, 26.8, 22.8, 14.1.

**4-(cyclohexylamino)-*N,N,N*-trimethyl-4-oxobutan-1-aminium iodide 4f**

Tan powder. Yield: 68%. m.p.:124-125°C. MS (ESI)  $m/z$ : 227.2(M+H)<sup>+</sup>.  $^1\text{H}$  NMR ( $\text{CDCl}_3$ , 300 MHz)  $\delta$ : 6.64 (d, 1H,  $J=7.9$  Hz), 3.75-3.66 (m, 2H), 3.39 (s, 9H), 2.43 (t, 2H,  $J=6.8$  Hz), 2.12 (t, 2H,  $J=8.0$  Hz), 1.86-1.56 (m, 5H), 1.32-1.19 (m, 6H).  $^{13}\text{C}$  NMR( $\text{CDCl}_3$ , 75 MHz)  $\delta$ : 172.4, 66.0, 54.7, 47.4, 35.3, 33.8, 28.0, 22.9, 22.8.

**4-(trimethylammonio)-1-(piperidin-1-yl)butan-1-one iodide 4g**

Pale yellow powder. Yield: 84%. m.p.:132-134°C. MS (ESI)  $m/z$ : 213.2(M+H)<sup>+</sup>.  $^1\text{H}$  NMR ( $\text{CDCl}_3$ , 300 MHz)  $\delta$ : 3.80-3.74 (m, 2H), 3.52-3.51 (m, 2H), 3.39 (s, 9H), 2.54 (t, 2H,  $J=6.1$  Hz), 2.16-2.08 (m, 2H), 1.65-1.53 (m, 8H).  $^{13}\text{C}$  NMR ( $\text{CDCl}_3$ , 75 MHz)  $\delta$ : 174.7, 66.0, 54.7, 44.8, 32.8, 25.6, 25.4, 23.1

**4-(trimethylammonio)-1-(morpholine-1-yl)butan-1-one iodide 4h**

White powder. Yield: 48%. m.p.:190-191°C. MS (ESI)  $m/z$ : 215.3(M+H)<sup>+</sup>.  $^1\text{H}$  NMR ( $\text{CDCl}_3$ , 300 MHz)  $\delta$ : 3.81-3.79 (m, 2H), 3.68 (t, 4H,  $J=4.8$  Hz), 3.57 (d, 2H,  $J=4.4$  Hz), 3.48-3.42 (m+s, 11H), 2.57 (t, 2H,  $J=6.2$  Hz), 2.18-2.08

(m, 2H).  $^{13}\text{C}$  NMR( $\text{CDCl}_3$ , 75 MHz)  $\delta$ :171.1, 66.3, 66.0, 54.7, 45.6, 32.8, 23.1.

**4-(trimethylammonio)-1-(pyrrolidin-1-yl)butan-1-one iodide 4i**

White powder. Yield: 95%. m.p.167-168°C. MS (ESI)  $m/z$ : 199.3(M+H) $^+$ .  $^1\text{H}$  NMR ( $\text{CDCl}_3$ , 300 MHz)  $\delta$ : 3.94-3.88 (m, 2H), 3.43-3.38 (m+s, 13H), 2.5 (t, 2H,  $J= 5.8$  Hz), 2.15-2.12 (m, 2H), 1.97-1.87 (m, 4H).  $^{13}\text{C}$  NMR ( $\text{CDCl}_3$ , 75 MHz)  $\delta$ : 174.7, 66.0, 54.7, 48.8, 32.8, 25.4, 23.1.

***N,N,N*-trimethyl-4-oxo-4-(phenylamine)butan-1- aminium iodide 4j**

Pale oil.Yield: 69%. MS (ESI)  $m/z$ : 222.3 (M+H) $^+$ .  $^1\text{H}$  NMR ( $\text{CD}_3\text{OD}$ , 300 MHz)  $\delta$ : 7.57 (d, 2H,  $J= 8.0$  Hz), 7.30 (t, 2H,  $J= 7.9$  Hz), 7.09 (s, 1H), 3.48-3.43 (m, 2H), 3.18 (s, 9H), 2.55 (t, 2H,  $J= 6.9$  Hz), 2.15 (t, 2H,  $J= 8.1$  Hz).  $^{13}\text{C}$  NMR ( $\text{CD}_3\text{OD}$ , 75 MHz)  $\delta$ : 173.0, 138.5, 129.0, 124.4, 121.6, 66.0, 54.7, 34.6, 22.8.

**4-[(4-methoxyphenyl)amino-*N,N,N*-trimethyl-4-oxobutan-1-aminium iodide 4k**

White powder. Yield: 83%. m.p: 189-190°C. MS (ESI)  $m/z$ : 252.2 (M+H) $^+$ .  $^1\text{H}$  NMR ( $\text{CDCl}_3$ , 300 MHz)  $\delta$ : 7.44 (d, 2H,  $J= 8.8$  Hz), 6.80 (d, 2H,  $J= 8.9$  Hz), 3.19 (s, 3H), 3.61-3.55 (m, 2H), 3.15 (d, 9H,  $J= 7.1$  Hz), 2.54 (t, 2H,  $J= 6.8$  Hz), 2.09 (t, 2H,  $J= 8.4$  Hz).  $^{13}\text{C}$  NMR ( $\text{CDCl}_3$ , 75 MHz)  $\delta$ : 173.0, 156.3, 130.8, 122.6, 114.5, 66.0, 55.9, 54.7, 34.6, 22.8.

**4-[(3,4-dimethylphenyl)amino]-*N,N,N*-trimethyl-4-oxobutan-1-aminium iodide 4l**

Yellow waxy gel. Yield: 82% MS (ESI) $m/z$ : 250.4 (M+H) $^+$ . $^1\text{H}$  NMR ( $\text{CDCl}_3$ , 300 MHz)  $\delta$ : 7.37 (d, 2H,  $J= 7.8$  Hz), 7.02 (d, 1H,  $J= 8.4$  Hz), 3.77-3.74 (m, 2H), 3.31 (s, 9H), 2.69 (t, 2H,  $J= 6.8$  Hz), 2.19 (d, 6H,  $J= 3.3$  Hz), 1.71 (s,

2H).  $^{13}\text{C}$  NMR ( $\text{CDCl}_3$ , 75 MHz)  $\delta$ : 173.0, 137.1, 135.4, 132.5, 129.2, 121.2, 117.5, 66.0, 54.7, 34.6, 22.8, 17.8.

**4-[(4-nitrophenyl)amino]-*N,N,N*-trimethyl-4-oxobutan-1-aminium iodide 4m**

White solid. Yield: 72%. m.p.: 244-245°C (dec.). MS (ESI)  $m/z$ : 265.2 (M+H) $^+$ .  $^1\text{H}$  NMR ( $\text{CDCl}_3$ , 300 MHz)  $\delta$ : 8.14 (d, 2H,  $J=7.0$  Hz), 7.77 (d, 2H,  $J=6.9$  Hz), 3.53-3.51 (m, 2H), 3.30 (s, 3H), 3.16 (s, 6H), 2.61 (m, 2H), 2.12 (m, 2H).  $^{13}\text{C}$  NMR ( $\text{CDCl}_3$ , 75 MHz)  $\delta$ : 173.0, 144.6, 122.5, 121.3, 66.0, 54.7, 34.6, 22.8.

***N,N,N*-trimethyl-4-oxo-4-(benzylamino)butan-1-aminium iodide 4n**

White solid. Yield: 98%. m.p.: 187-188°C (dec.). MS (ESI)  $m/z$ : 234.2 (M+H) $^+$ .  $^1\text{H}$  NMR ( $\text{DMSO-d}_6$ , 400 MHz)  $\delta$ : 7.32-7.22 (m, 5H), 4.25 (s, 2H), 3.26-3.23 (m, 2H), 3.12 (s, 9H), 2.20 (t, 2H,  $J=7.2$  Hz), 1.93-1.88 (m, 2H).  $^{13}\text{C}$  NMR ( $\text{DMSO-d}_6$ , 100 MHz)  $\delta$ : 173.0, 141.7, 128.6, 127.0, 126.8, 66.0, 54.7, 44.1, 35.0, 22.8.

**4-[(4-chlorobenzyl)amino]-*N,N,N*-trimethyl-4-oxobutan-1-aminium iodide 4o**

White solid. Yield: 98%. m.p.: 108-109 °C. MS (ESI)  $m/z$ : 269.8 (M+H) $^+$ .  $^1\text{H}$  NMR ( $\text{CDCl}_3$ , 300 MHz)  $\delta$ : 7.28 (m, 4H), 7.11 (bs, 1H), 4.36 (d, 2H,  $J=5.9$  Hz), 3.84-3.78 (m, 2H), 3.30 (s, 9H), 2.54 (t, 2H,  $J=6.6$  Hz), 2.18-2.13 (m, 2H).  $^{13}\text{C}$  NMR ( $\text{CDCl}_3$ , 75 MHz)  $\delta$ : 173.0, 139.8, 132.3, 128.7, 128.4, 66.0, 54.7, 44.1, 35.0, 22.8.

**4-[(4-methoxybenzyl)amino]-*N,N,N*-trimethyl-4-oxobutan-1-aminium iodide 4p**

White solid. Yield: 89%. m.p.: 110-111 °C. MS (ESI)  $m/z$ : 265.5 (M+H)<sup>+</sup>. <sup>1</sup>H NMR (CDCl<sub>3</sub>, 300 MHz)  $\delta$ : 7.20 (d, 2H,  $J$ = 7.3 Hz), 6.87 (d, 2H,  $J$ = 7.1 Hz), 4.29 (s, 2H), 3.76 (s, 3H), 3.36 (s, 2H), 3.13 (s, 9H), 2.33 (t, 2H,  $J$ = 6.7 Hz), 2.09-2.04 (m, 2H). <sup>13</sup>C NMR (CDCl<sub>3</sub>, 75 MHz)  $\delta$ : 173.0, 158.7, 134.0, 128.0, 114.1, 66.0, 55.9, 54.7, 44.1, 35.0, 22.8.

***N,N,N*-trimethyl-4-[(4-nitrobenzyl)amino]-4-oxobutan-1-aminium iodide  
4q**

Orange gel. Yield: 89%. MS (ESI)  $m/z$ : 279.4 (M+H)<sup>+</sup>. <sup>1</sup>H NMR (CDCl<sub>3</sub>, 300 MHz)  $\delta$ : 8.18 (d, 2H,  $J$ = 8.5 Hz), 7.54 (d, 2H,  $J$ = 8.4 Hz), 4.49 (s, 2H), 3.47-3.42 (m, 2H), 3.19 (s, 9H), 2.45 (t, 2H,  $J$ = 7.1 Hz), 2.17-2.00 (m, 2H). <sup>13</sup>C NMR (CDCl<sub>3</sub>, 75 MHz)  $\delta$ : 173.0, 147.8, 146.4, 127.9, 120.9, 66.0, 54.7, 44.1, 35.0, 22.8.

***(RS)*-*N,N,N*-trimethyl-4-oxo-4-[(1-phenylethyl)amino]butan-1-aminium  
iodide 4r**

White solid. Yield: 73%. m.p.: 153-154 °C. MS (ESI)  $m/z$ : 249.4 (M+H)<sup>+</sup>. <sup>1</sup>H NMR (CDCl<sub>3</sub>, 300 MHz)  $\delta$ : 7.36-7.26 (m, 5H), 7.22 (bs, 1H), 5.06-4.99 (m, 1H), 3.41-3.34 (m, 2H), 3.16 (s, 9H), 2.46-2.38 (m, 2H), 2.12-2.00 (m, 2H), 1.48 (d, 3H,  $J$ = 7.0 Hz). <sup>13</sup>C NMR (CDCl<sub>3</sub>, 75 MHz)  $\delta$ : 172.7, 143.5, 128.6, 127.0, 126.8, 66.0, 54.7, 49.5, 35.3, 22.8, 21.6.

**4-[(3,5-dimethoxybenzyl)amino]-*N,N,N*-trimethyl-4-oxobutan-1-aminium  
iodide 4s**

White solid. Yield: 98%. M.p.: 86-87°C. MS (ESI)  $m/z$ : 295.4 (M+H)<sup>+</sup>. <sup>1</sup>H NMR (CDCl<sub>3</sub>, 250 MHz)  $\delta$ : 8.06 (bs, 1H), 6.98 (s, 2H), 6.81 (s, 1H), 4.80 (d, 2H,  $J$ = 5.6 Hz), 4.26 (s, 6H), 4.15-4.12 (m, 2H), 3.79 (s, 9H), 2.97 (t, 2H,  $J$ = 6.7 Hz), 2.61 (m, 2H). <sup>13</sup>C NMR (CDCl<sub>3</sub>, 75 MHz)  $\delta$ : 173.0, 161.5, 143.7, 103.3, 98.4, 66.0, 55.9, 54.7, 44.7, 22.8.

**4-[(4-methoxyphenylethyl)amino]-*N,N,N*-trimethyl-4-oxobutan-1-aminium iodide 4t**

Waxy solid. Yield: 84%. MS (ESI)  $m/z$ : 279.4 (M+H)<sup>+</sup>. <sup>1</sup>H NMR (CDCl<sub>3</sub>, 300 MHz)  $\delta$ : 7.15 (d, 2H,  $J$ = 6.6 Hz), 6.84 (d, 2H,  $J$ = 6.6 Hz), 6.46 (bs, 1H), 3.77 (s, 3H), 3.69 (t, 2H,  $J$ = 8.2 Hz), 3.50-3.46 (m, 2H), 3.32 (s, 9H), 2.79 (t, 2H,  $J$ = 7.0 Hz), 2.42 (t, 2H,  $J$ = 6.3 Hz), 2.12-2.07 (m, 2H). <sup>13</sup>C NMR (CDCl<sub>3</sub>, 75 MHz)  $\delta$ : 172.7, 157.9, 131.8, 128.8, 114.2, 66.0, 55.9, 54.7, 40.7, 35.7, 35.0, 22.8.

***N,N,N*-trimethyl-4-[(4-nitrophenylethyl)amino]-4-oxobutan-1-aminium iodide 4u**

Yellow oil. Yield: 92% . MS (ESI)  $m/z$ : 293.4 (M+H)<sup>+</sup>. <sup>1</sup>H NMR (CDCl<sub>3</sub>, 300 MHz)  $\delta$ : 8.16 (d, 2H,  $J$ = 8.4 Hz), 8.10 (bs, 1H), 7.48 (d, 2H,  $J$ = 8.4 Hz), 3.50-3.30 (m, 4H), 3.16 (s, 9H), 2.95 (t, 2H,  $J$ = 6.9 Hz), 2.30 (t, 2H,  $J$ = 6.9 Hz), 2.05-2.02 (m, 2H). <sup>13</sup>C NMR (CDCl<sub>3</sub>, 75 MHz)  $\delta$ : 172.7, 145.6, 128.7, 121.0, 66.0, 54.7, 40.7, 35.7, 35.0, 22.8.

***N,N,N*-trimethyl-4-(phenylpropyl)amino-4-oxobutan-1-aminium iodide 4v**

Yellow oil. Yield: 74%. MS (ESI)  $m/z$ : 293.4 (M+H)<sup>+</sup>. <sup>1</sup>H NMR (CDCl<sub>3</sub>, 300 MHz)  $\delta$ : 7.24 (q, 5H,  $J$ = 5.9 Hz), 6.96 (bs, 1H), 3.71 (s, 2H), 3.33-3.25 (m, 9H), 2.66 (t, 2H,  $J$ = 6.9 Hz), 2.46 (s, 2H), 2.12 (s, 2H), 1.87-1.83 (m, 4H). <sup>13</sup>C NMR (CDCl<sub>3</sub>, 75 MHz)  $\delta$ : 172.7, 138.1, 128.9, 128.2, 126.1, 66.0, 54.9, 40.0, 35.0, 33.1, 29.1, 22.8.

## 6.2 Biological *in vitro* assay

### 6.2.1 Cell culture and treatments

NIH-3T3 is a murine fibroblast cell line and NRK is a rat kidney cell line.

Both these cell lines were grown and subcultured in Dulbecco's modified essential medium (EuroClone, Milan, Italy), supplemented with 10% fetal bovine serum (EuroClone), 2 mM glutamine, 10 units/ml penicillin, 100 µg/ml streptomycin. STHdh<sup>Q109/109</sup> and STHdh<sup>Q7/7</sup> were maintained at the permissive temperature of 37 °C, in a humidified incubator with 5% CO<sub>2</sub> [111].

STHdh<sup>Q109/109</sup> and STHdh<sup>Q7/7</sup> cells were a kind gift of Elena Cattaneo (Milan, Italy). STHdh<sup>Q109/109</sup> cells are derived from the striata of homozygous Htt knock-in mice with each Htt allele bearing 109 CAG repeats; STHdh<sup>Q7/7</sup> cells are derived from the wild-type mice with each allele bearing 7 CAG repeats [112]. Cells were grown and subcultured in Dulbecco's modified essential medium (EuroClone, Milan, Italy), supplemented with 10% fetal bovine serum (EuroClone), 2 mM glutamine, 10 units/ml penicillin, 100 µg/ml streptomycin. STHdh<sup>Q109/109</sup> and STHdh<sup>Q7/7</sup> were maintained at the permissive temperature of 33 °C, in a humidified incubator with 5% CO<sub>2</sub> [111].

### 6.2.2 Cell proliferation assay

Following 24, 48 and 72h treatment with Mildronate 10, 20 and 50 µM and with mildronate structurally related compounds (4a-v) 25, 50 and 100 µM (in triplicate) NIH-3T3, NRK, STHdh<sup>Q109/109</sup> and STHdh<sup>Q7/7</sup> cell lines proliferation was determined by MTT assay following manufacturer's protocol (Sigma-Aldrich, Italy). The absorbance of each well was measured with a microplate reader (Cytation3, ASHI) at 570 nm.

### **6.2.3 Western blotting**

Protein lysates from STHdh<sup>Q109/109</sup> and STHdh<sup>Q7/7</sup> cells were used for sodium dodecyl sulphate-polyacrylamide gel electrophoresis (SDS page). SDS page and immunoblotting were carried out according to standard procedures in triplicate using 15 µg of total proteins lysate. Membranes were pre-blocked then incubated with mouse monoclonal primary antibodies anti-Polyglutamine-Expansion (1:2000, Merck Millipore) and mouse monoclonal anti-β-Actin (ACTB, 1:1000; Sigma-Aldrich). Blots were washed and incubated with anti-mouse secondary antibody (1:10.000). Blots were then washed again, incubated in lumi-light enhanced chemiluminescence substrate and exposed to lumi-film. The relative expression, normalized respect to the housekeeping protein ACTB, was quantified densitometrically using Quantity One® 1-D analysis software (BioRad, Italy).

### **6.2.4 RNA isolation and quantitative Real-time PCR**

Total RNA was extracted from cells using QIAzol reagent (Qiagen, Italy). Retro-transcription (0.2 µg RNA) was performed according to the manufacturer's instructions (Promega Italy). To qPCR amplification specific primers for PGC-1α (forward: GATGGCACGCAGCCCTAT, reverse: CTCGACACGGAGAGTTAAAGGAA)[53] and for β-actin (forward: TTAGTTGCGTTACACCCTTTC, reverse: ACCTTCACCGTTCCAGTT) were used. Quantitative PCR (qPCR) was run on an 7900HT Fast Real time-PCR System. The reactions were performed according to the manufacturer's instructions using SYBR Green PCR Master mix (Invitrogen). All reactions were run in triplicate, normalized to the housekeeping gene, and the results expressed as mean ±SD. 2-ΔΔCT method was used to determine the relative quantification.

### **6.2.5 Statistical Analyses**

All quantitative data are presented as the mean  $\pm$  SD. Each experiment was performed at least three times. Statistical significance was evaluated using a t-test or one-way ANOVA analysis, followed by Bonferroni's test for multiple comparisons to determine statistical differences between groups. All the data were analyzed with the GraphPad Prism version 5.01 statistical software package (GraphPad, CA, USA).

### **6.3 Mitotracker fluorescence assay**

Cells were cultured on 12-mm diameter glass coverslips and incubated with 200 nM MitoTracker<sup>®</sup> Red CMXRos (Molecular Probes) for 20 min in culture medium. After incubation, cells were fixed with cold methanol for 5 min, washed with PBS and then mounted in 50% glycerol in PBS. Images were acquired using a Laser Scanning Microscope (LSM 510 META, Carl Zeiss Microimaging, Inc.) equipped with a Plan Apo 63x oil-immersion (NA 1.4) objective lens. Z-slices from the top to the bottom of the cell were collected and 3D reconstruction were carried out using LSM 510 software.

## **6.4 Biological assay in *Drosophila melanogaster***

### **6.4.1 *Drosophila melanogaster* stocks and crosses**

Flies were cultured in a humidified, temperature-controlled incubator with a 12-h on/offlight cycle at 25 °C in vials containing standard cornmeal medium unless specified otherwise.

Fly stocks used in the present study were obtained from the Bloomington Stock center w; P[9]f27b -Bloomington 33809-, that expresses human Huntingtin (HTT) with a long polyQ (glutamine) repeat of 128 amino acids under UAS control. that and w; P{GAL4- elav.L}2 –Bloomington 55635, that expresses the GAL4 protein under the pan-neural promoter elav.

Expression of polyglutamine-containing human huntingtin (hHtt) was driven by the bipartite expression system upstream activator sequence (UAS)-GAL4 in transgenic flies, so appropriate crosses were carried out in order to obtain desired genotypes [113]. Flies bearing the hHtt construct under the control of a yeast UAS were crossed to flies expressing the yeast GAL4 transcriptional activator driven by the neuron-specific promoter elav that is expressed in all neurons from embryogenesis onwards.

Their adult progenies carrying P{UAS-HTT.128Q.FL}f27b/P{GAL4-elav.L}2 were selected and analyzed for locomotor activity.

#### **6.4.2 Climbing behavioral assay**

The climbing assay takes advantages of the natural tendency of flies to move against gravity when agitated in order to study genes or conditions that may hinder locomotor capacities [114].

We used the negative geotaxis climbing reflex of *Drosophila* to examine motor deficits in flies overexpressing human Htt with 128Q in the central nervous system grown on food supplemented with the compounds and comparing their performance to those of flies grown on food devoid of compounds.

In principle, flies are tapped to the bottom of an empty vial and the number of flies that can climb above a certain height is recorded.

#### **Preparing the flies**

Flies were maintained on standard cornmeal medium in a humidified,

temperature-controlled incubator with a 12-h light/dark cycle at 25 °C.

After crosses, newly emerged adult flies with desired genotype were collected under cold-induced anesthesia, sorted by sex, grouped in cohorts of 10 animals in vials containing 3 ml of food supplemented or not with drugs and reared at 28°C. Mildronate and compounds 4k, 4l, 4m and 4v were dissolved in water and absorbed on Adult Food (AF) at 50 µM while normal AF food devoid of compounds was used for the control.

Flies were transferred to fresh vials without anesthesia and scored for motor function every 2 days for 15 days. The gender difference on behavior is significant so the assay was carried out without mix male and female flies.

### **Motor function assay**

The motor function was addressed by their ability to climb up a climbing apparatus prepared for each group by joining vertically two empty polystyrene vials by tape. The vials (diameter, 2,2 cm) faced each other with the openings perfectly aligned to provide an even climbing surface for the flies. 10 cm above the bottom surface of the lower vial, was drawn a circle around the entire circumference.

Before to start the assay, group of ten flies were acclimatized to the new setting for 1 hour after their transfer to the climbing apparatus.

The flies were gently tapped down to the bottom of the vial and the number of flies that could climb above the 10-cm mark within 10 seconds after the tap was recorded.

This assay was repeated for the same group two times, allowing for 1 minute rest period between each trial. The number of flies per group that passed the 10-cm mark was recorded as a percentage of total flies.

The test was repeated 3 times for each compound at the specified age.

### **6.4.3 Data Interpretation and Statistical Analysis**

The raw data generated from the climbing assay represents the number of flies crossing the 10 cm mark in 10 seconds in each group. These values were converted to percentage and the average pass rate for each group over 6 sessions was computed.

Data were represented graphically as an average pass rate per group with the standard error of mean (SEM).

## **6.5 Biological assay in *Caenorhabditis elegans***

### **6.5.1 *Caenorhabditis elegans* strain**

Pmec-3htt57Q128::GFP strain was a gift from J. Alex Parker, University of British Columbia, Vancouver, BC, Canada [115]. Transgenic animals were generated by standard transformation techniques [116]. The htt57Q128 construct was derived from pGBT9 plasmids containing 128 CAG repeats. GFP plasmids were coinjected with a wild-type lin-15 marker plasmid into the gonads of young, adult lin-15 hermaphrodites.

Nematodes are maintained on Nematode Growth (NG) agar plates seeded with OP50, a uracilrequiring mutant of *E. coli*, and incubated at 20°C in Petri dishes. Cultures require subculturing every 3 days.

### **6.5.2 Mechanosensory behavioral assay**

Following a 72h incubation with mildronate, compounds 4k, 4l, 4m and 4v 10µM (dissolved in water and absorbed on NG agar) were tested through the behavioral mechanosensory Assay.

It is the most generally used method to test *C. elegans* gentle touch sensitivity. It consists of stroking the animals with an eyebrow hair finely tapered, sterilized by dipping it into a 70% ethanol solution [117].

Test consists of touching animals five times at the head (just behind the pharynx), for the anterior touch response, and five times at the tail (just before the anus), for the posterior touch response. The responses were scored for every animal separately at both, anterior and posterior touch: for example, if animal responds 6 times out of 10 following anterior touch, this result is given as 60% of anterior responsiveness. Strain that failed to respond to the light

touch at the appropriate area is called posterior or anterior mechanosensory defective phenotype (Pmec).

### **6.5.3 Data Interpretation and Statistical Analysis**

The raw data generated from the mechanosensory assay represent the number of nematodes that failed to respond to the light touch. These values were converted to percentage and the average mechanosensory defective for each group was computed.

Data were represented graphically as an average pass rate per group with the standard error of mean (SEM).

# Results



## 7. Results

### 7.1 Mildronate biological activity in *in vitro* HD model

Mildronate is clinically used as cardioprotective and neuroprotective drug in Eastern Europe and it is able to affect FA mitochondrial metabolism.

This compound has never been investigated in HD. Thus, we have evaluated the effects of the compound on the striatal murine cell lines, STHdh<sup>Q109/109</sup> and STHdh<sup>Q7/7</sup>. STHdh<sup>Q109/109</sup> was obtained from the striata of homozygous Htt knock-in mice with each Htt allele bearing 109 CAG repeats, while STHdh<sup>Q7/7</sup> was obtained from the striata of homozygous Htt knock-in mice with each Htt allele bearing 7 CAG repeats (fig.5) [111].

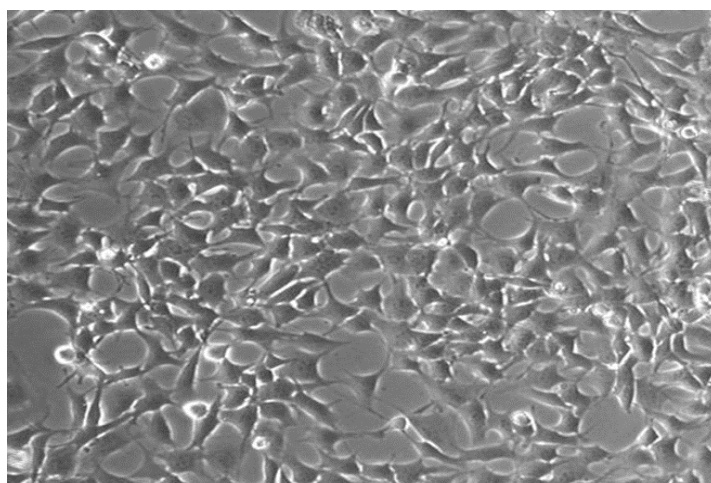
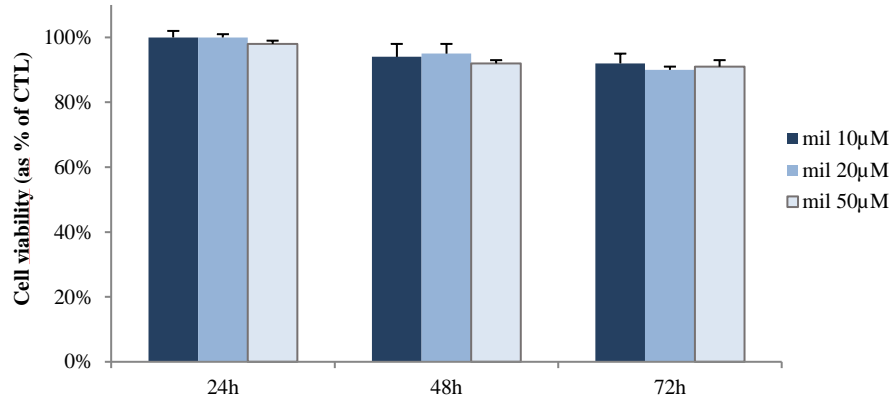


**Figure 5.** Striatal STHdh<sup>Q109/109</sup> and STHdh<sup>Q7/7</sup> cell lines.

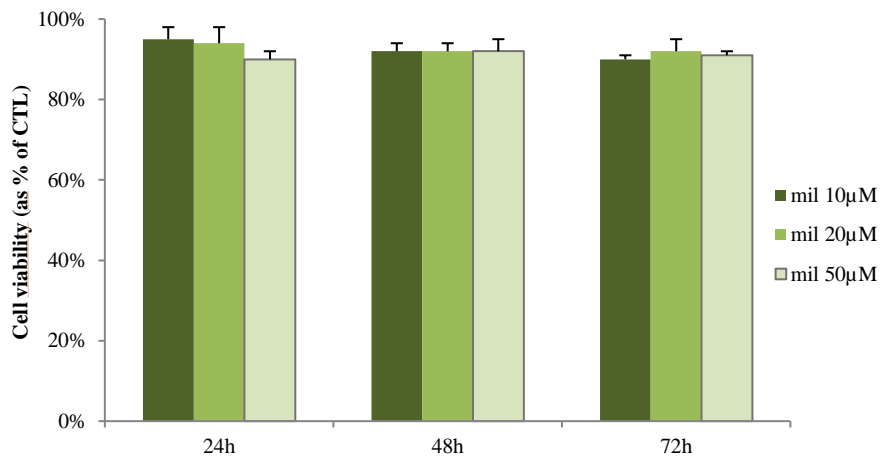
To investigate whether mildronate interfered with striatal cell viability, we incubated both STHdh<sup>Q109/109</sup> and STHdh<sup>Q7/7</sup> cell lines with 10, 20 and 50  $\mu$ M mildronate for 24, 48 and 72h.

Striatal cells viability was measured by MTT assay.

As shown in figure 6, treatment with mildronate did not affect the viability of any of the two cell lines treated compared to untreated.



A



B

**Figure 6.** Cell viability in STHdh<sup>Q7/7</sup> (A) and STHdh<sup>Q109/109</sup> (B) cell lines incubated for 24h, 48h and 72h in presence of mildronate (10 μM, 20 μM and 50μM). Bars represent mean cell viability percentage normalised to untreated control (mean ± SD; n=3).

### **7.1.1 Mildronate and mHtt aggregation**

Mutant Htt aggregation seems to be crucial in the pathogenesis of HD. For this reason, it is proposed a therapeutic approach to treat HD through inhibition of mHtt aggregation [76].

To evaluate whether mildronate was able to inhibit and/or to decrease mHtt aggregates, STHdh<sup>Q109/109</sup> cells were incubated for 72h with 50µM mildronate. mHtt aggregates were assayed by Western blotting analysis following the incubation time.

Results evidenced that mildronate induced a strong decrease in mHtt aggregates in STHdh<sup>Q109/109</sup> (figure 7).

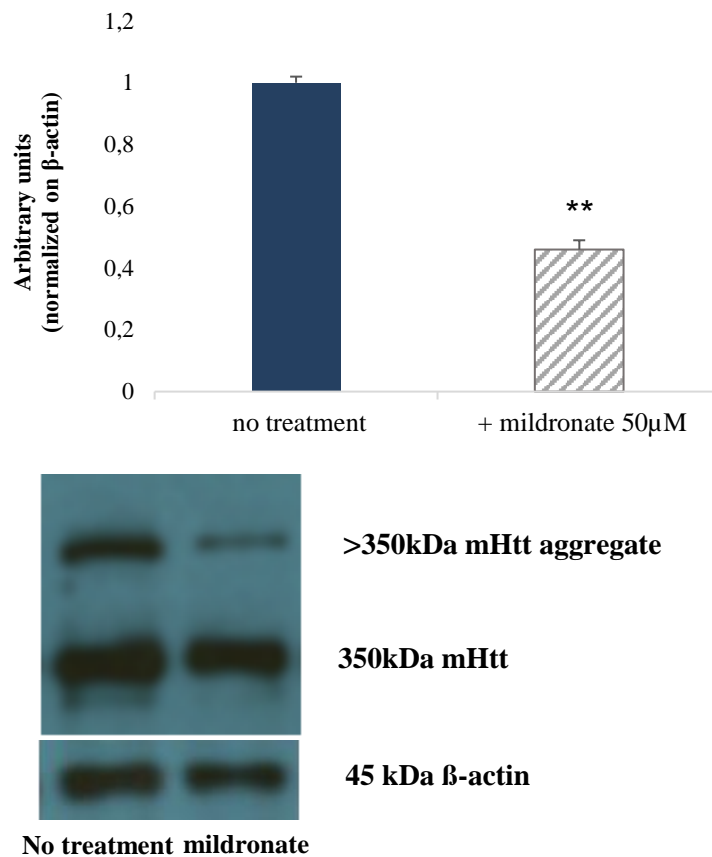


**Figure 7.** Western blot analysis of mHtt aggregates in STHdh<sup>Q109/109</sup> cell lines incubated for 72h in presence of 50 $\mu$ M mildronate. Densitometric analysis was performed using Quantity One® 1-D analysis software (BioRad, Italy). The bars represent means  $\pm$  standard deviation (n = 3). Statistical significance: \*\*  $p < 0.01$  versus control.

Again, mildronate inhibited mHtt aggregates without affecting the level of transfected normal Htt. Furthermore, Western blotting indicated that the same compound did not influence the expression of mutant Htt.

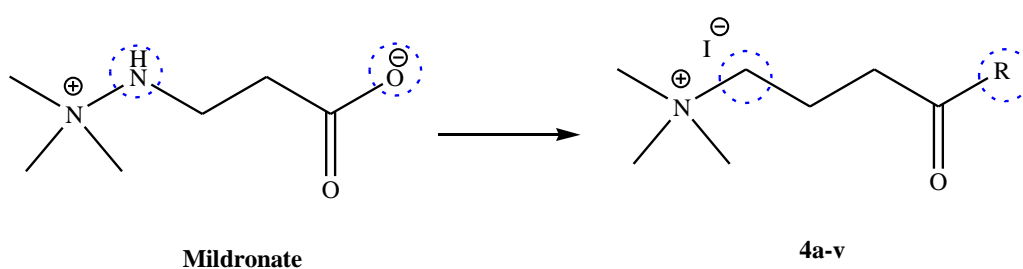
## 7.2 Synthesis of mildronate structurally related compounds: 4a-v

Starting from the promising results arising from our preliminaries studies, we have designed and synthesized new compounds structurally related to mildronate.

Recently Tars et al. also described the design, synthesis and properties of 51 compounds, which include both gamma butyrobetaine (GBB) and mildronate analogues. Their study, however, was aimed to discover novel  $\gamma$ -Butyrobetaine dioxygenase BBOX inhibitors with improved IC<sub>50</sub> [118]. Otherwise in the present study we designed, synthesized and characterized 22 compounds in order to find molecules more active on mHtt aggregation than the commercially available mildronate.

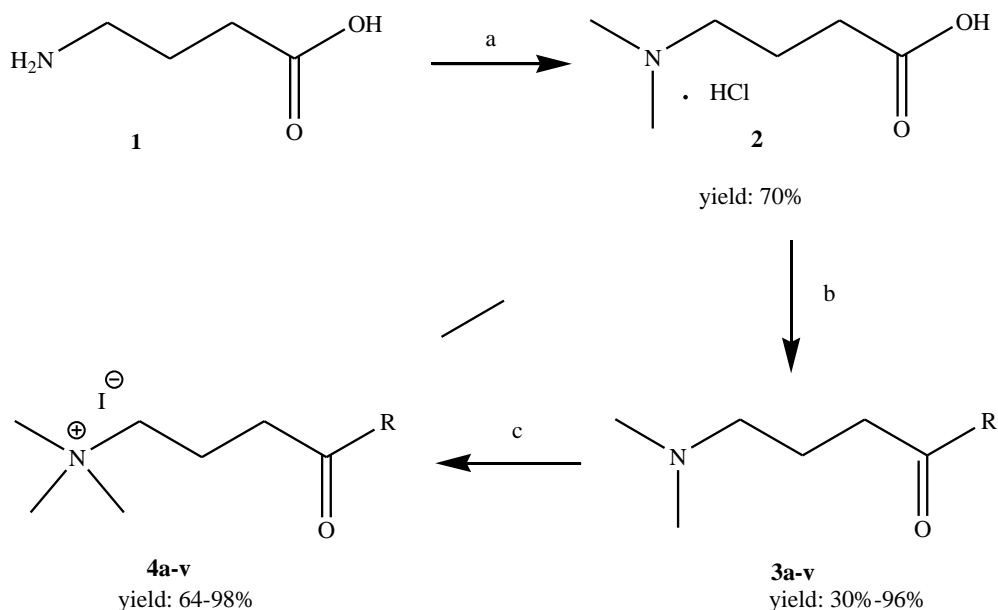
Differently from Tars, we have maintained the quaternary nitrogen, bearing the three methyl groups.

The structural modifications carried out on mildronate have included the replacing of the -NH group with the -CH<sub>2</sub> group and the transformation of the carboxyl group in highly functionalized aliphatic and aromatic amides (scheme 1, compounds 4a-v). The quaternary nitrogen, bearing the three methyl groups, was maintained.



**Scheme 1.** Structural modification carried out on mildronate.

Ammonium salts **4a-v** were prepared following the route depicted in Scheme 2.



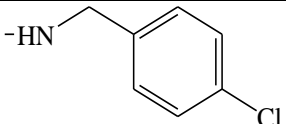
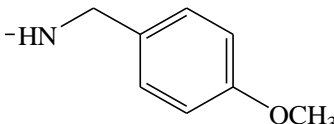
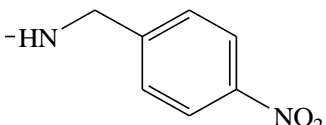
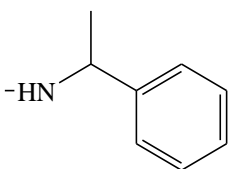
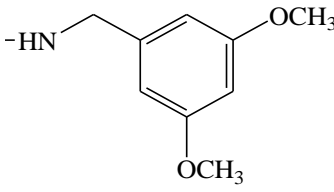
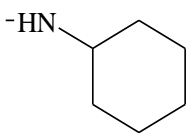
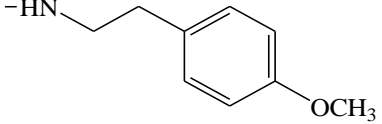
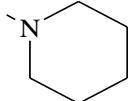
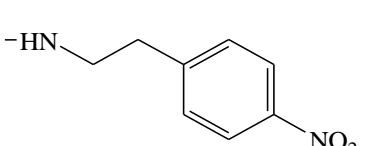
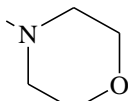
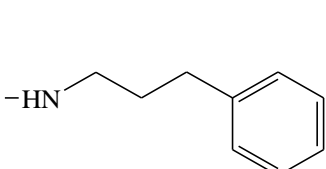
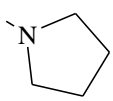
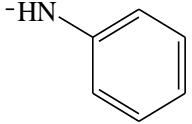
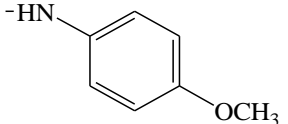
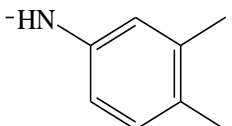
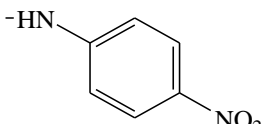
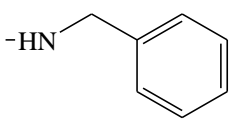
**Scheme 2.** a) HCOH 37%, HCOOH, 60°C, 16 h; b) amine, DCC, HOBT, Et<sub>3</sub>N, CH<sub>2</sub>Cl<sub>2</sub> or THF, r. t., 24h; PCl<sub>3</sub>, pyridine, 3h, 40°C (for 4m); c) CH<sub>3</sub>I, acetone, 18h, r.t.A

As reported in Scheme 2,  $\gamma$ -amino butyric acid **1** was submitted to Eschweiler-Clarke reductive amination reaction using formaldehyde and formic acid at reflux at 60°C for 16h [119]. The obtained 4-(dimethylamino)butanoic acid **2** was treated with DCC, HOBT and triethylamine in THF or CH<sub>2</sub>CH<sub>2</sub> with the suitable amines at room temperature for 24 h [120], to obtain the amides **3a-v**. All compounds **3a-v** were fully characterized by spectroscopic analysis (<sup>1</sup>HNMR, <sup>13</sup>CNMR and mass spectra) after purification. In some cases a simple extraction was sufficient to give moderate-good yields, in other cases a further purification on silica gel was necessary using a mixture of

CH<sub>2</sub>CH<sub>2</sub>/MeOH/Et<sub>3</sub>N. Only for the amide **3m**, due to the low reactivity of the aromatic amine (4-nitroaniline), by applying the same procedure of the preceding reactions, it was not possible to isolate the amide. Thus a new procedure was followed, by reacting the 4-nitroaniline with phosphorous trichloride in pyridine at 40 °C [121]. The desired ammonium salts **4a-v** were obtained by simple methylation reaction with iodomethane in acetone for 18 h [118]. Crystallization with diethyl ether, let to recover the products in yields between 64% and 98%.

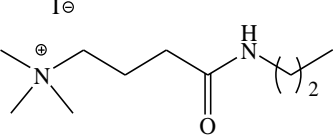
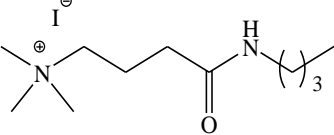
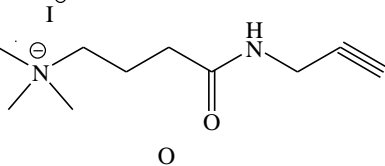
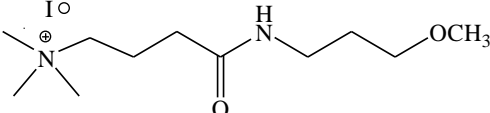
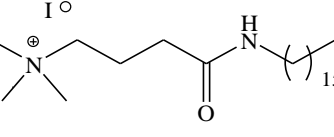
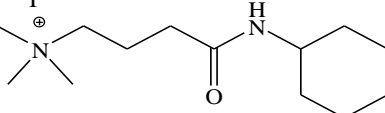
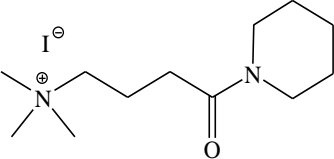
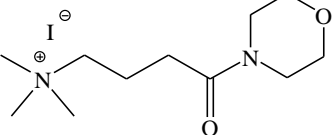
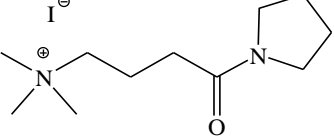
The amines used in reductive amination reaction were acyclic short and long chain alkyl amines, cyclic aliphatic amines, aromatic amines and phenyl alkyl amines (table 1). The amines containing an aromatic ring were chosen considering the spacer between the amino group and the aromatic ring (from none spacer to a spacer up to three carbon atoms) and taking into account of the substituents nature on the aromatic ring in terms of electron withdrawing groups or electron donor groups.

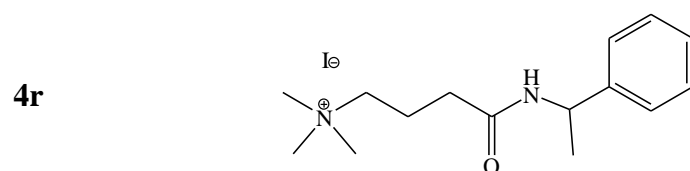
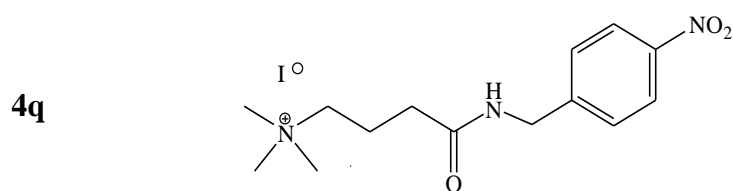
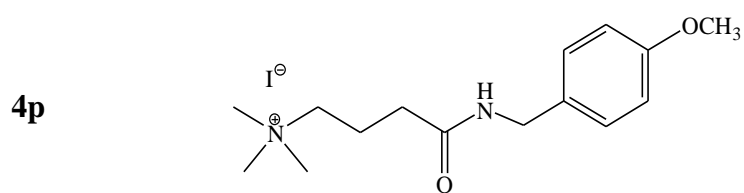
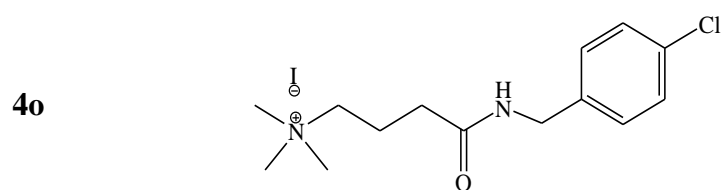
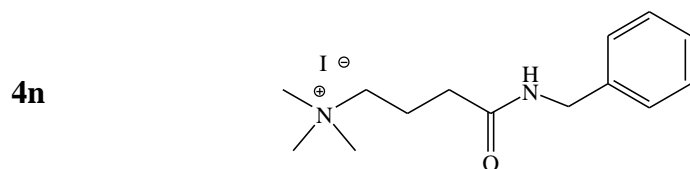
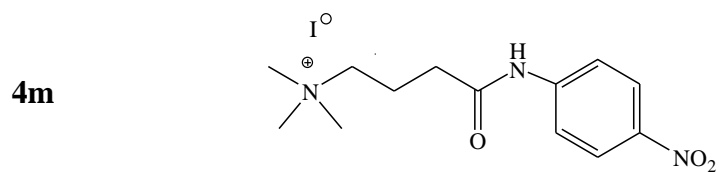
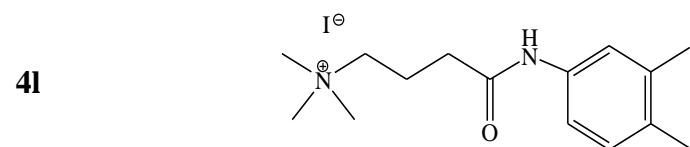
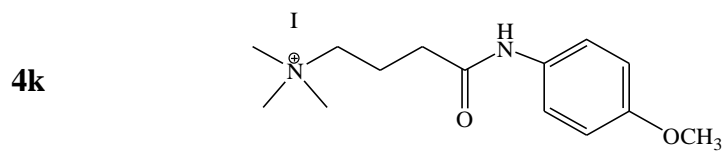
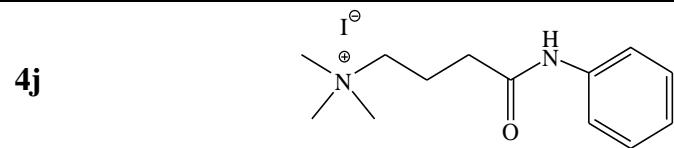
**Table 1.** Amines used in reductive amination reaction.

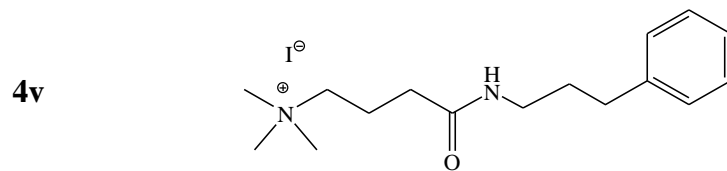
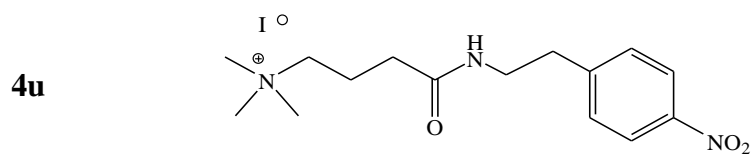
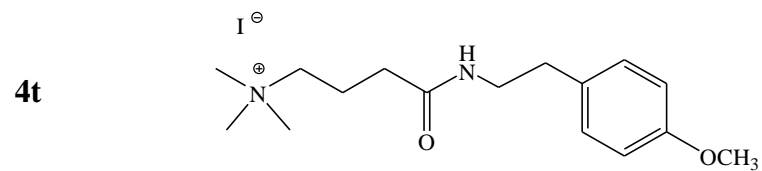
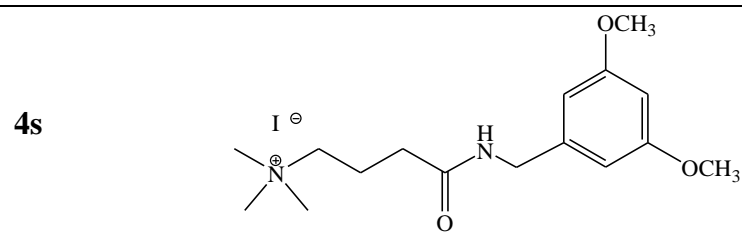
Compound	R	Compound	R
<b>4a</b>	-NHCH <sub>2</sub> CH <sub>2</sub> CH <sub>3</sub>	<b>4o</b>	
<b>4b</b>	-NHCH <sub>2</sub> CH <sub>2</sub> CH <sub>2</sub> CH <sub>3</sub>	<b>4p</b>	
<b>4c</b>	-NHCH <sub>2</sub> CCH	<b>4q</b>	
<b>4d</b>	-NHCH <sub>2</sub> CH <sub>2</sub> CH <sub>2</sub> OCH <sub>3</sub>	<b>4r</b>	
<b>4e</b>	-NHCH <sub>2</sub> (CH <sub>2</sub> ) <sub>14</sub> CH <sub>3</sub>	<b>4s</b>	
<b>4f</b>		<b>4t</b>	
<b>4g</b>		<b>4u</b>	
<b>4h</b>		<b>4v</b>	
<b>4i</b>			
<b>4j</b>			
<b>4k</b>			
<b>4l</b>			
<b>4m</b>			
<b>4n</b>			

These modifications resulted in the synthesis of the 22 ammonium salts 4a-v, showed in table 2.

**Table 2.** Ammonium salts 4a-v.

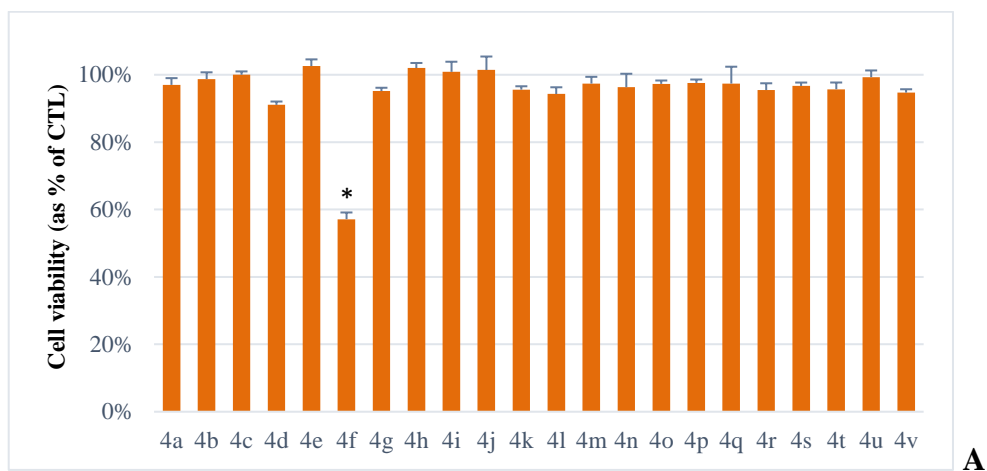
Compound	Structure
4a	
4b	
4c	
4d	
4e	
4f	
4g	
4h	
4i	





### 7.3 Evaluation of mildronate structurally related compounds in *in vitro* HD models

Differently from mildronate, already known in the literature as safe compound for clinical use, 4a-v compounds were newly synthesized and their cytotoxicity was assessed. We evaluated their biocompatibility on two non-neuronal cell lines, such as the rat kidney cell line (NRK) and the murine fibroblast cell line (NIH). We incubated both cells with the compounds at a concentration of 25, 50 and 100  $\mu$ M for 24, 48 and 72h. In figure 8, we only report the results for the most stressful treatment for the cells, such as 72h at 100 $\mu$ M concentration. Almost all of the compounds showed no toxicity on NRK and NIH cell lines (figure 8). Only 4f partially affected cell viability in both cell lines compared to untreated cells.



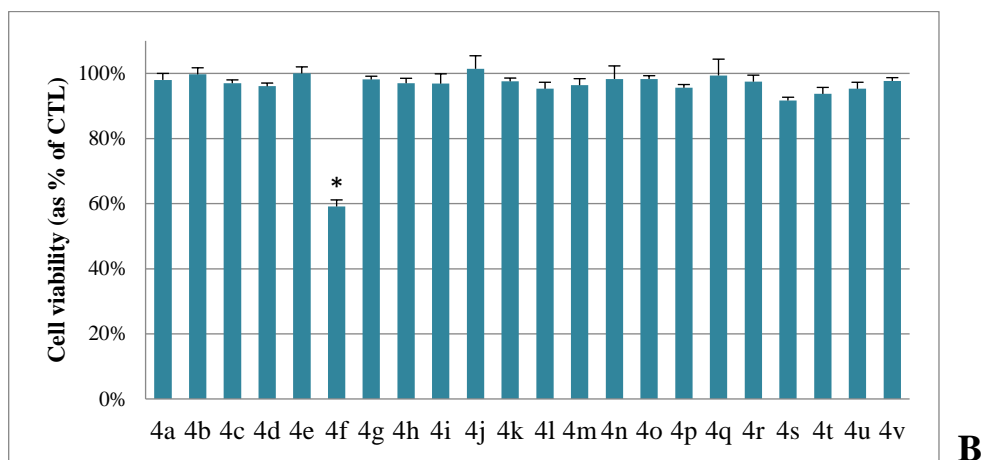
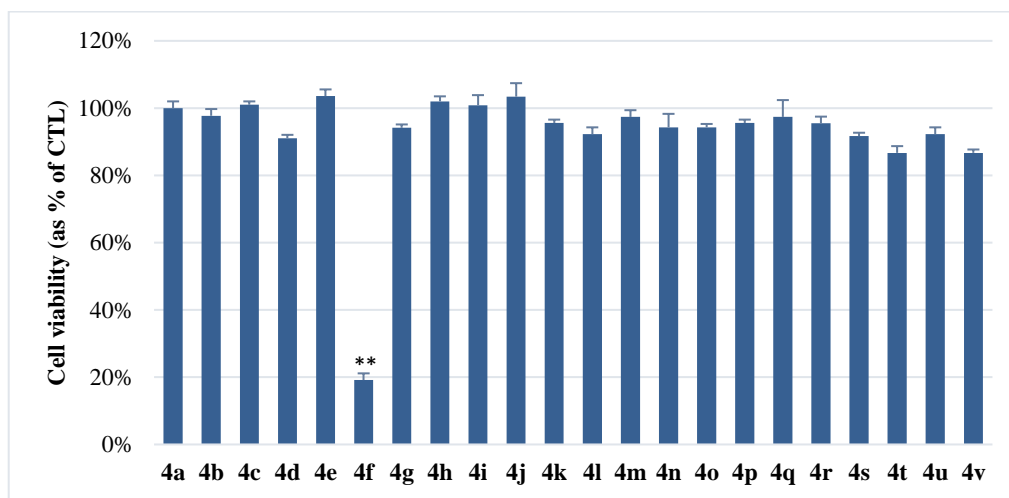


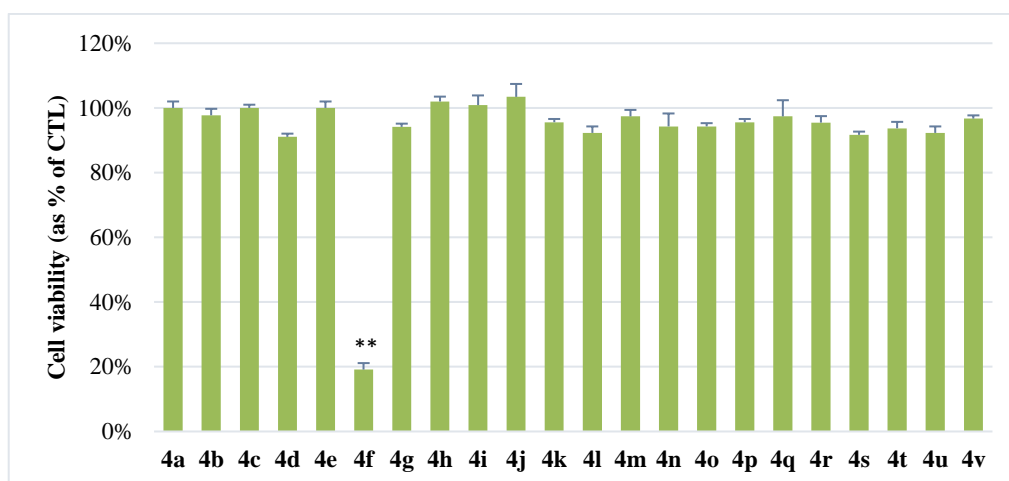
**Figure 8.** Cell viability in NRK (A) and NIH-3T3 (B) cell lines incubated for 72h in presence of 100  $\mu$ M 4a-v compounds. Bars represent mean cell viability percentage normalised to untreated control (mean  $\pm$  SD; n=3). Statistical significance: \*  $p < 0.05$  versus CTL.

Once established 4a-v compounds did not affect cell viability in non-neuronal cell lines, we tested these compounds on STHdh<sup>Q109/109</sup> and STHdh<sup>Q7/7</sup> striatal cell lines. We incubated both cells with the compounds at a concentration of 25, 50 and 100 $\mu$ M for 24, 48 and 72h.

In figure 9, we only report the results for the most stressful treatment for the cells, such as 72h at 100 $\mu$ M concentration. As shown, compound 4f significantly affected cell viability in both STHdh<sup>Q109/109</sup> and STHdh<sup>Q7/7</sup> compared to untreated cells, while we found that all other compounds did not interfere with striatal cell lines viability.



A



B

**Figure 9.** Cell viability in in STHdh<sup>Q7/7</sup> (A) and STHdh<sup>Q109/109</sup> (B) cell lines incubated for 72h in presence of 100μM 4a-v compounds. Bars represent mean cell viability percentage normalised to untreated control (mean ± SD; n=3). Statistical significance: \*\* p<0.01 versus CTL.

The results obtained from cell viability assays led us to avoid the 4f compound in subsequent studies.

Contrariwise, the other 21 compounds showed a good biocompatibility on neuronal and non-neuronal cellular models. Therefore, their biological activity was further investigated on other HD models.

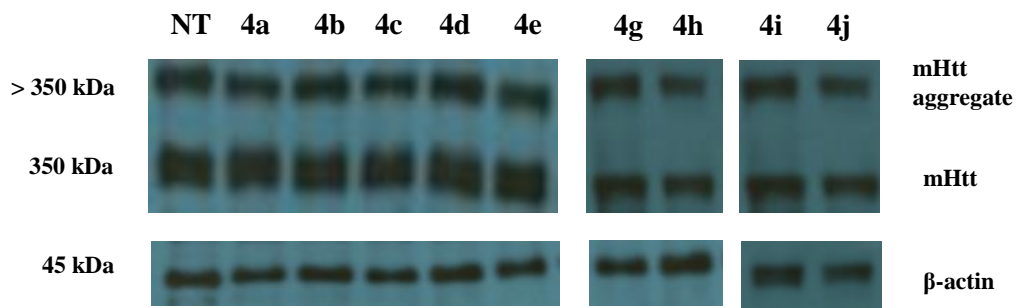
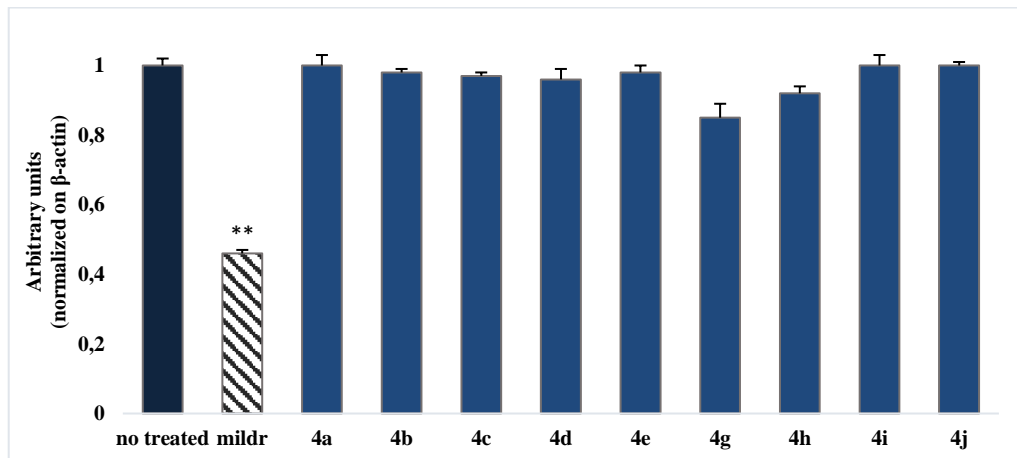
### **7.3.1 Mildronate structurally related compounds and mHtt aggregation**

Following these preliminary assessments, we evaluated the effect of compounds newly synthesized on mHtt aggregation.

Tests were conducted under the same conditions used previously for mildronate: STHdh<sup>Q109/109</sup> were incubated in presence of the different compounds for 72h at a concentration of 50µM.

We found that compounds 4k, 4l, 4m and 4v significantly decreased mHtt aggregates compared to untreated cultures.

Interestingly, they showed an effect on mHtt aggregates higher than mildronate, (figure 10) without affecting the expression of both mHtt and wHtt.



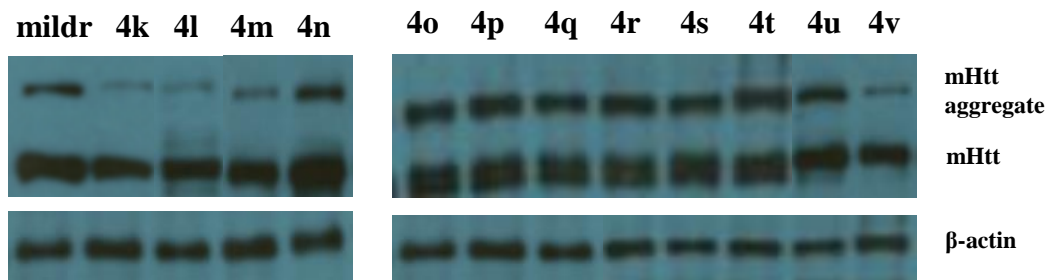
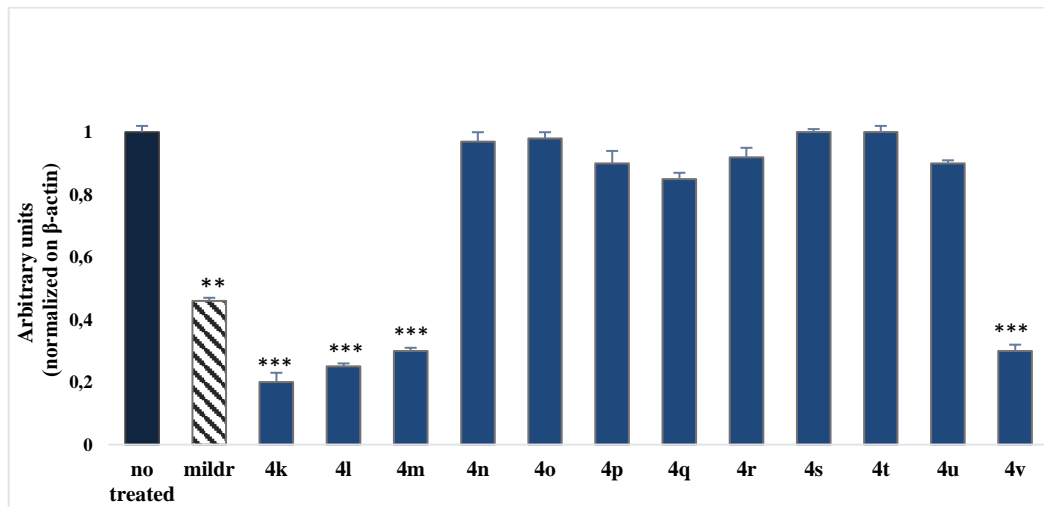


**Figure 10.** Western blot analysis of mHtt aggregates in STHdh<sup>Q109/109</sup> cell lines incubated for 72h in presence of 4a-v compounds 50μM. Densitometric analyses were performed using Quantity One® 1-D analysis software (BioRad, Italy). The bars represent means ± SD (n = 3). Statistical significance: \*\* p<0.01, \*\*\*p<0.005 *versus* no treated.

The results arising from biological studies allowed us to select the most active compounds 4k, 4l, 4m and 4v for the next phases of this study, involving evaluation of mildronate and selected compounds activity on mitochondrial dynamics and behavioral assays on *in vivo* HD models.

## 7.4 Modulation of *Pgc-1 $\alpha$* mRNA expression by mildronate and its structurally related analogues

As discussed above, there is substantial evidence that PGC-1 $\alpha$  promotes clearance of mHtt protein aggregates, decreasing mHtt neurotoxicity [96].

In order to evaluate whether mildronate and the neo-synthesized compounds 4k, 4l, 4m and 4v decreased mHtt aggregates by modulating PGC-1 $\alpha$  pathway, we examined the *Pgc-1 $\alpha$*  mRNA expression in STHdh<sup>Q109/109</sup> cell line before and after treatment with selected compounds.

First, the *Pgc-1 $\alpha$*  mRNA expression levels were determined by quantitative Real-Time PCR in STHdh<sup>Q7/7</sup> and STHdh<sup>Q109/109</sup> cell lines.

We found that *Pgc-1 $\alpha$*  mRNA expression is significantly downregulated in STHdh<sup>Q109/109</sup> cell line compared to STHdh<sup>Q7/7</sup> cell line (figure 11).

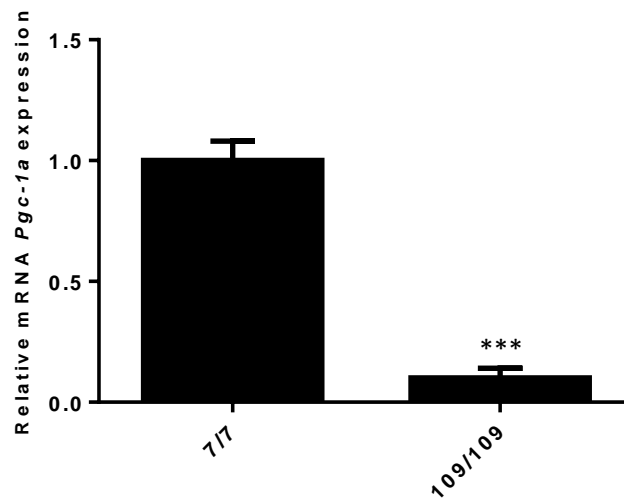


**Figure 11.** Relative mRNA *Pgc-1 $\alpha$*  expression in STHdh<sup>Q7/7</sup> and STHdh<sup>Q109/109</sup> cell lines. The expression of *Pgc-1 $\alpha$*  mRNA was normalized to the housekeeping gene  $\beta$ -actin. The bars represent means  $\pm$  SD (n = 3). Statistical significance: \*\*\* $p$ <0.005 versus STHdh<sup>Q7/7</sup> cell line.

Quantitative Real-Time PCR analysis of STHdh<sup>Q109/109</sup> cell line incubated for 24h with 50μM mildronate revealed that *Pgc-1α* mRNA expression was significantly upregulated, compared to untreated cells (figure 12).

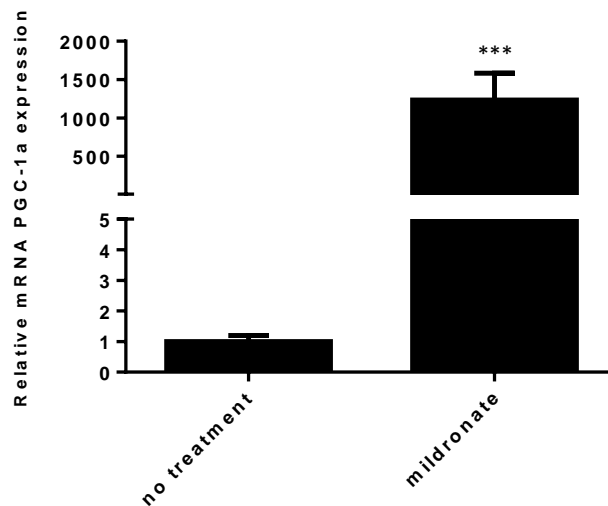


**Figure 12.** Relative mRNA *Pgc-1α* expression in 24h 50μM mildronate treated STHdh<sup>Q109/109</sup> cell line compared to untreated STHdh<sup>Q109/109</sup> cell line. The expression of *Pgc-1α* mRNA was normalized to the housekeeping gene β-actin. The bars represent means ± SD (n = 3). Statistical significance: \*\*\**p*<0.005 versus untreated.

Interestingly, our data show that the 4k and 4l mildronate derivatives were able to increase *Pgc-1α* mRNA expression more significantly than mildronate, at 24 h incubation time (figure 13).

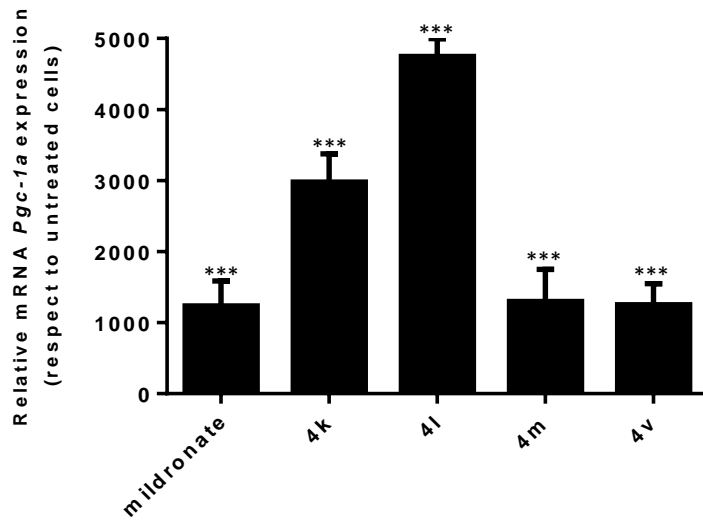


**Figure 13.** Relative mRNA *Pgc-1α* expression in 24h 50μM 4k, 4l, 4m and 4v treated STHdh<sup>Q109/109</sup> cell line. The expression of *Pgc-1α*. The expression of *Pgc-1α* mRNA was normalized to the housekeeping gene β-actin. The bars represent means ± SD (n = 3). Statistical significance: \*\*\**p*<0.005 versus untreated.

## **7.5 Regulation of mitochondrial dynamics by mildronate and its structurally related compounds**

Increasing evidences show that mitochondrial dynamics are mechanistically linked to mitochondrial function [122]. Hence, we examined the overall organization of the mitochondrial network in  $STHdh^{Q7/7}$  and  $STHdh^{Q109/109}$  cell lines by confocal microscope incubating the cells with the MitoTracker Red dye, a reagent that stains mitochondria in live cells according to their membrane potential. While in  $STHdh^{Q7/7}$  mitochondrial network exhibited a branched, tubular morphology, in  $STHdh^{Q109/109}$  cells expressing mutated Htt it appeared fragmented with many small and short mitochondria (figure 14).

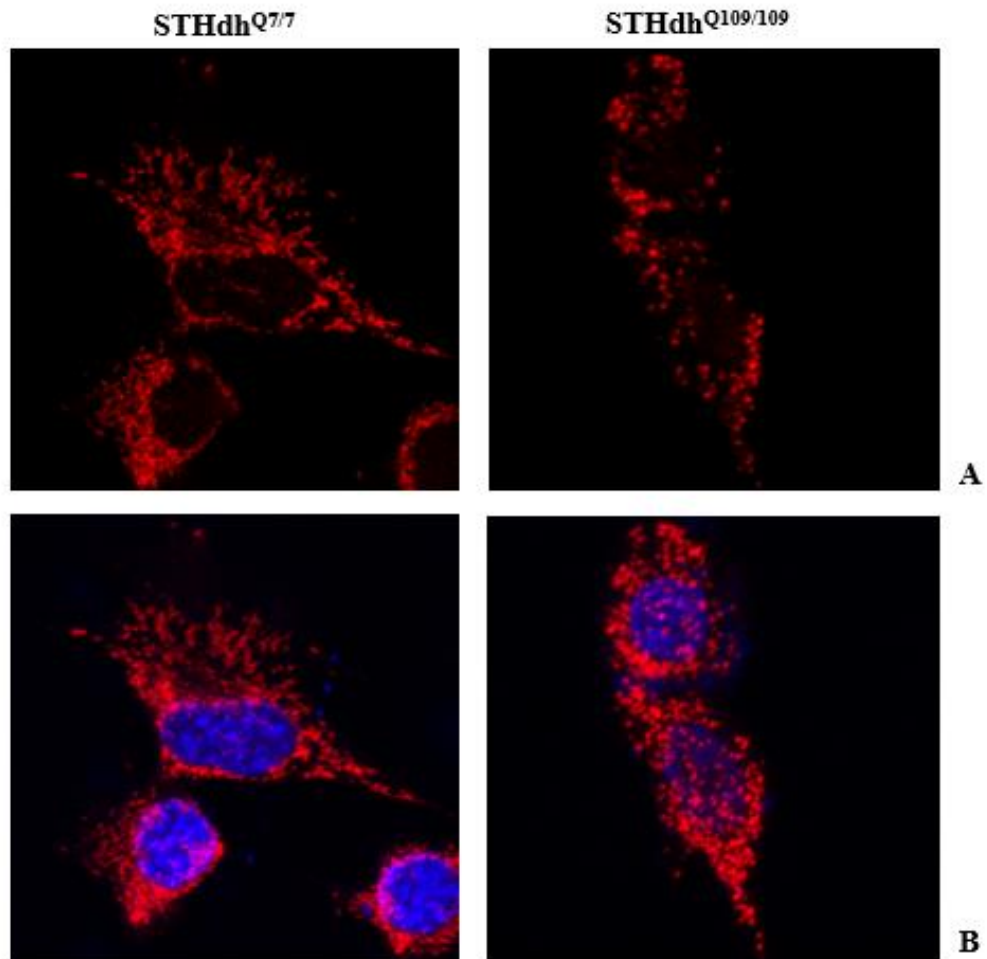


**Figure 14.** Mitochondria in STHdh<sup>Q7/7</sup> and STHdh<sup>Q109/109</sup> cell lines at the confocal microscope. (A) Mitotracker (B). Mitotracker and DAPI.

We then investigated whether 72h 50 $\mu$ M treatment with mildronate affected the mitochondrial network in STHdh<sup>Q109/109</sup>. Confocal microscopy analysis revealed a rescue of the tubular morphology of mitochondria upon mildronate treatment (figure 15). Mitochondria appear as long tubular structures extending in the whole cytosol and only in few cells the mitochondrial network resulted still fragmented (5-8%).

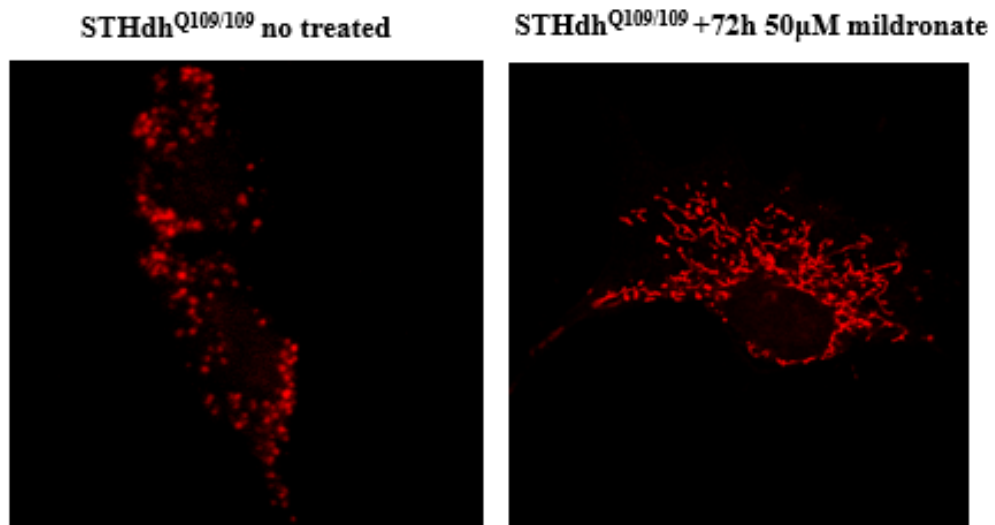


**Figure 15.** Confocal microscopy analysis of STHdh<sup>Q109/109</sup> cell line incubated 72h in presence of 50µM mildronate.

Finally we investigated whether treatment with 4k, 4l, 4m and 4v affected the mitochondrial network in STHdh<sup>Q109/109</sup> at the same extent of mildronate.

Confocal microscopy analysis revealed a full rescue of the tubular morphology of mitochondria upon 4k and 4l treatment. A less efficient reversion was observed upon 4m derivative treatments since many mitochondria appear shorter in a lot of cells. Moreover, we found partial rescue with 4v derivative (figure 16).

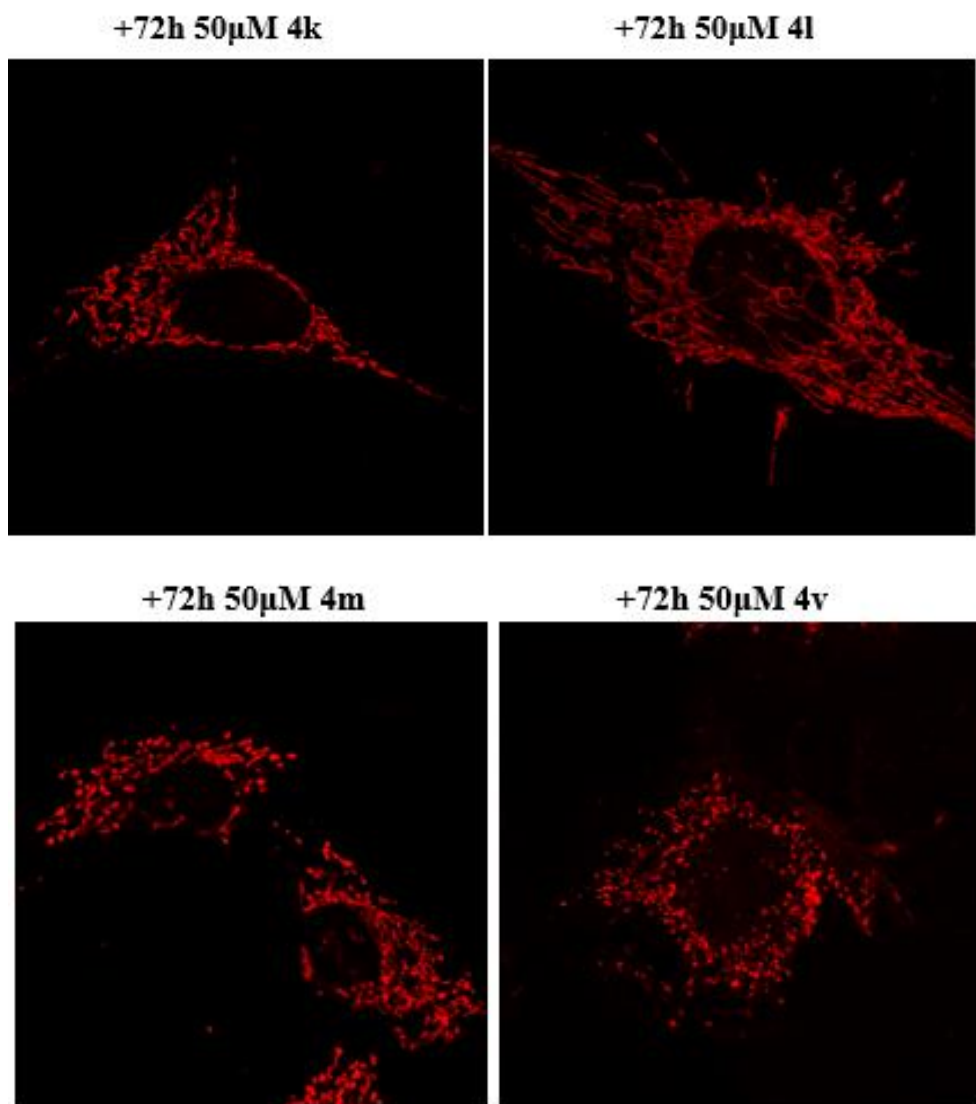


**Figure 16.** Confocal microscopy analysis of STHdh<sup>Q109/109</sup> cell line incubated 72h in presence of 50μM 4k, 4l, 4m and 4v compounds.

## **7.6 Rescue of neurological deficits in HD animal model by mildronate and its structurally related compounds**

To investigate the effect of mildronate and the selected compounds on neurological deficits related to HD pathology, behavioural assays were carried out in *Drosophila melanogaster* and *Caenorhabditis elegans*, both expressing human Htt with a long polyQ repeat (128 residues).

### **7.6.1 *Drosophila melanogaster* HD stock**

A significant contribution to understating of HD arises from studies utilizing *Drosophila melanogaster*.

The short lifespan of flies, low cost of maintaining and propagation stocks, genome completely sequenced and genetic tools available for *in vivo* manipulation make them ideal for testing new therapeutic compounds [123]. Transgenic flies engineered to overexpress the human mHtt gene show protein aggregation, neurodegeneration, a reduced lifespan and behavioral deficits [124].

The transgenic fly stock used in the present study is the elav-HTT.128Q.FL that expresses human mHtt with a long polyQ repeat of 128 CAG under UAS control.

The expression of polyglutamine-containing human huntingtin was driven by the bipartite expression system upstream activator sequence (UAS)-GAL4 in transgenic flies, so appropriate crosses were carried out in order to obtain desired genotypes (figure 17) [117].

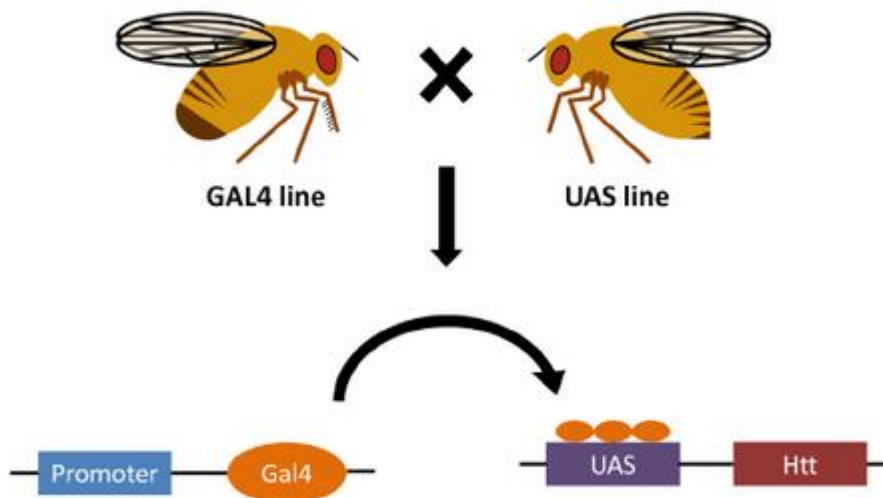


**Figure 17.** A schematic representation of the GAL4/upstream activation sequence (UAS) bitransgenic system. This system allows one to “humanize” *Drosophila* by expressing human Htt constructs. By crossing transgenic yeast GAL4 transcription activator flies with flies carrying UAS sites controlling Htt expression, progeny possessing both transgenes are obtained.

Adapted from: Mason R.P., C. Modeling Huntington Disease in Yeast and Invertebrates. [125]

### 7.6.2 Mildronate and its structurally related compounds on neuronal deficits in the HD *Drosophila* model

Overexpression of human mHtt in the fly stock elav-HTT.128Q.FL used in this study lead to the onset of neurological deficits in these organisms. In particular, they exhibit motor deficits in the climbing behavior (negative geotaxis).

Flies have a natural tendency to move against gravity when agitated: the negative geotaxis climbing reflex [126].

Climbing behavioral assay takes advantages of this feature in order to study genes or conditions that may hinder locomotor capacities.

Therefore, in order to examine the motor deficits correlated to overexpression of human Htt in these flies, we carried out climbing assay that allowed us to evaluate the negative geotaxis climbing reflex of *Drosophila* grown on food

supplemented with the compounds and comparing their performance to those of flies grown on food devoid of compounds.

The motor function was assessed by their ability to climb up: we scored the number of flies crossing the 10 cm mark in 10 seconds in each group. Mildronate and compounds 4k, 4l, 4m and 4v were dissolved in water and absorbed on Adult Food (AF) at 50  $\mu$ M while normal AF food devoid of compounds was used for the control.

The motor function was assessed by their ability to climb up: we scored the number of flies crossing the 10 cm mark in 10 seconds in each group (fig. 18).

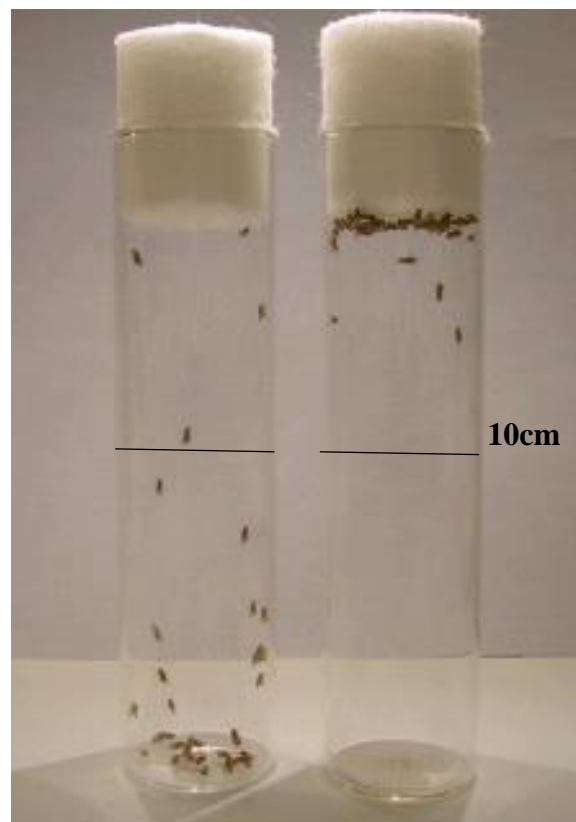


**Figure 18.** Exemplification of climbing assay.

The number of flies per group that passed the 10-cm mark was recorded as a percentage of total flies.

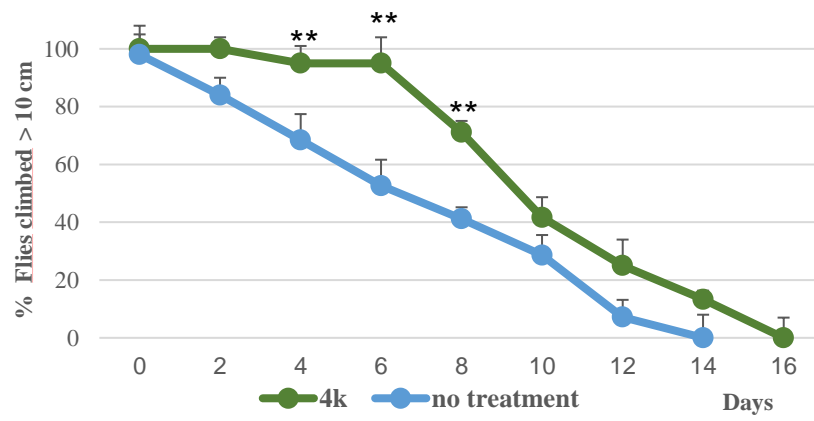
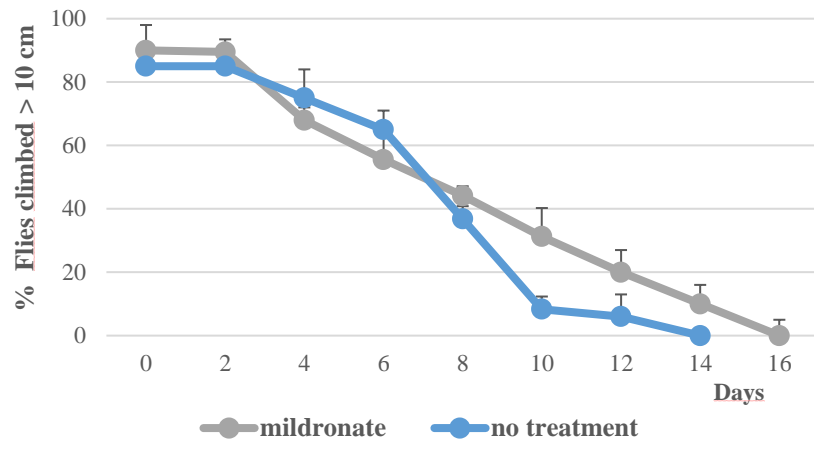
The test was repeated 3 times for each compound at the specified age.

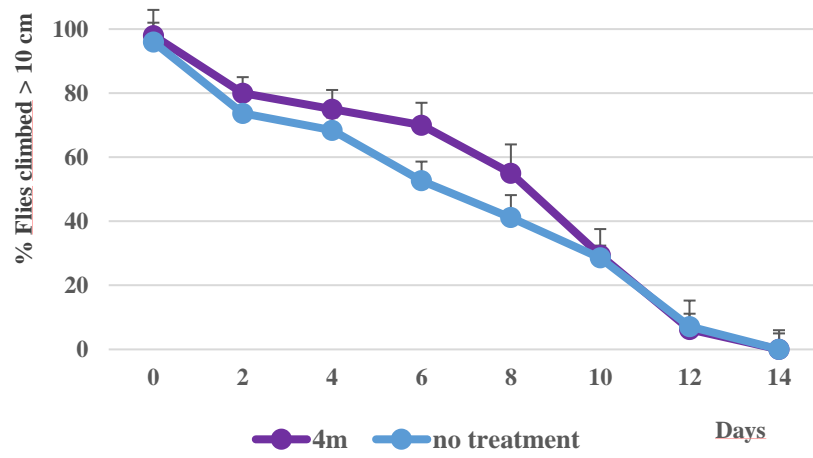
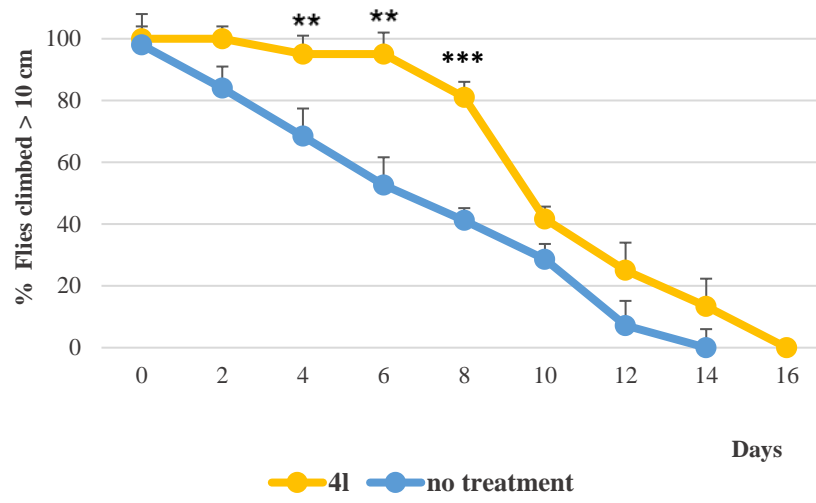
Mildronate and compounds 4k, 4l, 4m and 4v were dissolved in water and absorbed on Adult Food (AF) at 50  $\mu$ M concentration while normal AF food devoid of compounds was used for the control.

As reported in figure 19 mildronate and 4v treated flies showed a delay in climbing disability onset, from day 14 to day 16, compared to untreated control.

Compounds 4k and 4l, as well as mildronate, postponed climbing disability onset, but, in addition, they also led to a considerable rescue in percentage of flies able to cross 10 cm, compared to untreated flies. This rescue was evident in the first half of the treatment, at day 4, 6 and 8.

Finally, 4m treated flies had a climbing behavior comparable to untreated flies.





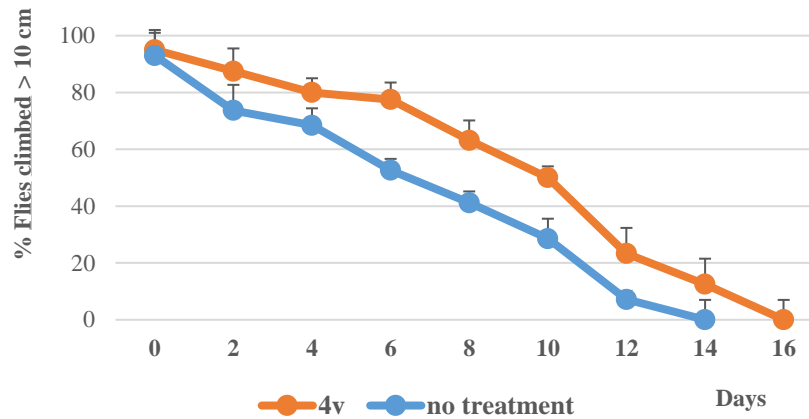


**Figure 19.** Climbing assay in fly stock elav-HTT.128Q.FL in presence of 50 $\mu$ M mildronate, 4k, 4l, 4m and 4v. Data were represented graphically as an average pass rate per group with the standard error of mean (SEM), n=50. Statistical significance: \*\* p<0.01, \*\*\*p<0.005 versus control.

Except the 4m compound, the other tested compounds showed a rescue of motor deficits in the flies model: they partially corrected impaired climbing behavior arising from overexpression of human mHtt.

## **7.7 *Caenorhabditis elegans* HD strain**

The ease by which *C. elegans* can be grown and maintained in a laboratory makes it extremely attractive as a model organism. Its short generation time and small size, together with the capacity to grow on agar plates seeded with *E. coli*, makes this organism ideal for high-throughput experiments. The transparency inherent to worms throughout their life span allows metabolic processes to be viewed in real time with the use of fluorescent markers. The simple nervous system of *C. elegans*, consisting of 302 neurons, provides a means of analyzing the underlying behavior of the neural circuitry (figure 20).

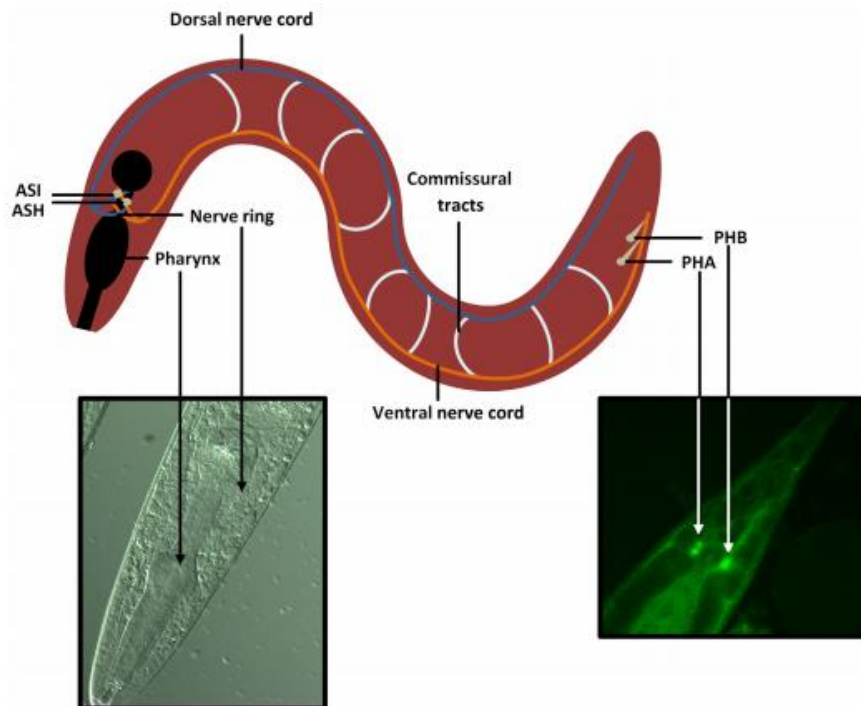


**Figure 20.** *C. elegans* nervous system possesses a simple nervous system comprising 302 sensory, motor, and interneurons. The entire nervous system consists of the nerve ring and two parallel nerve cords (dorsal and ventral). The majority of the neuron cell bodies are located in the head, forming large ganglia or the “brain” of the worm. Four sensory neurons are highlighted in the diagram: the ASH, ASI, PHA, and PHB neurons.

Source: Mason R.P., *C. Modeling Huntington Disease in Yeast and Invertebrates*

*C. elegans* is the only organism to have its entire nervous system mapped, a task facilitated by the simplicity of the synaptic connectivity [127]

Because of the lack of an Htt orthologue in *C. elegans*, HD has been studied using transgenic strains expressing portions of the human gene.

*C. elegans* strain we used in our analysis is Pmec-3htt57Q128::GFP. In this strain Parker and his group expressed the first 57 aminoacids of human Htt expanded polyQ fused to a fluorescent protein marker in touch receptor neurons by using the mec-3 promoter (Pmec-3) [127].

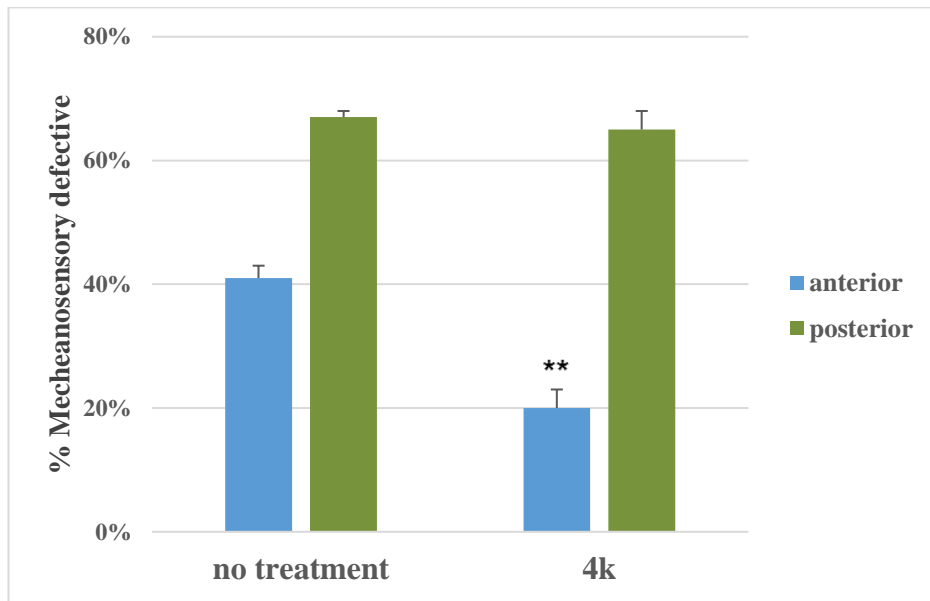
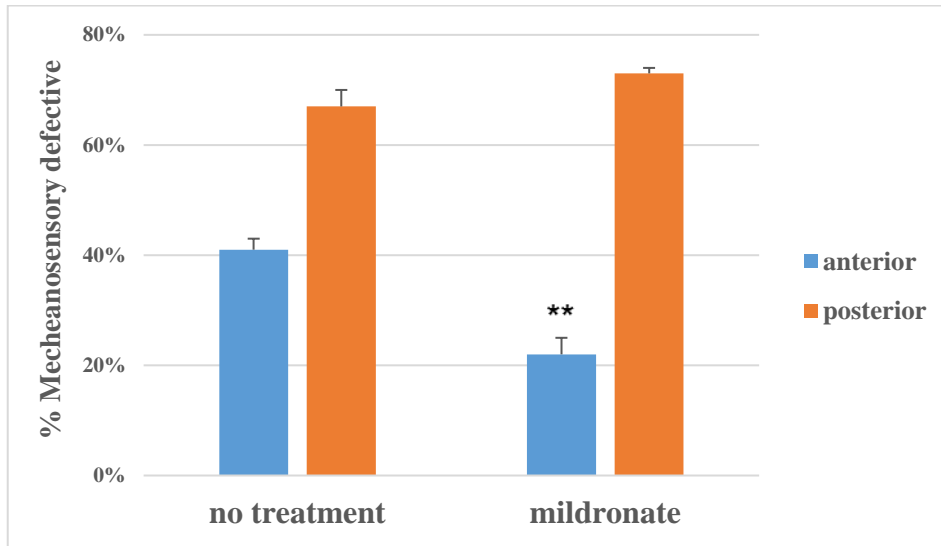
### **7.7.1 Mildronate and its structurally related compounds on neuronal deficits in the HD *C.elegans* model**

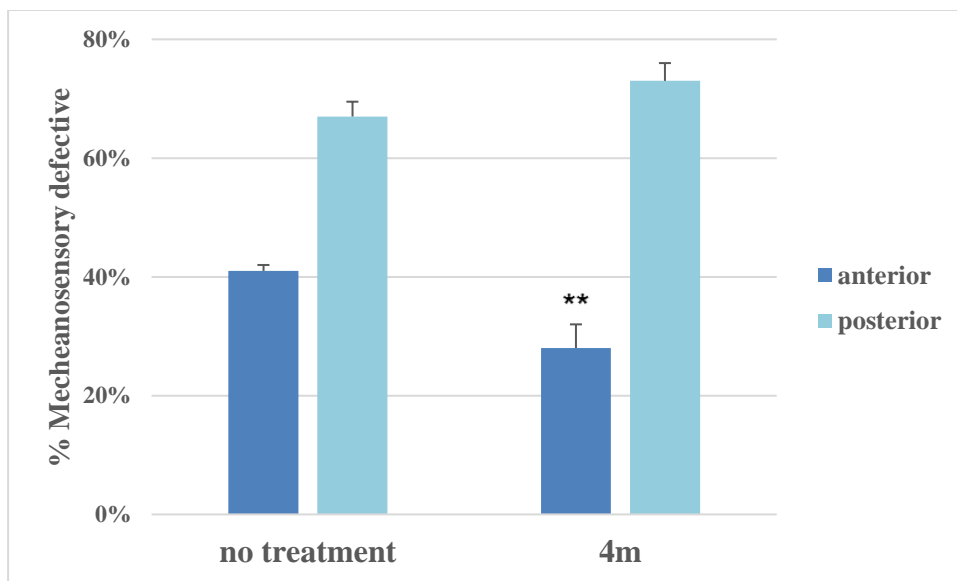
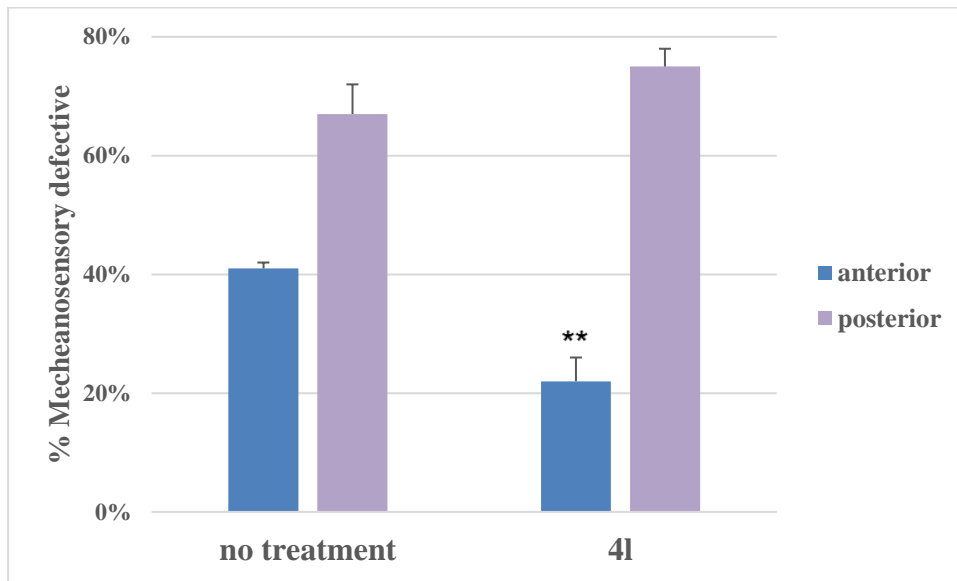
Increased polyQ expansion in these animals led to a significant mechanosensory defective (Mec) phenotype: nematodes fail to respond to a light touch at the tail.

To test whether mildronate and selected compounds were able to rescue this neurological deficit, we used mechanosensory behavioral assays.

This is the most generally used method to test *C. elegans* gentle touch sensitivity. It consists of stroking the animals with an eyebrow five times at the head (just behind the pharynx), for the anterior touch response, and five times at the tail (just before the anus), for the posterior touch response. The responses were scored for every animal separately at both, anterior and posterior touch: for example, if animal responds 6 times out of 10 following anterior touch, this results is given as 60% of anterior responsiveness.

In figure 21 we reported the percentage of mechanosensory defective in *Pmec-3htt57Q128::GFP* nematodes following 72h incubation with mildronate, compounds 4k, 4l, 4m and 4v 10  $\mu$ M (dissolved in water and absorbed on NG agar). All tested compounds significantly rescued the neuronal dysfunction induced by 128Q in anterior responsiveness compared to *Pmec-3htt57Q128::GFP* nematodes untreated. On contrary, posterior responsiveness seems not to be affected by incubation with compounds.





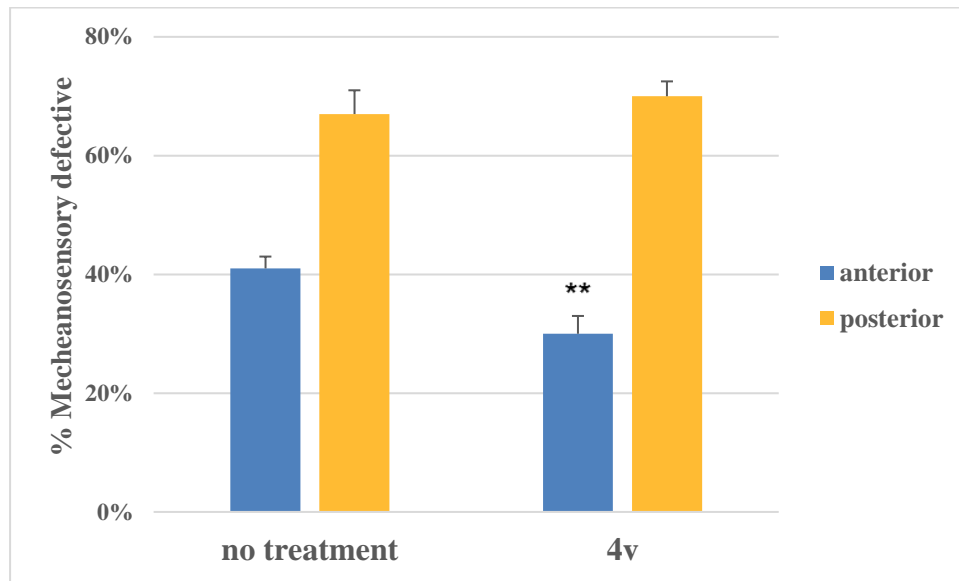


**Figure 21.** Mechanosensory behavioral assay on *Pmec-3htt57Q128::GFP* nematodes following 72h incubation with mildronate, compounds 4k, 4l, 4m and 4v 10 $\mu$ M. Data were represented graphically as average of the percentage of mechanosensory defective in anterior and posterior touch response per group with the standard error of mean (SEM), n=50. Statistical significance: \*\* p<0.01 *versus* control untreated.

# Discussion



## 8. Discussion

HD shares many pathological features with other neurodegenerative diseases that are caused by protein misfolding. These pathological features include age-dependent accumulation of misfolded proteins and selective degeneration of neuronal cells. Since HD is a monogenetic disorder caused by polyQ expansion in Htt, it provides an ideal model for us to find therapeutics for neurodegenerative diseases. However, there is still lack of effective treatments for HD, despite large efforts being made to identify its therapeutics.

Recently, it has been suggested that mHtt may impair neuronal mitochondrial dynamics and quality control by several mechanisms. Mitochondrial biogenesis may be decreased through reduced PGC-1 $\alpha$  expression, coupled with impaired protein import attributed to mHtt interaction with TIM23. Reduced expression of fusion proteins and increased expression/activity of fission-associated Drp1 are associated with excessive mitochondrial fission in the HD striatum. These cumulative effects of mHtt on mitochondrial dynamics and biogenesis are predictably detrimental to mitochondrial bioenergetics and quality control, and are likely to impact neuronal homeostasis, given the high-energy requirements, postmitotic nature, and polarized morphology of the neuron.

Pharmacological strategies that modulate mitochondrial function have been showing promising results in several HD models. Approaches to upregulate the PGC-1 $\alpha$  pathway (e.g. PPAR agonists) were neuroprotective in cellular and mouse models of HD [69], and pharmacological inhibition of mitochondrial fission with P110 prevented striatal neuronal loss and reduced mortality of R6/2 HD mice [69].

Another study reported the beneficial effects of Mdivi1, a cell-permeable selective mitochondrial fission inhibitor that arrests GTPase Drp1 activity by blocking the self-assembly of Drp1, resulting in a reversible formation of

elongated and tubular mitochondria. Mdivi1-treated HD striatal cells showed restored mitochondrial dynamics and function through down-regulation of fission genes and increased expression of fusion and synaptic genes [90].

Mildronate has been found to have protective effects on a wide range of neuropathological events [102]. Indeed, mildronate has demonstrated protective effect on (a) stress- and haloperidol-induced impairment in memory in rats [128], (b) brain damage by anoxia-reoxygenation and (c) loss of learning/memory in trained rats.

Several studies investigated the mechanisms of mildronate neuroprotective action. Acute mildronate administration was shown to modulate nitric oxide and adrenergic signalling [129]. In a rat model of Parkinson's disease, mildronate treatment prevented 6-hydroxydopamine-induced alterations of the neuronal-glia pathways [105]. In addition, a recent study suggested that the cholinergic and glutamatergic pathways are involved in mildronate action [110].

Interestingly, in the current study we found that mildronate can effectively improve motor function of *Drosophila* and *C.elegans*. This improvement is evident by the significant increase in performance on the behavioral assays after mildronate treatment.

In an effort to increase the activity of mildronate on HD, we have designed, synthesized, and characterized 22 mildronate structurally related compounds, among which 4 of these display superior ability to reduce pathological biomarkers of HD as well as ameliorate mitochondrial dysfunction of HD in *in vitro* and *in vivo* assays in comparison to mildronate.

In particular, compounds 4k, 4l, 4m and 4v decrease the level of HD aggregates in transfected cells more significantly than mildronate, without affecting the level of transfected normal Htt. Furthermore, Western blotting indicates that the same compounds do not influence the expression of mutant Htt, though they can reduce the formation of Htt aggregates in the HD cells.

The present study supports the hypothesis that the decrease of mutant Htt accumulation may be mediated by the ability of mildronate to activate the PPAR- $\alpha$ /PGC1- $\alpha$  signaling pathway [110, 128]

Indeed quantitative Real-Time PCR analysis revealed that *Pgc-1 $\alpha$*  mRNA expression was significantly upregulated in transfected cells treated with mildronate and selected compounds, compared to untreated cells. Particularly, compounds 4k and 4l showed an activity higher than mildronate.

Several studies have indicated that PGC1- $\alpha$  is able to promote clearance of Htt protein aggregates and rescue Htt neurotoxicity by the induction of transcription factor EB (TFEB), a master regulator of the autophagy-lysosome pathway.

This therapeutic effect is different from the previous findings for other therapeutics, which rely on improving transcriptional function [130] metabolic function [131], neurotrophic factor signaling pathways [132], mutant Htt conformation, and its interactions with other proteins [133, 134].

Finally, the compound 4k and 4l have shown the ability to significantly decrease the mitochondrial fragmentation. Though the mechanisms underlying the abnormal mitochondrial fragmentation in HD neurons are not yet completely understood, perturbation in mitochondrial dynamics, particularly those affecting the control of the complementary processes of fission and fusion, may increase neuronal susceptibility to brain injuries and contribute to the onset and progression of distinct neurodegenerative disorders [135]. Thus, correcting mitochondrial fragmentation, it was shown to reduce motor deficits, neuropathology, and mortality in HD animals [89].

Although our findings demonstrate that mildronate structurally related compounds reduce mutant Htt accumulation, abnormal mitochondrial dynamics and the associated neurological phenotypes in HD animal models, it remains to be investigated whether they can be used in other neurodegenerative diseases. Such investigation would require more in-depth

studies with sophisticated tools that can explore whether these compounds can affect the expression of other misfolded proteins.

In fact, the increased autophagic function by mildronate structurally related compounds could be beneficial for other pathological conditions in which the accumulation of misfolded proteins leads to neurodegeneration. Consistent with this idea, mildronate has been found to reduce the neuropathology in AD transgenic mice. It is also known that the accumulation of toxic forms of peptides and misfolded proteins can lead to a variety of pathological events such as inflammation and altered cellular signaling [136], which could allow the use of our mildronate structurally related compounds on a variety of pathological events.

# References



## 9. References

- [1] E.M. Coppen, R.A. Roos, Current Pharmacological Approaches to Reduce Chorea in Huntington's Disease, *Drugs*, 77 (2017) 29-46.
- [2] X. Yin, M. Manczak, P.H. Reddy, Mitochondria-targeted molecules MitoQ and SS31 reduce mutant huntingtin-induced mitochondrial toxicity and synaptic damage in Huntington's disease, *Human molecular genetics*, 25 (2016) 1739-1753.
- [3] S.L. Mason, R.A. Barker, Advancing pharmacotherapy for treating Huntington's disease: a review of the existing literature, *Expert opinion on pharmacotherapy*, 17 (2016) 41-52.
- [4] A. Kumar, S. Kumar Singh, V. Kumar, D. Kumar, S. Agarwal, M.K. Rana, Huntington's disease: an update of therapeutic strategies, *Gene*, 556 (2015) 91-97.
- [5] E.J. Wild, S.J. Tabrizi, Biomarkers for Huntington's disease, *Expert opinion on medical diagnostics*, 2 (2008) 47-62.
- [6] G.M. Halliday, D.A. McRitchie, V. Macdonald, K.L. Double, R.J. Trent, E. McCusker, Regional Specificity of Brain Atrophy in Huntington's Disease, *Experimental Neurology*, 154 (1998) 663-672.
- [7] R.H. Myers, Huntington's disease genetics, *NeuroRx : the journal of the American Society for Experimental NeuroTherapeutics*, 1 (2004) 255-262.
- [8] P.C. Nopoulos, Huntington disease: a single-gene degenerative disorder of the striatum, *Dialogues in Clinical Neuroscience*, 18 (2016) 91-98.
- [9] K.B. Kegel, A.R. Meloni, Y. Yi, Y.J. Kim, E. Doyle, B.G. Cuiffo, E. Sapp, Y. Wang, Z.H. Qin, J.D. Chen, J.R. Nevins, N. Aronin, M. DiFiglia, Huntingtin is present in the nucleus, interacts with the transcriptional corepressor C-terminal binding protein, and represses transcription, *The Journal of biological chemistry*, 277 (2002) 7466-7476.
- [10] P. Harjes, E.E. Wanker, The hunt for huntingtin function: interaction partners tell many different stories, *Trends in biochemical sciences*, 28 (2003) 425-433.
- [11] M. Tartari, C. Gissi, V. Lo Sardo, C. Zuccato, E. Picardi, G. Pesole, E. Cattaneo, Phylogenetic comparison of huntingtin homologues reveals the

appearance of a primitive polyQ in sea urchin, *Molecular biology and evolution*, 25 (2008) 330-338.

[12] E. Cattaneo, C. Zuccato, M. Tartari, Normal huntingtin function: an alternative approach to Huntington's disease, *Nature reviews. Neuroscience*, 6 (2005) 919-930.

[13] J. Gafni, E. Hermel, J.E. Young, C.L. Wellington, M.R. Hayden, L.M. Ellerby, Inhibition of calpain cleavage of huntingtin reduces toxicity: accumulation of calpain/caspase fragments in the nucleus, *The Journal of biological chemistry*, 279 (2004) 20211-20220.

[14] X.-J.L. Shi-Hua Li, Huntingtin–protein interactions and the pathogenesis of Huntington's disease, *Trends in Genetics* 20 (2004) 146-154.

[15] J.P. Caviston, J.L. Ross, S.M. Antony, M. Tokito, E.L. Holzbaur, Huntingtin facilitates dynein/dynactin-mediated vesicle transport, *Proceedings of the National Academy of Sciences of the United States of America*, 104 (2007) 10045-10050.

[16] J. Nasir, S.B. Floresco, J.R. O'Kusky, V.M. Diewert, J.M. Richman, J. Zeisler, A. Borowski, J.D. Marth, A.G. Phillips, M.R. Hayden, Targeted disruption of the Huntington's disease gene results in embryonic lethality and behavioral and morphological changes in heterozygotes, *Cell*, 81 (1995) 811-823.

[17] J.K. White, W. Auerbach, M.P. Duyao, J.P. Vonsattel, J.F. Gusella, A.L. Joyner, M.E. MacDonald, Huntingtin is required for neurogenesis and is not impaired by the Huntington's disease CAG expansion, *Nature genetics*, 17 (1997) 404-410.

[18] D. Rigamonti, J.H. Bauer, C. De-Fraja, L. Conti, S. Sipione, C. Sciorati, E. Clementi, A. Hackam, M.R. Hayden, Y. Li, J.K. Cooper, C.A. Ross, S. Govoni, C. Vincenz, E. Cattaneo, Wild-type huntingtin protects from apoptosis upstream of caspase-3, *The Journal of neuroscience : the official journal of the Society for Neuroscience*, 20 (2000) 3705-3713.

[19] I. Dragatsis, M.S. Levine, S. Zeitlin, Inactivation of *Hdh* in the brain and testis results in progressive neurodegeneration and sterility in mice, *Nature genetics*, 26 (2000) 300-306.

[20] B.R. Leavitt, J.M. van Raamsdonk, J. Shehadeh, H. Fernandes, Z. Murphy, R.K. Graham, C.L. Wellington, L.A. Raymond, M.R. Hayden, Wild-

type huntingtin protects neurons from excitotoxicity, *Journal of neurochemistry*, 96 (2006) 1121-1129.

[21] F.G. Gervais, R. Singaraja, S. Xanthoudakis, C.A. Gutekunst, B.R. Leavitt, M. Metzler, A.S. Hackam, J. Tam, J.P. Vaillancourt, V. Houtzager, D.M. Rasper, S. Roy, M.R. Hayden, D.W. Nicholson, Recruitment and activation of caspase-8 by the Huntingtin-interacting protein Hip-1 and a novel partner Hip1, *Nature cell biology*, 4 (2002) 95-105.

[22] C. Zuccato, A. Ciammola, D. Rigamonti, B.R. Leavitt, D. Goffredo, L. Conti, M.E. MacDonald, R.M. Friedlander, V. Silani, M.R. Hayden, T. Timmusk, S. Sipione, E. Cattaneo, Loss of huntingtin-mediated BDNF gene transcription in Huntington's disease, *Science*, 293 (2001) 493-498.

[23] R. Smith, P. Brundin, J.Y. Li, Synaptic dysfunction in Huntington's disease: a new perspective, *Cellular and molecular life sciences : CMLS*, 62 (2005) 1901-1912.

[24] D.M. Hatters, Protein misfolding inside cells: the case of huntingtin and Huntington's disease, *IUBMB life*, 60 (2008) 724-728.

[25] E. Scherzinger, A. Sittler, K. Schweiger, V. Heiser, R. Lurz, R. Hasenbank, G.P. Bates, H. Lehrach, E.E. Wanker, Self-assembly of polyglutamine-containing huntingtin fragments into amyloid-like fibrils: implications for Huntington's disease pathology, *Proceedings of the National Academy of Sciences of the United States of America*, 96 (1999) 4604-4609.

[26] C.A. Ross, M.A. Poirier, Protein aggregation and neurodegenerative disease, *Nature medicine*, 10 Suppl (2004) S10-17.

[27] P.H. Reddy, P. Mao, M. Manczak, Mitochondrial structural and functional dynamics in Huntington's disease, *Brain research reviews*, 61 (2009) 33-48.

[28] P.H. Reddy, Increased mitochondrial fission and neuronal dysfunction in Huntington's disease: implications for molecular inhibitors of excessive mitochondrial fission, *Drug discovery today*, 19 (2014) 951-955.

[29] J.M. Oliveira, Nature and cause of mitochondrial dysfunction in Huntington's disease: focusing on huntingtin and the striatum, *Journal of neurochemistry*, 114 (2010) 1-12.

[30] Z.X. Yu, S.H. Li, J. Evans, A. Pillarisetti, H. Li, X.J. Li, Mutant huntingtin causes context-dependent neurodegeneration in mice with

Huntington's disease, *The Journal of neuroscience : the official journal of the Society for Neuroscience*, 23 (2003) 2193-2202.

[31] A.L. Orr, S. Li, C.E. Wang, H. Li, J. Wang, J. Rong, X. Xu, P.G. Mastroberardino, J.T. Greenamyre, X.J. Li, N-terminal mutant huntingtin associates with mitochondria and impairs mitochondrial trafficking, *The Journal of neuroscience : the official journal of the Society for Neuroscience*, 28 (2008) 2783-2792.

[32] S.E. Browne, R.J. Ferrante, M.F. Beal, Oxidative stress in Huntington's disease, *Brain pathology*, 9 (1999) 147-163.

[33] M.A. Sorolla, G. Reverter-Branchat, J. Tamarit, I. Ferrer, J. Ros, E. Cabiscol, Proteomic and oxidative stress analysis in human brain samples of Huntington disease, *Free radical biology & medicine*, 45 (2008) 667-678.

[34] N.N. Naseri, H. Xu, J. Bonica, J.P. Vonsattel, E.P. Cortes, L.C. Park, J. Arjomand, G.E. Gibson, Abnormalities in the tricarboxylic Acid cycle in Huntington disease and in a Huntington disease mouse model, *Journal of neuropathology and experimental neurology*, 74 (2015) 527-537.

[35] S.E. Browne, A.C. Bowling, U. MacGarvey, M.J. Baik, S.C. Berger, M.M. Muqit, E.D. Bird, M.F. Beal, Oxidative damage and metabolic dysfunction in Huntington's disease: selective vulnerability of the basal ganglia, *Annals of neurology*, 41 (1997) 646-653.

[36] M. Gu, M.T. Gash, V.M. Mann, F. Javoy-Agid, J.M. Cooper, A.H. Schapira, Mitochondrial defect in Huntington's disease caudate nucleus, *Annals of neurology*, 39 (1996) 385-389.

[37] S.J. Tabrizi, M.W. Cleeter, J. Xuereb, J.W. Taanman, J.M. Cooper, A.H. Schapira, Biochemical abnormalities and excitotoxicity in Huntington's disease brain, *Annals of neurology*, 45 (1999) 25-32.

[38] P. Guidetti, V. Charles, E.Y. Chen, P.H. Reddy, J.H. Kordower, W.O. Whetsell, Jr., R. Schwarcz, D.A. Tagle, Early degenerative changes in transgenic mice expressing mutant huntingtin involve dendritic abnormalities but no impairment of mitochondrial energy production, *Exp Neurol*, 169 (2001) 340-350.

[39] C.L. Benn, T. Sun, G. Sadri-Vakili, K.N. McFarland, D.P. DiRocco, G.J. Yohrling, T.W. Clark, B. Bouzou, J.H. Cha, Huntingtin modulates transcription, occupies gene promoters in vivo, and binds directly to DNA in a

polyglutamine-dependent manner, *The Journal of neuroscience : the official journal of the Society for Neuroscience*, 28 (2008) 10720-10733.

[40] B.I. Bae, H. Xu, S. Igarashi, M. Fujimuro, N. Agrawal, Y. Taya, S.D. Hayward, T.H. Moran, C. Montell, C.A. Ross, S.H. Snyder, A. Sawa, p53 mediates cellular dysfunction and behavioral abnormalities in Huntington's disease, *Neuron*, 47 (2005) 29-41.

[41] S. Sameni, A. Syed, J.L. Marsh, M.A. Digman, The phasor-FLIM fingerprints reveal shifts from OXPHOS to enhanced glycolysis in Huntington Disease, *Scientific reports*, 6 (2016) 34755.

[42] Q. Zhang, D.W. Piston, R.H. Goodman, Regulation of corepressor function by nuclear NADH, *Science*, 295 (2002) 1895-1897.

[43] C. Meisinger, A. Sickmann, N. Pfanner, The mitochondrial proteome: from inventory to function, *Cell*, 134 (2008) 22-24.

[44] D.J. Pagliarini, S.E. Calvo, B. Chang, S.A. Sheth, S.B. Vafai, S.E. Ong, G.A. Walford, C. Sugiana, A. Boneh, W.K. Chen, D.E. Hill, M. Vidal, J.G. Evans, D.R. Thorburn, S.A. Carr, V.K. Mootha, A mitochondrial protein compendium elucidates complex I disease biology, *Cell*, 134 (2008) 112-123.

[45] R.C. Scarpulla, Metabolic control of mitochondrial biogenesis through the PGC-1 family regulatory network, *Biochimica et biophysica acta*, 1813 (2011) 1269-1278.

[46] O. Schmidt, N. Pfanner, C. Meisinger, Mitochondrial protein import: from proteomics to functional mechanisms, *Nature reviews. Molecular cell biology*, 11 (2010) 655-667.

[47] A.B. Harbauer, M. Opalinska, C. Gerbeth, J.S. Herman, S. Rao, B. Schonfisch, B. Guiard, O. Schmidt, N. Pfanner, C. Meisinger, Mitochondria. Cell cycle-dependent regulation of mitochondrial preprotein translocase, *Science*, 346 (2014) 1109-1113.

[48] C. Schulz, A. Schendzielorz, P. Rehling, Unlocking the presequence import pathway, *Trends in Cell Biology*, 25 (2015) 265-275.

[49] J. Lin, P.-H. Wu, P.T. Tarr, K.S. Lindenberg, J. St-Pierre, C.-y. Zhang, V.K. Mootha, S. Jäger, C.R. Vianna, R.M. Reznick, L. Cui, M. Manieri, M.X. Donovan, Z. Wu, M.P. Cooper, M.C. Fan, L.M. Rohas, A.M. Zavacki, S. Cinti, G.I. Shulman, B.B. Lowell, D. Krainc, B.M. Spiegelman, Defects in

Adaptive Energy Metabolism with CNS-Linked Hyperactivity in PGC-1 $\alpha$  Null Mice, *Cell*, 119 (2004) 121-135.

[50] C. Puddifoot, M.-A. Martel, F.X. Soriano, A. Camacho, A. Vidal-Puig, D.J.A. Wyllie, G.E. Hardingham, PGC-1 $\alpha$  Negatively Regulates Extrasynaptic NMDAR Activity and Excitotoxicity, *The Journal of Neuroscience*, 32 (2012) 6995-7000.

[51] T. Hering, N. Birth, J.W. Taanman, M. Orth, Selective striatal mtDNA depletion in end-stage Huntington's disease R6/2 mice, *Exp Neurol*, 266 (2015) 22-29.

[52] A.M. Pickrell, H. Fukui, X. Wang, M. Pinto, C.T. Moraes, The striatum is highly susceptible to mitochondrial oxidative phosphorylation dysfunctions, *The Journal of neuroscience : the official journal of the Society for Neuroscience*, 31 (2011) 9895-9904.

[53] L. Cui, H. Jeong, F. Borovecki, C.N. Parkhurst, N. Tanese, D. Krainc, Transcriptional Repression of PGC-1 $\alpha$  by Mutant Huntingtin Leads to Mitochondrial Dysfunction and Neurodegeneration, *Cell*, 127 (2006) 59-69.

[54] P. Weydt, V.V. Pineda, A.E. Torrence, R.T. Libby, T.F. Satterfield, Eduardo R. Lazarowski, M.L. Gilbert, G.J. Morton, T.K. Bammler, A.D. Strand, L. Cui, R.P. Beyer, C.N. Easley, A.C. Smith, D. Krainc, S. Luquet, Ian R. Sweet, M.W. Schwartz, A.R. La Spada, Thermoregulatory and metabolic defects in Huntington's disease transgenic mice implicate PGC-1 $\alpha$  in Huntington's disease neurodegeneration, *Cell Metabolism*, 4 (2006) 349-362.

[55] P. Guedes-Dias, B.R. Pinho, T.R. Soares, J. de Proenca, M.R. Duchen, J.M. Oliveira, Mitochondrial dynamics and quality control in Huntington's disease, *Neurobiology of disease*, 90 (2016) 51-57.

[56] I. Tellez-Nagel, A.B. Johnson, R.D. Terry, Studies on brain biopsies of patients with Huntington's chorea, *Journal of neuropathology and experimental neurology*, 33 (1974) 308-332.

[57] V. Costa, M. Giacomello, R. Hudec, R. Lopreiato, G. Ermak, D. Lim, W. Malorni, K.J. Davies, E. Carafoli, L. Scorrano, Mitochondrial fission and cristae disruption increase the response of cell models of Huntington's disease to apoptotic stimuli, *EMBO molecular medicine*, 2 (2010) 490-503.

[58] J. Kim, J.P. Moody, C.K. Edgerly, O.L. Bordiuk, K. Cormier, K. Smith, M.F. Beal, R.J. Ferrante, Mitochondrial loss, dysfunction and altered

dynamics in Huntington's disease, *Human molecular genetics*, 19 (2010) 3919-3935.

[59] W. Song, J. Chen, A. Petrilli, G. Liot, E. Klinglmayr, Y. Zhou, P. Poquiz, J. Tjong, M.A. Pouladi, M.R. Hayden, E. Masliah, M. Ellisman, I. Rouiller, R. Schwarzenbacher, B. Bossy, G. Perkins, E. Bossy-Wetzel, Mutant huntingtin binds the mitochondrial fission GTPase dynamin-related protein-1 and increases its enzymatic activity, *Nature medicine*, 17 (2011) 377-382.

[60] P. Guedes-Dias, J. de Proenca, T.R. Soares, A. Leitao-Rocha, B.R. Pinho, M.R. Duchon, J.M. Oliveira, HDAC6 inhibition induces mitochondrial fusion, autophagic flux and reduces diffuse mutant huntingtin in striatal neurons, *Biochimica et biophysica acta*, 1852 (2015) 2484-2493.

[61] U.P. Shirendeb, M.J. Calkins, M. Manczak, V. Anekonda, B. Dufour, J.L. McBride, P. Mao, P.H. Reddy, Mutant huntingtin's interaction with mitochondrial protein Drp1 impairs mitochondrial biogenesis and causes defective axonal transport and synaptic degeneration in Huntington's disease, *Human molecular genetics*, 21 (2012) 406-420.

[62] M. Gray, D.I. Shirasaki, C. Cepeda, V.M. Andre, B. Wilburn, X.H. Lu, J. Tao, I. Yamazaki, S.H. Li, Y.E. Sun, X.J. Li, M.S. Levine, X.W. Yang, Full-length human mutant huntingtin with a stable polyglutamine repeat can elicit progressive and selective neuropathogenesis in BACHD mice, *The Journal of neuroscience : the official journal of the Society for Neuroscience*, 28 (2008) 6182-6195.

[63] O.J. Martin, L. Lai, M.M. Soundarapandian, T.C. Leone, A. Zorzano, M.P. Keller, A.D. Attie, D.M. Muoio, D.P. Kelly, A role for peroxisome proliferator-activated receptor gamma coactivator-1 in the control of mitochondrial dynamics during postnatal cardiac growth, *Circulation research*, 114 (2014) 626-636.

[64] J. Lin, C. Handschin, B.M. Spiegelman, Metabolic control through the PGC-1 family of transcription coactivators, *Cell Metab*, 1 (2005) 361-370.

[65] C. Handschin, B.M. Spiegelman, Peroxisome proliferator-activated receptor gamma coactivator 1 coactivators, energy homeostasis, and metabolism, *Endocrine reviews*, 27 (2006) 728-735.

[66] S.J. McConoughey, M. Basso, Z.V. Niatsetskaya, S.F. Sleiman, N.A. Smirnova, B.C. Langley, L. Mahishi, A.J. Cooper, M.A. Antonyak, R.A. Cerione, B. Li, A. Starkov, R.K. Chaturvedi, M.F. Beal, G. Coppola, D.H. Geschwind, H. Ryu, L. Xia, S.E. Iismaa, J. Pallos, R. Pasternack, M. Hils, J.

Fan, L.A. Raymond, J.L. Marsh, L.M. Thompson, R.R. Ratan, Inhibition of transglutaminase 2 mitigates transcriptional dysregulation in models of Huntington disease, *EMBO molecular medicine*, 2 (2010) 349-370.

[67] J. St-Pierre, S. Drori, M. Uldry, J.M. Silvaggi, J. Rhee, S. Jager, C. Handschin, K. Zheng, J. Lin, W. Yang, D.K. Simon, R. Bachoo, B.M. Spiegelman, Suppression of reactive oxygen species and neurodegeneration by the PGC-1 transcriptional coactivators, *Cell*, 127 (2006) 397-408.

[68] D. Hinerfeld, M.D. Traini, R.P. Weinberger, B. Cochran, S.R. Doctrow, J. Harry, S. Melov, Endogenous mitochondrial oxidative stress: neurodegeneration, proteomic analysis, specific respiratory chain defects, and efficacious antioxidant therapy in superoxide dismutase 2 null mice, *Journal of neurochemistry*, 88 (2004) 657-667.

[69] A. Johri, N.Y. Calingasan, T.M. Hennessey, A. Sharma, L. Yang, E. Wille, A. Chandra, M.F. Beal, Pharmacologic activation of mitochondrial biogenesis exerts widespread beneficial effects in a transgenic mouse model of Huntington's disease, *Human molecular genetics*, 21 (2012) 1124-1137.

[70] H.S. Group, Tetrabenazine as antichorea therapy in Huntington disease: a randomized controlled trial, *Neurology*, 66 (2006) 366-372.

[71] Y.L. Wang, W. Liu, E. Wada, M. Murata, K. Wada, I. Kanazawa, Clinico-pathological rescue of a model mouse of Huntington's disease by siRNA, *Neuroscience research*, 53 (2005) 241-249.

[72] S.Q. Harper, P.D. Staber, X. He, S.L. Eliason, I.H. Martins, Q. Mao, L. Yang, R.M. Kotin, H.L. Paulson, B.L. Davidson, RNA interference improves motor and neuropathological abnormalities in a Huntington's disease mouse model, *Proceedings of the National Academy of Sciences of the United States of America*, 102 (2005) 5820-5825.

[73] H.B. Kordasiewicz, L.M. Stanek, E.V. Wancewicz, C. Mazur, M.M. McAlonis, K.A. Pytel, J.W. Artates, A. Weiss, S.H. Cheng, L.S. Shihabuddin, G. Hung, C.F. Bennett, D.W. Cleveland, Sustained therapeutic reversal of Huntington's disease by transient repression of huntingtin synthesis, *Neuron*, 74 (2012) 1031-1044.

[74] C.A. Ross, S.J. Tabrizi, Huntington's disease: from molecular pathogenesis to clinical treatment, *The Lancet. Neurology*, 10 (2011) 83-98.

[75] C. Vacher, L. Garcia-Oroz, D.C. Rubinsztein, Overexpression of yeast hsp104 reduces polyglutamine aggregation and prolongs survival of a

transgenic mouse model of Huntington's disease, *Human molecular genetics*, 14 (2005) 3425-3433.

[76] S. Kim, K.T. Kim, Therapeutic Approaches for Inhibition of Protein Aggregation in Huntington's Disease, *Experimental neurobiology*, 23 (2014) 36-44.

[77] I. Sanchez, C. Mahlke, J. Yuan, Pivotal role of oligomerization in expanded polyglutamine neurodegenerative disorders, *Nature*, 421 (2003) 373-379.

[78] M. Tanaka, Y. Machida, S. Niu, T. Ikeda, N.R. Jana, H. Doi, M. Kurosawa, M. Nekooki, N. Nukina, Trehalose alleviates polyglutamine-mediated pathology in a mouse model of Huntington disease, *Nature medicine*, 10 (2004) 148-154.

[79] V. Chopra, J.H. Fox, G. Lieberman, K. Dorsey, W. Matson, P. Waldmeier, D.E. Housman, A. Kazantsev, A.B. Young, S. Hersch, A small-molecule therapeutic lead for Huntington's disease: preclinical pharmacology and efficacy of C2-8 in the R6/2 transgenic mouse, *Proceedings of the National Academy of Sciences of the United States of America*, 104 (2007) 16685-16689.

[80] Y. Nagai, N. Fujikake, K. Ohno, H. Higashiyama, H.A. Popiel, J. Rahadian, M. Yamaguchi, W.J. Strittmatter, J.R. Burke, T. Toda, Prevention of polyglutamine oligomerization and neurodegeneration by the peptide inhibitor QBP1 in *Drosophila*, *Human molecular genetics*, 12 (2003) 1253-1259.

[81] R.K. Chaudhary, K.A. Patel, M.K. Patel, R.H. Joshi, I. Roy, Inhibition of Aggregation of Mutant Huntingtin by Nucleic Acid Aptamers In Vitro and in a Yeast Model of Huntington's Disease, *Molecular therapy : the journal of the American Society of Gene Therapy*, 23 (2015) 1912-1926.

[82] M.V. Karpuj, M.W. Becher, J.E. Springer, D. Chabas, S. Youssef, R. Pedotti, D. Mitchell, L. Steinman, Prolonged survival and decreased abnormal movements in transgenic model of Huntington disease, with administration of the transglutaminase inhibitor cystamine, *Nature medicine*, 8 (2002) 143-149.

[83] G.O. Abdulrahman, Jr., Therapeutic advances in the management of Huntington's disease, *The Yale journal of biology and medicine*, 84 (2011) 311-319.

- [84] R.K. Chaturvedi, M.F. Beal, Mitochondrial approaches for neuroprotection, *Annals of the New York Academy of Sciences*, 1147 (2008) 395-412.
- [85] M.F. Beal, Neuroprotective effects of creatine, *Amino acids*, 40 (2011) 1305-1313.
- [86] C.A. Ross, S.J. Tabrizi, Huntington's disease: from molecular pathogenesis to clinical treatment, *The Lancet Neurology*, 10 (2011) 83-98.
- [87] B. Martin, E. Golden, O.D. Carlson, P. Pistell, J. Zhou, W. Kim, B.P. Frank, S. Thomas, W.A. Chadwick, N.H. Greig, G.P. Bates, K. Sathasivam, M. Bernier, S. Maudsley, M.P. Mattson, J.M. Egan, Exendin-4 improves glycemic control, ameliorates brain and pancreatic pathologies, and extends survival in a mouse model of Huntington's disease, *Diabetes*, 58 (2009) 318-328.
- [88] Z. Xun, S. Rivera-Sanchez, S. Ayala-Pena, J. Lim, H. Budworth, E.M. Skoda, P.D. Robbins, L.J. Niedernhofer, P. Wipf, C.T. McMurray, Targeting of XJB-5-131 to mitochondria suppresses oxidative DNA damage and motor decline in a mouse model of Huntington's disease, *Cell reports*, 2 (2012) 1137-1142.
- [89] X. Guo, M.H. Disatnik, M. Monbureau, M. Shamloo, D. Mochly-Rosen, X. Qi, Inhibition of mitochondrial fragmentation diminishes Huntington's disease-associated neurodegeneration, *The Journal of clinical investigation*, 123 (2013) 5371-5388.
- [90] M. Manczak, P.H. Reddy, Mitochondrial division inhibitor 1 protects against mutant huntingtin-induced abnormal mitochondrial dynamics and neuronal damage in Huntington's disease, *Human molecular genetics*, 24 (2015) 7308-7325.
- [91] J.M. Oliveira, S. Chen, S. Almeida, R. Riley, J. Goncalves, C.R. Oliveira, M.R. Hayden, D.G. Nicholls, L.M. Ellerby, A.C. Rego, Mitochondrial-dependent Ca<sup>2+</sup> handling in Huntington's disease striatal cells: effect of histone deacetylase inhibitors, *The Journal of neuroscience : the official journal of the Society for Neuroscience*, 26 (2006) 11174-11186.
- [92] M.C. Chiang, C.M. Chen, M.R. Lee, H.W. Chen, H.M. Chen, Y.S. Wu, C.H. Hung, J.J. Kang, C.P. Chang, C. Chang, Y.R. Wu, Y.S. Tsai, Y. Chern, Modulation of energy deficiency in Huntington's disease via activation of the peroxisome proliferator-activated receptor gamma, *Human molecular genetics*, 19 (2010) 4043-4058.

- [93] R.A. Quintanilla, Y.N. Jin, K. Fuenzalida, M. Bronfman, G.V. Johnson, Rosiglitazone treatment prevents mitochondrial dysfunction in mutant huntingtin-expressing cells: possible role of peroxisome proliferator-activated receptor-gamma (PPARgamma) in the pathogenesis of Huntington disease, *The Journal of biological chemistry*, 283 (2008) 25628-25637.
- [94] Z. Wu, P. Puigserver, U. Andersson, C. Zhang, G. Adelmant, V. Mootha, A. Troy, S. Cinti, B. Lowell, R.C. Scarpulla, B.M. Spiegelman, Mechanisms controlling mitochondrial biogenesis and respiration through the thermogenic coactivator PGC-1, *Cell*, 98 (1999) 115-124.
- [95] Y. Chen, J. Zhang, Y. Lin, Q. Lei, K.L. Guan, S. Zhao, Y. Xiong, Tumour suppressor SIRT3 deacetylates and activates manganese superoxide dismutase to scavenge ROS, *EMBO reports*, 12 (2011) 534-541.
- [96] T. Tsunemi, T.D. Ashe, B.E. Morrison, K.R. Soriano, J. Au, R.A. Roque, E.R. Lazarowski, V.A. Damian, E. Masliah, A.R. La Spada, PGC-1alpha rescues Huntington's disease proteotoxicity by preventing oxidative stress and promoting TFEB function, *Science translational medicine*, 4 (2012) 142ra197.
- [97] C. Settembre, C. Di Malta, V.A. Polito, M. Garcia Arencibia, F. Vetrini, S. Erdin, S.U. Erdin, T. Huynh, D. Medina, P. Colella, M. Sardiello, D.C. Rubinsztein, A. Ballabio, TFEB links autophagy to lysosomal biogenesis, *Science*, 332 (2011) 1429-1433.
- [98] M. Jiang, J. Wang, J. Fu, L. Du, H. Jeong, T. West, L. Xiang, Q. Peng, Z. Hou, H. Cai, T. Seredenina, N. Arbez, S. Zhu, K. Sommers, J. Qian, J. Zhang, S. Mori, X.W. Yang, K.L. Tamashiro, S. Aja, T.H. Moran, R. Luthi-Carter, B. Martin, S. Maudsley, M.P. Mattson, R.H. Cichewicz, C.A. Ross, D.M. Holtzman, D. Krainc, W. Duan, Neuroprotective role of Sirt1 in mammalian models of Huntington's disease through activation of multiple Sirt1 targets, *Nature medicine*, 18 (2011) 153-158.
- [99] H. Jeong, D.E. Cohen, L. Cui, A. Supinski, J.N. Savas, J.R. Mazzulli, J.R. Yates, 3rd, L. Bordone, L. Guarente, D. Krainc, Sirt1 mediates neuroprotection from mutant huntingtin by activation of the TORC1 and CREB transcriptional pathway, *Nature medicine*, 18 (2011) 159-165.
- [100] T. Yang, N.Y. Chan, A.A. Sauve, Syntheses of nicotinamide riboside and derivatives: effective agents for increasing nicotinamide adenine dinucleotide concentrations in mammalian cells, *Journal of medicinal chemistry*, 50 (2007) 6458-6461.

- [101] N. Sjakste, A. Gutcaits, I. Kalvinsh, Mildronate: An Antiischemic Drug for Neurological Indications, *CNS Drug Reviews*, 11 (2005) 151-168.
- [102] M. Dambrova, M. Makrecka-Kuka, R. Vilskersts, E. Makarova, J. Kuka, E. Liepinsh, Pharmacological effects of meldonium: Biochemical mechanisms and biomarkers of cardiometabolic activity, *Pharmacological research*, 113 (2016) 771-780.
- [103] E. Liepinsh, E. Skapare, J. Kuka, M. Makrecka, H. Cirule, E. Vavers, E. Sevostjanovs, S. Grinberga, O. Pugovics, M. Dambrova, Activated peroxisomal fatty acid metabolism improves cardiac recovery in ischemia-reperfusion, *Naunyn-Schmiedeberg's archives of pharmacology*, 386 (2013) 541-550.
- [104] P. Degrace, L. Demizieux, J. Gresti, M. Tsoko, A. André, L. Demaison, P. Clouet, Fatty acid oxidation and related gene expression in heart depleted of carnitine by mildronate treatment in the rat, *Molecular and cellular biochemistry*, 258 (2004) 171-182.
- [105] E. Liepinsh, R. Vilskersts, E. Skapare, B. Svalbe, J. Kuka, H. Cirule, O. Pugovics, I. Kalvinsh, M. Dambrova, Mildronate decreases carnitine availability and up-regulates glucose uptake and related gene expression in the mouse heart, *Life Sciences*, 83 (2008) 613-619.
- [106] J. Kuka, R. Vilskersts, H. Cirule, M. Makrecka, O. Pugovics, I. Kalvinsh, M. Dambrova, E. Liepinsh, The cardioprotective effect of mildronate is diminished after co-treatment with L-carnitine, *Journal of cardiovascular pharmacology and therapeutics*, 17 (2012) 215-222.
- [107] B.Z. Simkhovich, Z.V. Shutenko, D.V. Meirena, K.B. Khagi, R.J. Mezapuke, T.N. Molodchina, I.J. Kalvins, E. Lukevics, 3-(2,2,2-Trimethylhydrazinium)propionate (THP)--a novel gamma-butyrobetaine hydroxylase inhibitor with cardioprotective properties, *Biochemical pharmacology*, 37 (1988) 195-202.
- [108] N. Asaka, Y. Muranaka, T. Kirimoto, H. Miyake, Cardioprotective profile of MET-88, an inhibitor of carnitine synthesis, and insulin during hypoxia in isolated perfused rat hearts, *Fundamental & clinical pharmacology*, 12 (1998) 158-163.
- [109] J. Pupure, S. Isajevs, E. Skapare, J. Rumaks, S. Svirskis, D. Svirina, I. Kalvinsh, V. Klusa, Neuroprotective properties of mildronate, a mitochondria-targeted small molecule, *Neuroscience letters*, 470 (2010) 100-105.

- [110] V. Klusa, R. Muceniece, S. Isajevs, D. Isajeva, U. Beitnere, I. Mandrika, J. Pupure, J. Rumaks, B. Jansone, I. Kalvinsh, H.V. Vinters, Mildronate enhances learning/memory and changes hippocampal protein expression in trained rats, *Pharmacology, biochemistry, and behavior*, 106 (2013) 68-76.
- [111] F. Trettel, D. Rigamonti, P. Hilditch-Maguire, V.C. Wheeler, A.H. Sharp, F. Persichetti, E. Cattaneo, M.E. MacDonald, Dominant phenotypes produced by the HD mutation in STHdh(Q111) striatal cells, *Human molecular genetics*, 9 (2000) 2799-2809.
- [112] C. Soldati, A. Bithell, C. Johnston, K.-Y. Wong, L.W. Stanton, N.J. Buckley, Dysregulation of REST-regulated coding and non-coding RNAs in a cellular model of Huntington's disease, *Journal of neurochemistry*, 124 (2013) 418-430.
- [113] A.H. Brand, N. Perrimon, Targeted gene expression as a means of altering cell fates and generating dominant phenotypes, *Development (Cambridge, England)*, 118 (1993) 401-415.
- [114] Y.O. Ali, R. McCormack, A. Darr, R.G. Zhai, Nicotinamide mononucleotide adenylyltransferase is a stress response protein regulated by the heat shock factor/hypoxia-inducible factor 1alpha pathway, *The Journal of biological chemistry*, 286 (2011) 19089-19099.
- [115] J.A. Parker, J.B. Connolly, C. Wellington, M. Hayden, J. Dausset, C. Neri, Expanded polyglutamines in *Caenorhabditis elegans* cause axonal abnormalities and severe dysfunction of PLM mechanosensory neurons without cell death, *Proceedings of the National Academy of Sciences of the United States of America*, 98 (2001) 13318-13323.
- [116] C. Mello, A. Fire, Chapter 19 DNA Transformation, in: F.E. Henry, C.S. Diane (Eds.) *Methods in Cell Biology*, Academic Press 1995, pp. 451-482.
- [117] M. Chalfie, J. Sulston, Developmental genetics of the mechanosensory neurons of *Caenorhabditis elegans*, *Developmental biology*, 82 (1981) 358-370.
- [118] K. Tars, J. Leitans, A. Kazaks, D. Zelencova, E. Liepinsh, J. Kuka, M. Makrecka, D. Lola, V. Andrianovs, D. Gustina, S. Grinberga, E. Liepinsh, I. Kalvinsh, M. Dambrova, E. Loza, O. Pugovics, Targeting carnitine biosynthesis: discovery of new inhibitors against gamma-butyrobetaine hydroxylase, *Journal of medicinal chemistry*, 57 (2014) 2213-2236.

- [119] T.C. Bruice, S.J. Benkovic, A Comparison of the Bimolecular and Intramolecular Nucleophilic Catalysis of the Hydrolysis of Substituted Phenyl Acylates by the Dimethylamino Group, *Journal of the American Chemical Society*, 85 (1963) 1-8.
- [120] N. Kanamitsu, T. Osaki, Y. Itsuji, M. Yoshimura, H. Tsujimoto, M. Soga, Novel water-soluble sedative-hypnotic agents: isoindolin-1-one derivatives, *Chemical & pharmaceutical bulletin*, 55 (2007) 1682-1688.
- [121] L. Guo, D. Wang, P.J. Edwards, N. Shobana, R.W. Roeske, Studies on synthesis of peptides with C-terminal glutamine paranitroanilide, *Peptides Frontiers of Peptide Science*, Springer2002, pp. 297-298.
- [122] N.P. Greene, D.E. Lee, J.L. Brown, M.E. Rosa, L.A. Brown, R.A. Perry, J.N. Henry, T.A. Washington, Mitochondrial quality control, promoted by PGC-1 $\alpha$ , is dysregulated by Western diet-induced obesity and partially restored by moderate physical activity in mice, *Physiological Reports*, 3 (2015) e12470.
- [123] C. Neri, *Frontiers in Neuroscience*  
Value of Invertebrate Genetics and Biology to Develop Neuroprotective and Preventive Medicine in Huntington's Disease, in: D.C. Lo, R.E. Hughes (Eds.) *Neurobiology of Huntington's Disease: Applications to Drug Discovery*, CRC Press/Taylor & Francis  
Llc., Boca Raton (FL), 2011.
- [124] E.A. Lewis, G.A. Smith, Using *Drosophila* models of Huntington's disease as a translatable tool, *Journal of neuroscience methods*, 265 (2016) 89-98.
- [125] R.P. Mason, C. Breda, G.S. Kooner, G.R. Mallucci, C.P. Kyriacou, F. Giorgini, M.T. Unit, *Modeling Huntington Disease in Yeast and Invertebrates*.
- [126] J.A. Linderman, M.C. Chambers, A.S. Gupta, D.S. Schneider, Infection-related declines in chill coma recovery and negative geotaxis in *Drosophila melanogaster*, *PLoS One*, 7 (2012) e41907.
- [127] M. Dimitriadi, A.C. Hart, Neurodegenerative disorders: insights from the nematode *Caenorhabditis elegans*, *Neurobiology of disease*, 40 (2010) 4-11.
- [128] U. Beitnere, Z. Dzirkale, S. Isajevs, J. Rumaks, S. Svirskis, V. Klusa, Carnitine congener mildronate protects against stress- and haloperidol-induced

impairment in memory and brain protein expression in rats, *European Journal of Pharmacology*, 745 (2014) 76-83.

[129] L. Zvejniece, B. Svalbe, M. Makrecka, E. Liepinsh, I. Kalvinsh, M. Dambrova, Mildronate exerts acute anticonvulsant and antihypnotic effects, *Behavioural pharmacology*, 21 (2010) 548-555.

[130] E.A. Thomas, G. Coppola, P.A. Desplats, B. Tang, E. Soragni, R. Burnett, F. Gao, K.M. Fitzgerald, J.F. Borok, D. Herman, The HDAC inhibitor 4b ameliorates the disease phenotype and transcriptional abnormalities in Huntington's disease transgenic mice, *Proceedings of the National Academy of Sciences*, 105 (2008) 15564-15569.

[131] Z. Qiu, F. Norflus, B. Singh, M.K. Swindell, R. Buzescu, M. Bejarano, R. Chopra, B. Zucker, C.L. Benn, D.P. DiRocco, J.H. Cha, R.J. Ferrante, S.M. Hersch, Sp1 is up-regulated in cellular and transgenic models of Huntington disease, and its reduction is neuroprotective, *The Journal of biological chemistry*, 281 (2006) 16672-16680.

[132] K. Gharami, Y. Xie, J.J. An, S. Tonegawa, B. Xu, Brain-derived neurotrophic factor over-expression in the forebrain ameliorates Huntington's disease phenotypes in mice, *Journal of neurochemistry*, 105 (2008) 369-379.

[133] C.-E. Wang, H. Zhou, J.R. McGuire, V. Cerullo, B. Lee, S.-H. Li, X.-J. Li, Suppression of neuropil aggregates and neurological symptoms by an intracellular antibody implicates the cytoplasmic toxicity of mutant huntingtin, *The Journal of cell biology*, 181 (2008) 803-816.

[134] N.L. Dudek, Y. Dai, N.A. Muma, Neuroprotective Effects of Calmodulin Peptide 76-121aa: Disruption of Calmodulin Binding to Mutant Huntingtin, *Brain Pathology (Zurich, Switzerland)*, 20 (2010) 176-189.

[135] E. Bossy-Wetzell, A. Petrilli, A.B. Knott, Mutant huntingtin and mitochondrial dysfunction, *Trends in neurosciences*, 31 (2008) 609-616.

[136] C. Soto, Unfolding the role of protein misfolding in neurodegenerative diseases, *Nature Reviews Neuroscience*, 4 (2003) 49-60.

## ***Acknowledgments***

*I wish to thank my advisor, Professor Carmela Saturnino: she has been supportive since the day I began working with her. She gave me the academic and moral support, as well as the freedom I needed to work on this research.*

*I would like to express my special appreciation and thanks to Professor Gianfranco Peluso. He has been a mentor to me and I would like to thank him for his advices and endless availability, for encouraging and supporting my research and for allowing me to grow and improve myself.*

*I wish to thank Orsolina Petillo for her precious support in this work. I would like to especially thank Sabrina Margarucci for the guidance she has given me over the past three years.*

*Similarly, I would like to thank Anna Calarco, Anna Di Salle, Maria D'Apolito and Mauro Finicelli for supporting me in this period.*

*I can't forget my colleague and friends Raffaele Conte, Angela Napoletano, Felicia Gioiello and Ilenia Del Luca for listening, offering me advice and making me smile through this entire process.*

*A special thanks goes to Anna Valentino for her moral and experimental support and to Adriana De Luise for her unconditional trust, timely encouragement and endless patience.*

*Right balance between lightness and seriousness resulting from my family allows me to always aim for goals greater than me, without fearing failures: it means a lot to me.*

*Finally, a profound thanks to You.*

*Your encouragement led me to finish what I had started.*

*We went through hard times together and we always came out victorious.*